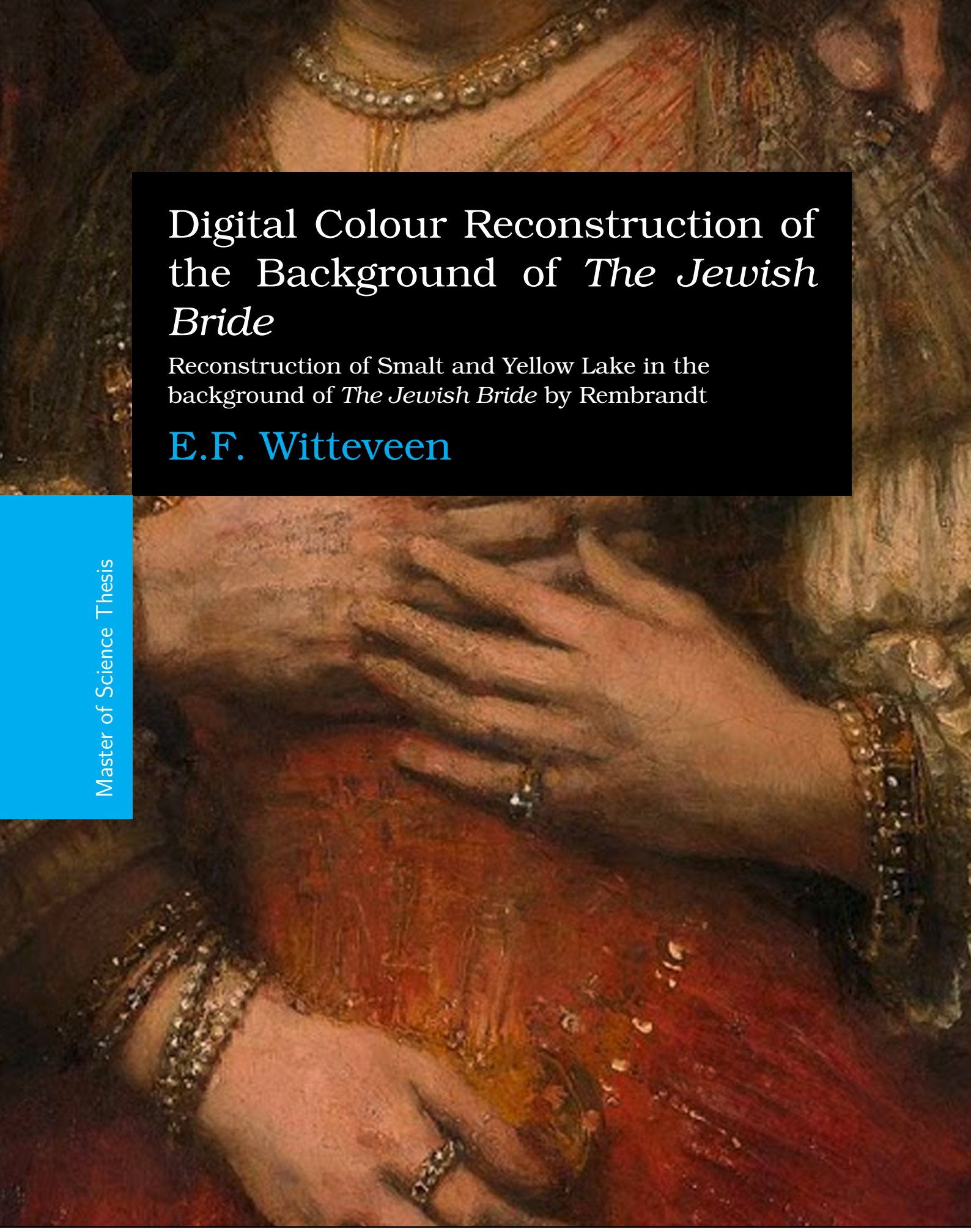

Digital Colour Reconstruction of the Background of *The Jewish Bride*

Reconstruction of Smalt and Yellow Lake in the background of *The Jewish Bride* by Rembrandt

E.F. Witteveen

Master of Science Thesis

TU Delft Delft University of Technology

Materials Science and Engineering

Digital Colour Reconstruction of the Background of *The Jewish Bride*

Reconstruction of Smalt and Yellow Lake in the background of *The Jewish Bride* by Rembrandt

Master of Science Thesis

For the degree of Master of Science in Mechanical Engineering at Delft University of Technology

E.F. Witteveen

October 1, 2017

Supervisors: prof.dr. J. Dik TU Delft

dr. A.van Loon TU Delft & Rijksmuseum

drs. P. Noble Rijksmuseum

Faculty of Mechanical, Maritime and Materials Engineering (3mE) · Delft University of Technology

Copyright © Materials Science and Engineering (MSE)
All rights reserved.

Abstract

Rembrandt was a unique painter of his era, and one of his most outstanding pieces is *The Jewish Bride*. He mastered the art of manipulating pigments to create unique paint mixtures and textures. This can be seen in his painting, *The Jewish Bride*.
In the background of The Jewish Bride, Rembrandt mixed five pigments together: bone black, red earth, smalt (a blue pigment), yellow earth and yellow lake. Smalt and yellow lake are unstable pigments in oil and their colour fades over time. Due to the degradation process of smalt, the oil matrix and the top layer have both changed its appearance into a transparent monochrome brown. The colour loss and change of colour affect the pictorial impression created by the painting.
The goal of this thesis is to digital colour reconstruct the background of *The Jewish Bride* to show how it might have looked when non-degraded smalt and yellow lake were present.
In this work, the painting is analysed with different micro and macro techniques: microscopy, SEM-EDX, Macro-XRF, and hyperspectral imaging. The outcomes of microscopy, SEM-EDX and Macro-XRF are combined to show the distribution and to quantify the amount of smalt and yellow lake in the background.
Knowing the distribution of smalt and yellow lake in the painting made it possible to digital mix the colours back to their primary appearance. To achieve this, the hyperspectral data were used, together with the Kubelka-Munk theory. This was later transferred to RGB values, which results in a digital colour reconstruction.
The digital colour reconstructions show a trend of what the painting might have looked like, at the time Rembrandt painted it, see Figure 5-1.

Table of Contents

Acknowledgements **xvii**

1 Introduction **1**
1-1 ReVisualizing late Rembrandt . . . 2
1-2 *The Jewish Bride* . . . 2
1-2-1 Pictorial image . . . 2
1-2-2 Background . . . 2
1-3 Degradation of the background in the painting . . . 3
1-4 Research goal . . . 4
1-4-1 Requirements for the method . . . 4
1-5 Previous research on *The Jewish Bride* . . . 4
1-6 New analyses on *The Jewish Bride* . . . 5

2 Theory **7**
2-1 Rembrandt . . . 7
2-1-1 Late painting techniques . . . 7
2-1-2 Pigments . . . 8
2-2 Digital colour reconstructions . . . 10
2-2-1 Digital colour space . . . 10
2-2-2 Previous work . . . 13
2-3 Colour prediction methods . . . 18
2-3-1 Physical background of colour appearance . . . 18
2-3-2 Colour prediction methods . . . 24
2-4 Analytical techniques . . . 26
2-4-1 Micro analytical techniques . . . 26
2-4-2 Macro analytical techniques . . . 28
2-4-3 Combination of outputs of measuring techniques . . . 32
2-5 Conclusion . . . 33

3 Method **35**
3-1 Section A . . . 38
3-1-1 Macro-XRF . . . 38
3-1-2 Pigment concentrations calculated from cross-sections of *The Jewish Bride* 38
3-1-3 Linking the Macro-XRF data with the pigment concentrations of smalt and yellow lake of the samples . . . 39
3-2 Section B . . . 39
3-3 Section C . . . 39
3-4 Section D . . . 40
3-5 Section E . . . 40
3-5-1 Section E.1 . . . 40
3-5-2 Section E.2 . . . 41
3-5-3 Section E.3 . . . 42
3-5-4 Section E.4 . . . 42

4 Results & Discussion **43**
4-1 Section A . . . 44
4-1-1 Macro-XRF images of *The Jewish Bride* - previous work . . . 45
4-1-2 Pigment detection of five cross-section samples of *The Jewish Bride*'s background . . . 52
4-1-3 Calculating the volume fractions of the pigments in the five different cross-section samples . . . 65
4-1-4 Smalt and yellow lake concentration in *The Jewish Bride* . . . 75
4-1-5 Conclusion section A and discussion . . . 76
4-2 Section B - Reflectance curves of *The Jewish Bride* . . . 78
4-2-1 Conclusion of section B and discussion . . . 79
4-3 Section C - Paint-outs . . . 83
4-3-1 First set of paint-outs . . . 83
4-3-2 Second set of paint-outs . . . 84
4-3-3 Third set of paint-outs . . . 85
4-3-4 Fourth set of paint-outs . . . 86
4-3-5 Hyperspectral analysis of smalt and yellow lake . . . 91
4-3-6 Conclusion of section C and discussion . . . 91
4-4 Section D - Cross-section analysis of paint-out reconstruction of sample 40_15 . 94
4-4-1 Conclusion of section D and discussion . . . 96
4-5 Section E . . . 98
4-5-1 Focus Area of *The Jewish Bride* . . . 99
4-5-2 Section E.1 . . . 101
4-5-3 Section E.2 . . . 105
4-5-4 Section E.3 . . . 111
4-5-5 Section E.4 . . . 115
4-5-6 Conclusion of section E and discussion . . . 117

5 Conclusion **119**
5-1 Discussion . . . 121
5-1-1 Smalt and yellow lake . . . 121
5-1-2 K/S values of smalt en yellow lake . . . 121
5-1-3 Hyperspectral data . . . 122
5-1-4 Mixing colour with Kubelka-Munk theory . . . 122
5-1-5 Requirements for the method . . . 122
5-1-6 Conclusion . . . 123
5-2 Further research . . . 123
5-2-1 Smalt and yellow lake . . . 124
5-2-2 The Kubelka-Munk theory and transparency pigments . . . 124
5-2-3 Accurate colour of degraded smalt . . . 124
5-2-4 Extrapolating the method to the whole painting . . . 124

A XRF **125**
A-1 Workings of the Macro-XRF . . . 125
A-2 Distributions of elements in *The Jewish Bride* . . . 125
A-2-1 Complete overview of the Macro-XRF Maps . . . 127

B Cross-section Samples **131**
B-1 Sample 215/2 . . . 132
B-2 Sample 215/3 . . . 133
B-3 Sample 40_7 . . . 134
B-4 Sample 40_12 . . . 135
B-5 Sample 40_15 . . . 136

C SEM-EDX **137**
C-1 SEM-EDX experimental details . . . 137
C-2 Sample 215/2 . . . 137
C-2-1 EDX spot analysis . . . 137
C-2-2 Element Map of Sample . . . 141
C-3 Sample 215/3 . . . 142
C-3-1 EDX spots . . . 142
C-3-2 Element map of sample . . . 144
C-4 Sample 40_7 . . . 145
C-4-1 EDX spot analysis . . . 145
C-4-2 Element Map of Sample . . . 147
C-5 Sample 40_12 . . . 148
C-5-1 EDX spots . . . 148
C-5-2 Element Map of Sample . . . 150

C-6 Sample 40_15 . . . 151
C-6-1 EDX Spots . . . 151
C-6-2 Element Map of Sample . . . 153
C-7 Reconstruction of Sample 40_15 . . . 154
C-7-1 Element maps of sample . . . 154

D Paintouts **155**
D-1 Paint-outs . . . 155
D-1-1 Material used and method . . . 155
D-1-2 Translation from volume to weight . . . 156
D-1-3 Paint-outs . . . 157
D-2 Tile set 1 . . . 158
D-3 Tile set 2 . . . 160
D-4 Tile set 3 . . . 161

E Digital Colour Reconstructions **163**
E-1 Yellow lake and Smalt . . . 163
E-2 The background without the colour of the degraded matrix and yellow lake . . . 163
E-3 The background without the colour of the degraded matrix and yellow lake . . . 163
E-4 Expansion of figure 4-57 . . . 165

F Matlab **169**

Bibliography **171**

List of Figures

1-1 Rembrandt Harmensz. van Rijn, *Portrait of a Couple as Isaac and Rebecca, known as 'The Jewish Bride'*, c. 1665 - c. 1669, oil on canvas, 121.5x166.5, Rijksmuseum Amsterdam.[1] 1

1-2 Rembrandt Harmensz. van Rijn, *King Abimelech looking down from his window sees Isaac and Rebecca making love*,c. 1665 - c. 1669, pen on paper, 145 x 185 mm, New York, private collection. [2]. This is a study for the painting. In the sketch Abimelech is visible in the top of the paper on the left side of the beam. . 3

2-1 How a digital image is build up in RGB On the left hand side, it shows how the image would be seen on the screen. The right hand side shows the three matrix planes, red, green and blue. For example, the red box is built up by R:255 G:0 and B:0, while the grey colour below the red box is built up from the values R:50, G:50 and B:50. 11

2-2 Method reflectance curve to XYZ [3] First the spectral reflectance curve R(λ), will be multiplied with the D65 light, E(λ)(65), normal daylight; see panel number 1. I. It is then multiplied with the light sensitive curves of the eye ($\bar{x}$, $\bar{y}$ and $\bar{z}$),; see panel number 2. The area beneath the curve is calculated, which gives three values X, Y, and Z; see panel number 3. X, Y, and Z are then converted to R, G, and B values with a matrix. 12

2-3 Three versions of *The conversion of the Magdalen* 14

2-4 Hendrick ter Brugghen, *The Evangelist Luke*, 1622, Museum De Waag, Deventer - Reconstruction of smalt in the cloak is shown on the left side, the right side isnot reconstructed[4].This reconstruction was carried out by Joris Dik (Antoni van Leeuwenhoek chair Materials in Art and Archaeology, TU Delft)[5] in 2002. It shows the effect of the smalt degradation and the effect on the pictorial image. . 15

2-5 Van Gogh, *The Bedroom*, 1888, Van Gogh Museum, Amsterdam - On the left side original painting and on the right side the reconstruction done by prof.dr. Roy Berns (Richard S. Hunter chair Color Science, Rochester Institute Of Technology) in 2016 [6]. There were two red lakes reconstructed eosin and cochineal, especially on the wall this had a great effect. In the present-day they appear blue, while in the digital reconstruction they became purple. 16

2-6 Different visible light interactions with an object. 18

2-7 Spectral curve of D65 (sun light) [7]. It shows that the relative power per wavelength differs. 19

2-8 Colour from a paint layer Here white light goes through the surface and interacts with the pigment particles. In the yellow particles all the light except yellow light is absorbed, and the same goes for the blue pigment particles where only the blue light is not absorbed. The yellow light is scattered by the yellow pigments and the blue light is scattered by blue pigments. Out of the surface comes blue and yellow light, and together it creates a green colour. 20

2-9 Colour from a transparent layer on top of a opaque layer The transparent layer scatters some of the yellow light back towards the surface, while part of the incoming white light goes through the transparent layer without interaction. This light reacts with the blue opaque layer after scattering the blue light towards the surface without interacting with the transparent yellow layer. The two coloured lights, blue and yellow, are mixed into green. 21

2-10 Hunter's experiment[8]. Here pebbles of the same colour are used with decreasing size. The light scatters more on the smaller pebbles, which therefore appear lighter of colour. 22

2-11 Simultaneous colour contrast Colours can appear the same due to the colour surrounding them, while when placed side by side they differ. For instance, inside the white and black box the grey colour appear the same grey tone, while placed side by side, they are actually a different colour. 23

2-12 Working principle of XRF [9] X-rays can eject an electron close to the core of an atom. When the hole is filled by an electron of an outer orbital, an X-ray (XRF) that is specific for that element is sent out. 28

2-13 Different Representation of Colours 31

3-1 Method sections A, B, C, and D Section A Paragraph 4-1 page 44 Section B Paragraph 4-2 page 78 Section C Paragraph 4-3 page 83 Section D Paragraph 4-4 page 94 36

3-2 Section E Section E Paragraph 4-5 page 98 Section E.1 Paragraph 4-5-2 page 101, Section E.2 Paragraph 4-5-3 page 105, Section E.3 Paragraph 4-5-4 page 111, Section E.4 Paragraph 4-5-5 page 115 37

3-3 Focus Area of *The Jewish Bride*, the plant beside Rebecca 41

4-1 A schematic overview of section A It also shows the different paragraphs containing section A. 44

4-2 *The Jewish Bride* is scanned in four sessions (1–4) using the Macro-XRF scanner. 45

4-3 Schematic representation of the steps taken to achieve Figures 5-4b, 5-5b, 5-6b and 5-7b 46

4-4 Distribution of Calcium in the Painting **(a)** White indicates a relatively high concentration, black indicates a relatively low concentration. **(b)** Grey areas indicate areas where there is a low amount of the element. Areas show original colour when there is a high concentration of the element present. The figure shows that the dark areas in background of the original painting correspond with high amounts of calcium. This element is linked in the background to bone black. 47

4-5 Distribution of iron in the painting **(a)** White indicates a relatively high concentration, black indicates a relatively low concentration. **(b)** Grey areas indicate areas where there is a low amount of the element. Areas show original colour when there is a high concentration of the element present. The figure shows that the iron distribution is homogeneous in the whole background, apart from some areas in the plant on the right side of Rebecca. This element is linked to earth pigments. 48

4-6 Distribution of cobalt in the painting **(a)** White indicates a relatively high concentration, black indicates a relatively low concentration. **(b)** Grey areas indicate areas where there is a low amount of the element. Areas show original colour when there is a high concentration of the element present. The figure shows that cobalt is used extensively in the whole background. This element is linked to smalt. . . 49

4-7 Distribution of potassium in the painting **(a)** White indicates a relatively high concentration, black indicates a relatively low concentration. **(b)** Grey areas indicate areas where there is a low amount of the element. Areas show original colour when there is a high concentration of the element present. The figure shows that in the background potassium is not homogeneously distributed, especially in the plant on the right side of Rebecca. The element is linked to lake pigments. 49

4-8 Close-up of the different elemental maps of the plant, in grey scale. White indicates a relatively high concentration of the element, black indicates a relatively low concentration. Each element can be linked to specific pigment(s). Notice that the painting is build-up by using different pigment mixtures. 51

4-9 Cross-section sample locations, descriptions can be found in Table 4-1. 52

4-10 Microscope images of cross-section of sample 215/2 depicting the three layers. In layer 1 and 2 smalt particles are visible, as angular particles. 54

4-11 Cross-section of sample 215/2 scanned by SEM-EDX. It shows the backscattered electron image and elemental maps. Silicon shows the smalt particles, while the combination of maps of sulphur and potassium show yellow lake particles. 55

4-12 Microscope images of cross-section of sample 215/3 depicting the three layers. In layer 2 & 3 smalt particles are visible in UV as angular particles. 56

4-13 Cross-section of sample 215/3 scanned by SEM-EDX. It shows the backscattered electron image and elemental maps. Silicon shows the smalt particles as angular particles, while the combination of sulphur, potassium and calcium show yellow lake particles. 57

4-14 Microscope images of cross-section of sample 40_7 depicting the three layers. In layer 2 & 3 smalt particles are visible in UV as angular particles. 58

4-15 Cross-section of sample 40_7 scanned by SEM-EDX. It shows the backscattered electron image and elemental maps. Silicon shows the smalt particles as angular particles, while the combination of sulphur, potassium and calcium show yellow lake particles. 59

4-16 Microscope images of cross-section of sample 40_12 depicting the three layers. In layer 2 & 3 smalt particles are visible in UV as angular particles. 60

4-17 Cross-section of sample 40_12 scanned by SEM-EDX. It shows the backscattered electron image and elemental maps. Silicon shows the smalt particles as angular particles, while the combination of sulphur, potassium and calcium show yellow lake particles. 61

4-18 Microscope images of cross-section of sample 40_15 depicting the three layers. In layer 3 smalt particles are visible in UV as angular particles. 62

4-19 Cross-section of sample 40_15 scanned by SEM-EDX. It shows the backscattered electron image and elemental maps. Silicon shows the smalt particles as angular particles, while the combination of sulphur, potassium and calcium show yellow lake particles. 63

4-20 Cross-section image of sample 40_15 in UV and scanned by SEM-EDX. **(a)** and **(b)** depict the same area and have the same pixel size. The region of interest is selected: the smalt containing layer, which is indicated as the black boundary around the cross-section sample images. 66

4-21 Process of filtering out smalt particles. **(a)** shows the input image **(b)** shows the output, where the white pixels represent the smalt particles 67

4-22 Process of filtering out yellow lake. Figures **(a)**, **(b)** and **(c)** shows the input elemental maps. **(d)** shows the output, where **(a)**, **(b)** and **(c)** are combined. White pixels represent the yellow lake clusters. 68

4-23 UV images with different mutations **(a)** is the input image. **(b)** shows **(a)** with a larger range of RGB values (stretched) and more distinct transitions between the pigment particles and the oil matrix (sharpened). 69

4-24 Steps of filtering out bone black 70

4-25 Steps of filtering out red earth 70

4-26 Steps of filtering out yellow earth 71

4-27 The Macro-XRF values for cobalt and potassium on the sample locations are plotted against the pigment concentrations of the non-normalised smalt and yellow lake calculated out of the samples, Table 4-3. The relationship that appears is that that low amount of cobalt means low amount of smalt and vice versa. The same holds for yellow lake and potassium. 77

4-28 Schematic representation hyperspectral data set of the focus area. The row and columns give the location of the scanned area, while the layers show the reflection per wavelength. 79

4-29 Hyperspectral scan in RGB of *The Jewish Bride* 80

4-30 The focus area in RGB based on the hyperspectral scan 80

4-31 Different pixels in the painting, which in Figure 4-32 are shown in RGB, hyperspectral curves and K/S curves 81

4-32 Pixels, from locations shown in Figure 5-31, represented in RGB, reflection curves and K/S values. 82

4-33 First set of paint-outs using pigment mixture described in Table 4-5 using no-degreaded smalt. The paint-outs based on the calculated pigment concentrations of 40_7, 40_15 and 215/3 and showing little colour difference between them. They all appear dark and cool of colour. 84

4-34 Second set of paint-outs using pigment mixture described in Table 4-6. The paint-outs shows the same samples as in the previous sub-paragraph 4-3-1, but without the use of non-degraded smalt. There is more colour difference between the samples and they appear browner than Figure 4-33. 84

4-35 RGB values of the three paint-outs based on the reflection curves. The paint-outs are very dark, this is also visible in the reflection curves, where the reflection is around 0.03. The little difference in the reflection curves do lead to colour differences. 85

4-36 Third set of paint-outs. The paint-outs are based on sample 40_15. The difference in percentages per pigment from sample 40_15 are shown in the figure, with only one pigment percentage changed per paint-out. There is no real colour difference between the different paint-outs. 86

4-37 Fourth set of paint-outs Here mixtures of non-degraded smalt and another pigments are shown. It is seen that every pigment has its own interaction with non-degraded smalt 87

4-38 Paint-out Smalt 4% cobalt made by Diana de Man [10][11] It shows that smalt is not evenly distributed over the surface. 87

4-39 RGB and reflection curves of bone black and smalt mixtures. It shows that smalt has little effect on the colour of the mixtures. 88

4-40 RGB and reflection curves of red earth and smalt mixtures. It shows that large amount of smalt make the colour more purple. 89

4-41 RGB and reflection curves of yellow earth and smalt mixtures. It shows that large amount of smalt make the colour more green. 89

4-42 RGB and reflection curves of yellow lake and smalt mixtures. It shows that smalt makes the colour darker. 90

4-43 Yellow lake and smalt represented in RGB, reflection curves and K/S values. . . 92

4-44 Microscope images of cross-section paint-out reconstruction of sample 40_15 and cross-section of sample 40_15. **(a)** the blue angular particles are non-degraded smalt. **(b)** shows degraded smalt as angular transparent particles. It shows that the smalt particles in **(a)** are bigger than in **(b)**. In both the smalt particles are evenly distributed. All the images show that the thickness of the paint-out reconstruction cross-section sample is bigger than that of cross-section of sample 40_15. 94

4-45 Backscattered electron image and silicon map of cross-section paint-out reconstruction of sample 40_15 and cross-section of sample 40_15. It shows that in both the cross-section smalt is evenly distributed. 95

4-46 Focus Area of *The Jewish Bride*. It shows the plant on the right side of Rebecca and the yellow border indicates the area of focus. 99

4-47 Close-up of focus area and Macro-XRF images of calcium, cobalt, iron and potassium. **(b)** calcium can be related with the pigment of bone black and the high calcium areas are related to the shadows underneath the leaves in the present-day image. **(c)** cobalt can be related to smalt and is present in whole of the focus area. **(d)**is related to red earth and yellow earth. It shows clearly that there is some concentration in the plant itself, but there is very little present in the leaves themselves. **(e)** potassium is related to the pigment of yellow lake. The highest concentration of potassium is in the leaves. 100

4-48 Four colours, all based on sample 40_7. The colour from the painting (1) is a bit more brownish compared to the paint-out 2). Using non-degraded smalt makes the colour darker and cooler of tone. 3,the colour is very blueish compared to the first two colours. This is due to the fact that the concentration measured is for transparent smalt, while when digital mixing smalt is seen as opaque. 4, only half the amount of smalt is used. It appears less blue and more in line with the first two colours. The calculated concentration of smalt should be decreased to make sure that the blue colour is not too dominant. In the next sections the concentration of smalt and yellow lake will vary in different concentration, since the exact concentration is unknown. *Note that the figure brightness is adjusted for printing* 103

4-49 Steps in the concentration of smalt and yellow lake The smalt distribution and concentration is based on the cobalt Macro- XRF image of the focus area. What becomes visible is that the images become progressively darker blue, beside a few spots smalt is very homogeneously distributed. The yellow lake distribution is based on the potassium Macro-XRF image. It shows that between the leaves the concentration is very large, while there is significantly less yellow lake surrounding the leaves. Also, it shows that the colour in the beginning is yellow, but turns into a more brownish/reddish colour when the concentration increases. *Note that the figure brightness is adjusted for printing* 106

4-50 Digital mixture of smalt and yellow lake The concentration distribution is based on the cobalt Macro-XRF image for smalt and on the potassium Macro-XRF image for yellow lake. The colour of the leaves becomes very dark. Due to the fact that the yellow lake in large concentrations is a brownish yellow. The leaves do not appear as green as one might have expected.*Note that the figure brightness is adjusted for printing* 107

4-51 Steps in concentration of the present-day image Between the different concentrations it shows that more specular reflection appears in lower percentages. Also, at the lower concentrations the different colours in the leaves become more visible. *Note that the figure brightness is adjusted for printing* 108

4-52 Yellow circle indicates the pixel, which represents the colour of degraded smalt The location was chosen using the Macro-XRF image, where there was a low amount of calcium, iron, and potassium in combination with a very high amount of cobalt. 109

4-53 Steps in the concentration of the colour degraded smalt. The distribution is based on the cobalt Macro-XRF images, since this indicates the smalt distribution. *Note that the figure brightness is adjusted for printing* 109

4-54 Steps in the concentration of degraded Smalt subtracted from the present day colour of the painting. What is interesting is that different highlights become better visible. The yellow highlight in the top right corner, for example, is better visible. *Note that the figure brightness is adjusted for printing* 110

4-55 Two sequences focusing on the effect of smalt and yellow lake on the focus area. The first array shows that different concentrations of smalt make the background very dark and cool of colour. The second array shows that different colour concentrations of yellow lake, have less an effect on the focus area. It makes the image a dark and brownish of colour. *Note that the figure brightness is adjusted for printing* . . 111

4-56 Two sequences focussing on the effect of filtering out degraded smalt In the top array 20% is filtered out and the bottom array 40% is filtered out, while in both the concentration of smalt and yellow increase in steps of 20%. There is little difference between the two arrays, only that in the bottom array, the specular reflection is larger. Both arrays show that the focus area becomes darker and cooler of tone. *Note that the figure brightness is adjusted for printing* 112

4-57 Two sequences focussing on the effect of the concentration of the present-day image and a combination of all The first array shows that by increasing the concentration the colour of the focus area becomes darker and cooler of tone. The second array shows that subtracting the brown colour of degraded smalt does influence the image. It appears to be even cooler in tone and more blueish dark compared to the first array. *Note that the figure brightness is adjusted for printing* 113

4-58 Possible digital colour reconstructions (the dark square in the plant) are placed back in the present-day painting. For this the digital colour reconstruction of Figure 4-57 is used. It shows that the colour change due to smalt and yellow lake degradation is drastic. The digital colour reconstruction is darker and cooler of tone compared to the present-day colour of *The Jewish Bride* *Note that the figure brightness is adjusted for printing* 115

5-1 Possible digital colour reconstructions (the dark square in the plant) are placed back in the present-day painting. For this the digital colour reconstruction sof Figure 4-57 is used. It shows that the colour change due to smalt and yellow lake degradation is drastic. The digital colour reconstructions are darker and cooler of tone compared to the present-day colour of *The Jewish Bride* *Note that the figure brightness is adjusted for printing* 120

A-1 Working principle of XRF [8] 126

A-2 Area scanned and X-ray transmission image 126

B-1 Sample 215/2 132

B-2 Sample 215/3 133

B-3 Sample 40_7 134

B-4 Sample 40_12 135

B-5 Sample 40_15 136

C-1 Sample 215/2 with indicated EDX spots 138

C-2 Spectra 9 - 19 140

C-3 Elemental maps of Sample 215/2 141

C-4 Sample 215/3 with indicated EDX spots 142
C-5 Elemental maps of Sample 215/3 144
C-6 Sample 40_7 with indicated EDX spots 145
C-7 Spectra 8 & 9 145
C-8 Elemental maps of Sample 40_7 147
C-9 Sample 40_12 with indicated EDX spots 148
C-10 Spectra 4-6 149
C-11 Elemental maps of Sample 40_12 150
C-12 Sample 40_15 with indicated EDX spots 151
C-13 Spectra 13, 16 and 17 152
C-14 Elemental maps of Sample 40_15 153
C-15 Elemental maps of reconstruction of sample 40_15 154

D-1 Steps from pigment prectage to total weight (pigment+oil) 157
D-2 Tile set 1 159
D-3 Tile set 2 160
D-4 Tile set 3 161

E-1 The focus area with increasing concentration of smalt and yellow lake It shows that in almost every concentration the area surrounding the leaves appear blue, while the leaves turn brownish due to the fact of the mix of blue and 'reddish' yellow. . 164
E-2 The focus area with increasing concentration of yellow lake and increasing amount of degraded smalt is filtered out. By subtracting the colour of degraded smalt the colour becomes lighter and more specular reflection appears. Smalt makes the painting progressively darker/bluer. 165
E-3 The focus area with increasing concentration of smalt and increasing amount of degraded smalt is filtered out. By subtracting the colour of degraded smalt the colour becomes lighter and more specular reflection appears. Yellow lake makes the painting progressively darker and more brown. 166
E-4 The original image set at 80% with increasing concentration in steps of 10% of smalt and yellow lake. It shows that that the focus area get progressively darker and cooler of tone. 167
E-5 The original image set at 80% and 20% of the colour of degraded smalt is subtracted, with increasing concentration in steps of 10% of smalt and yellow lake. It shows that that the focus area get progressively darker and cooler of tone. 168

List of Tables

2-1 Pigments used by Rembrandt and their main chemical composition 8
2-2 Image areas of Figure 2-5 and lake used on those locations 16
2-3 Colour and wavelength [12] 18
2-4 Overview of the Theories with there Advantages and Limitations 26
2-5 Overview of the Theories with their advantages and limitations 32

4-1 Cross-section sample spots and description 53
4-2 Comparison of the smalt particles in wt% using EDX spot analysis 64
4-3 Non-normalised fraction of pigments in samples 215/2, 215/3, 40_7, 40_12 and 40_15 72
4-4 Normalised fraction of pigments in the samples 215/3, 40_7, 40_12 and 40_15 . 72
4-5 Amount of pigment without oil in percentages on which paint-outs seen in Figure 4-33 are made 84
4-6 Amount of oil per pigment and fraction on which paint-outs seen in Figure 4-34 are made 85
4-7 Calculated pigment concentration of the cross-section of sample 40_15 and of paint-out reconstruction of 40_15 96
4-8 Calculated yellow pigment of the cross-section of sample 40_15 and of paint-out reconstruction of 40_15 96

C-1 Quantitative spectrum data of sample 215/2 138
C-2 Average wt% and standard deviation of sample 215/2 spectrum spots 139
C-3 Quantitative spectra data of sample 215/3 142
C-4 Average wt% and standard deviation of sample 215/3 sample spots 143
C-5 Quantitative spectra data of sample 40_7 145
C-6 Average wt% and standard Deviation of sample 40_7 sample spots 146
C-7 Quantitative spectrum data of sample 40_12 148

C-8 Average wt% and standard Deviation of sample 40_12 sample spots 149
C-9 Quantitative spectra data of sample 40_15 151
C-10 Elements of smalt particles in sample 40_15 152

D-1 Pigments used for Paint outs 155
D-2 Volume and weight per dry pigment and oil 156
D-3 Amount of oil per pigment and fraction 156
D-4 Third set of paint-outs 158

F-1 Matlab functions 169

Acknowledgements

I would like to thank everyone who contributed to this work, and I want to specifically thank the following people:

All my supervisors, Annelies van Loon (TU Delft/Rijksmuseum), Joris Dik (TU Delft) and Petria Noble (Rijksmuseum), for their input and help, especially during the writing part of my thesis. Also many thanks to John Delaney (National Gallery of Art in Washington) for scanning The Jewish Bride and his help with the data analysis. Lastly, big thanks to Barend Thijsse (TU Delft) for the final check of my thesis.

I have learned a lot during my thesis, not only about Rembrandt and *The Jewish Bride*, but also about structuring and explaining my thoughts on paper.

I would like to thank my father, Menno Witteveen and my sisters, Maaike and Willemijn Witteveen, for making the time to check my thesis. I have received a lot of support from my family and friends, many thanks for that.

Thank you all!

Delft, University of Technology — E.F. Witteveen
October 1, 2017

Chapter 1

Introduction

The Portrait of a Couple as Isaac and Rebecca, known as *The Jewish Bride*, is one of Rembrandt's masterpieces and on view in the Rijksmuseum in Amsterdam; see Figure 1-1. The painting is dated around 1665 - 1669, which is known as Rembrandts late period.[1] The degraded background in this painting is the subject of research for this thesis.



Figure 1-1: Rembrandt Harmensz. van Rijn, *Portrait of a Couple as Isaac and Rebecca, known as 'The Jewish Bride'*, c. 1665 - c. 1669, oil on canvas, 121.5x166.5, Rijksmuseum Amsterdam.[1]

1-1 ReVisualizing late Rembrandt

This thesis was conceived as part of the NWO-sponsored Science4Arts ReVisualizing late Rembrandt (ReVisRembrandt) project. The project started in 2012 and will continue till 2018. ReVisRembrandt focuses on applying and developing new non-invasive imaging techniques, including Macro X-ray fluorescence (Macro-XRF); see chapter 2-4-2-1 and 2-4-2-1-1. These imaging techniques can help determine which painting materials were used, and show how these materials are distributed in the painting. This not only gives new insight about the experimental painting technique of the late Rembrandt, but provides a better understanding of the condition of these complex paintings.

1-2 *The Jewish Bride*

The Jewish Bride (SK-C-216) has been painted with oil paint on canvas. The painting measures 121.5 cm in height by 166.5 cm in width.[1] In this section the pictorial image will be discussed, including the present appearance of the background that now appears monochrome brown with indistinct blackish patches.

1-2-1 Pictorial image

The image depicts a couple as Isaac and Rebecca, see Figure 1-1. Isaac and Rebecca are two characters from the Old Testament. In this story, Isaac is sent by God to the Philistine land of Gerar. His wife Rebecca, who is much younger and very beautiful, accompanies him. Isaac fears that he will be murdered by the men who desire Rebecca. For that reason he pretends to be her brother, instead of her husband. At a moment when Isaac and Rebecca are in an intimate embrace, they are spotted by the King of Gerar, Abimelech. This is the moment that Rembrandt captures in the painting. In the sketch Rembrandt made as a study for the painting, Abimelech is visible, but in the painting he is absent; see Figure 1-2. Luckily, the story has a happy ending. King Abimelech is merciful, and after this incident Isaac and Rebecca are able to live together as husband and wife in Gerar under Abimelech's protection.

1-2-2 Background

The background of this painting is hard to distinguish. The main features of the background will be discussed here.
In both the sketch and (initially in the) painting, the couple sits on a bench; see Figures 1-1 and 1-2. This is more clearly visible in the sketch. In the painting it is very difficult to see, and the couple appear to be standing. Rebecca's dress is bunched up on the right side, from which it becomes clear that she is actually seated.
On the right side, there is a potted plant, which is clearly visible in the sketch and less so in the painting. In the sketch there is more space between Rebecca and the plant. The pilasters below the plant in the sketch are replaced in the painting by steps.
Above Rebecca, there is a column, with shading around it. The column is also visible in the



Figure 1-2: Rembrandt Harmensz. van Rijn, *King Abimelech looking down from his window sees Isaac and Rebecca making love*,c. 1665 - c. 1669, pen on paper, 145 x 185 mm, New York, private collection. [2]. This is a study for the painting. In the sketch Abimelech is visible in the top of the paper on the left side of the beam.

sketch. The rest of the background does not show any specific features. From the sketch, it appears that in the top left there are also some plants. If these were part of the painting, they have faded away over time.

1-3 Degradation of the background in the painting

All paintings suffer from some form of degradation and ageing, which can lead to changes in their appearance. This evidently can influence the pictorial depiction that was intended by the artist. As already stated, colour degradation has taken place in the background of *The Jewish Bride*. Previous research has shown that in the paint mixture of the background of *The Jewish Bride*, degraded pigments are also present, in addition to stable pigments. The degraded pigments are smalt, a blue pigment, and yellow lake, an organic yellow dyestuff. Both of these pigments are known to degrade and become colourless over time. High quantities of smalt are mixed with other pigments to create the colour of the background. The background is now a translucent monochrome brown. This is not the colour Rembrandt intended, and its present condition is due to the colour loss of the smalt and yellow lake.

1-4 Research goal

The aim of this thesis is to show that with a new scientifically based method, the original colour of the two pigments smalt and yellow lake can be digitally colour reconstructed in their mixture as painted by Rembrandt.
Using this method the background of *The Jewish Bride* can be digitally reconstructed. The digital colour reconstruction of *The Jewish Bride* can give an insight into how the painting might have looked at the time when Rembrandt created it.

1-4-1 Requirements for the method

For a new method to be of use, it has to meet a number of requirements:

It must have a scientific basis.
The method must be easy to use.
The method must be applicable to paint mixtures.
It should have the possibility of being extrapolated to the whole painting.
The method should also be applicable for other paintings.

The method developed in this thesis will be evaluated in the discussion, Chapter 5-1.

1-5 Previous research on *The Jewish Bride*

The Jewish Bride has been researched in the past.

In 1992 dr. Karin Groen (chemist & research technician, Rembrandt Research Project)[13] took cross-section paint samples from the painting. The aim was to distinguish the different paint layers and to identify the pigments used. These results are documented at the Rijksmuseum.
In 2011 prof. dr. Arie Wallert (chair Atelier Practice, University of Amsterdam/Rijksmuseum)[14] took cross-section paint samples. The purpose was to investigate the difference in paint materials between the hat of Isaac and a shadow area beside the pillar. These results are documented at the Rijksmuseum.
In 2012 the painting was taken up in the Science4Arts ReVisRembrandt project. Annelies van Loon (Conservation scientist, Rijksmuseum/TU Delft)[15] and Petria Noble (Head of Paintings Conservation, Rijksmuseum)[16] are both actively researching late Rembrandt paintings in this project.
In the spring of 2013 *The Jewish Bride* was scanned with Macro X-ray fluorescence (Macro-XRF). This was done in partnership between the University of Antwerp and Delft University of Technology (TU Delft). This gave insight into the paint materials used and the distribution of materials in the painting. These results were documented at the Rijksmuseum. The experimental description of this test will be given in Paragraph 2-4.
In December 2013, John Delaney, (Senior Scientist, National Gallery of Art in Washington D.C.)[17] who is also partner in the ReVisRembrandt project, scanned *The Jewish Bride* with a hyperspectral scanner in the wavelength range of 1000 nm – 2500 nm. These results are documented at the Rijksmuseum.

In 2015, Diana de Man (MA Conservation and Restoration of Paintings, University of Amsterdam)[11] made paint-outs using smalt and yellow lake based on historic recipes.[10] New paint-outs have been made for this research using the same pigments as used by Diana de Man, and are therefore are an extension of her paint-outs. Diana de Man's research was carried out for her Master thesis at the University of Amsterdam in the context of the ReVisRembrandt project.

1-6 New analyses on *The Jewish Bride*

For this thesis different analyses have been done. The experimental description of these tests will be given in Paragraph 2-4.
The existing paint cross-sections and paint cross-sections from a paint-out made for this thesis were studied under a microscope and with the SEM-EDX. By analysing the paint cross-sections through a microscope and SEM-EDX, it is possible to calculate the fraction of pigments used in the paint. In previous research, the focus was on the build-up of the paint layers and the pigments used.
In November 2016, John Delaney (Senior Scientist, National Gallery of Art in Washington D.C.)[17] scanned *The Jewish Bride* with a hyperspectral scanner in the wavelength range of 400 nm – 1000 nm. The new scan is in the visible light range and will be the basis for the digital colour reconstruction.

Chapter 2

Theory

The focus of this chapter is on the theory and analytical measuring techniques on which the digital reconstruction is based. Rembrandt's painting techniques, digital colour reconstruction, colour prediction methods, and analytical techniques will be discussed.

2-1 Rembrandt

Rembrandt van Rijn (1606-1669) was a unique painter of his era. His genius also shows in the way he experimented with painting techniques and in his manipulation of the materials that he used.[18]

2-1-1 Late painting techniques

Rembrandt worked his paintings from the bottom up. There are different stages distinguishable: the ground layer, dead colouring, second colouring/working up and final glazing and highlights.[19]

The ground layer was painted directly on the prepared canvas or panel. Its purpose was to prepare the canvas or panel for the actual painting. The late Rembrandt works used grey, grey brown, and ochre brown grounds. The grounds of the late Rembrandts are darker than those of his early work.[18]
After this step, whereas usually painters would make an under drawing, Rembrandt differed from that technique. He used the dead colouring stage to outline the main shapes and shadows. Dead paint does not have a specific colour. It is usually a monochrome colour of different shades of brown or grey paint. Rembrandt used a mixture of leftover paints from his other pallets to create the dead paint.
After the dead colouring layer, there would be the working up or second colouring. In this stage, he laid in the colours. Finally, there could be some final glazing and highlights were painted on.[18][19]

It is not only the build-up of the paint layers that is unique. Rembrandt created mixtures with different texture roughness, which he applied to give texture to the paintings. In the case of *The Jewish Bride*, this is best seen in the sleeve of Isaac. Besides the colour, the texture of the paint shows the richness of the fabric.

2-1-2 Pigments

There were only a limited number of pigments available in Rembrandt's time. Table 2-1 presents an overview of the pigments used by Rembrandt. As is stated in Table 2-1, ,

Table 2-1: Pigments used by Rembrandt and their main chemical composition

Colour	Pigment	Main chemical composition
White	Lead White	$2PbCO_3 * (OH)_2 + PbCO_3$
	Chalk	$CaCO_3$
Yellow	Lead Tin Yellow	$PbSnO_4$
	Yellow Earth	$FeO(OH)$
	Yellow Lake	Varying on the substrate
Browns	Earth pigments	Fe_2O_3
	Umber	Fe_2O_3/MnO
Red	Vermilion	HgS
	Red Earth	Fe_2O_3
	Red Lake	Varying on the substrate
Blue	Azurite	$2CuCO_3 * Cu(OH)_2$
	Smalt	$SiO_2 + K_2O + CoO$
Black	Bone Black	$Ca_3(PO_4)_2 + CaCO_3 + C$

the yellow and red lake pigments are dependent on the substrate on which the lake dye is precipitated, often alum or chalk. The main elements identified in a lake as substrate are aluminium, sulphur, calcium, and potassium.
Rembrandt used mixtures of different pigments to create colours. He sometimes used as many as six different pigments. He also manipulated the pigments by grinding them in different ways to achieve the best texture and/or colour for a certain area.[18]
In this thesis, the focus will be on the background of *The Jewish Bride*. Here five pigments have been found: bone black, red earth, smalt, yellow earth, and yellow lake. With these five pigments, Rembrandt could create a range of different colours and textures. Bone black, red earth, and yellow earth are stable, but smalt and yellow lake are unstable and degrade over time. Smalt and yellow lake will be discussed further in the next sections.

2-1-2-1 Smalt degradation

Smalt ($SiO_2 + K_2O + CoO$) is made from ground, potassium rich glass. The blue colour of the glass is created by adding cobalt to the melt. [20]
The amount of cobalt in the glass can vary, but if the pigment was used in paintings it is normally between 2 wt% and 7 wt%.[21][22] The amount of cobalt and the particle size of the pigment both influence the colour.[23][12] A higher cobalt content will create a more intense blue pigment. The particle size influences the amount of light scattered by the glass particles. If the particles are small, there will be a greater scattering effect of the light, giving them a lighter appearance, and the colour will be a less saturated blue. For larger particles, the amount of scattering will be less and they will appear darker and a more saturated blue.[12]
There are also impurities found in the smalt particles, which stem from the cobalt ore and silica source. The most common impurities are: aluminium and iron, originating from the silica; and arsenic, nickel, iron, and bismuth originating from the cobalt ore.[24] It is still not known whether and how much the impurities do influence the colour of smalt.
Smalt is an instable pigment in oil, but can be stable in a different medium. During the degradation of smalt, the pigment particles change colour. Over time, the blue pigment particles become grey and colourless. This is due to the fact that potassium leaches out of the particles. This influences the coordination of the cobalt oxide that changes from a tetrahedral into an octahedral coordination. Through this change the blue colour fades[21] What remain are glass-like particles that contain the elements silicone, cobalt and the other impurities which were present in the pigment from the beginning.
The top layer of the paint also changes due to the migration of the potassium. The potassium binds to the fatty acids in the oil and forms potassium soaps which can migrate further to the top surface. Here they form a brown curst. Also, the oil matrix itself changes colour and turns brown as a result of the formation of potassium soaps.[25][22]
The late Rembrandt used smalt extensively in the paintings, especially in mixtures.

2-1-2-2 Yellow lake degradation

Yellow lake colours are plant based and made from unripe buckthorn berries, quercitron and weld.[26] The colour is extracted from the plants by soaking them in water or an alkaline solution. The dyestuff diffuses out of the plants and can precipitate on an inert and inorganic substrate, usually alum or chalk or a combination of these two. Over time, yellow lake fades in colour, due to a photochemical proces.[25] This process is not yet understood, but the substrate on which the pigment particles precipitate and the dye source can influence the degradation process. [25] This is not investigated here.
Interestingly, it was a common practice for the 17th century Dutch painters to use yellow lake in combination with a blue pigment to achieve a plant-like green.[25][26] The green colour in those paintings was not made only with smalt, but also with azurite or ultramarine combined with yellow lake, and/or lead-tin yellow and yellow earth. The result is that the foliage in 17th century Dutch paintings may have turned blue in colour over time.

2-2 Digital colour reconstructions

In this section, digital colour space is discussed, as also selected examples of previous digital colour reconstruction.

2-2-1 Digital colour space

Colour can be represented in different colour spaces, the most common one is RGB. There are many other colour spaces, such as CIE LAB and HSV (Hue, Saturation and Value). Those are related to each other by a conversion matrix, and it is easy to switch between them. RGB is used in this thesis and therefore will be discussed here.
To see the comparison between different colour spaces, the book Principles of Colour and Appearance Measurement by Asim Kumar Roy Choudhury (2014) could be used. In volume 1 chapter 7, all the main colour spaces are discussed in depth and compared.

2-2-1-1 RGB colour space

Most of the monitors and/or images are based on the RGB colour space. RGB is based on the three additive primary colours of light: red, green, and blue. The standard values of the three components are between 0-255. This is also known as an 8-bit image. It is possible to create 16.7 million colours by combining the three different colour values of red, green, and blue.
Every RGB image is built up of 3 matrices; these are shown in Figure 2-1. On the left hand side, it shows how the image would be seen on the screen. The right hand side shows the three matrix planes, red, green and blue. For example, the red box is built up by R:255 G:0 and B:0, while the grey colour below the red box is built up from the values R:50, G:50 and B:50.

There is a downside to this colour space, namely that it is not a linear space.[3] This implies that to change colour to a lighter shade or to a darker shade, one does not follow linear steps. Also, it is impossible to add two RGB values together to create a colour mixture of both.

There is a standard routine to retrieve an RGB colour from a spectral reflectance curve. A spectral reflectance curve shows the amount of light that is scattered back from a surface. This is illustrated in Figure 2-2. First the spectral reflectance curve R(λ), will be multiplied with the D65 light, E(λ)(65), normal daylight; see panel number 1 in Figure 2-2. I. It is then multiplied with the light sensitive curves of the eye ($\bar{x}$, $\bar{y}$ and $\bar{z}$),; see panel number 2 in Figure 2-2. The area beneath the curve is calculated, which gives three values X, Y, and Z; see panel number 3 in Figure 2-2. X, Y, and Z are then converted to R, G, and B values with a matrix. The matrix used is:

$$\begin{bmatrix} R \\ G \\ B \end{bmatrix} = \begin{bmatrix} 3.2404542 & -1.5371385 & -0.4985314 \\ -0.9692660 & 1.8760108 & 0.0415560 \\ 0.0556434 & -0.2040259 & 1.0572252 \end{bmatrix} \begin{bmatrix} X \\ Y \\ Z \end{bmatrix}$$

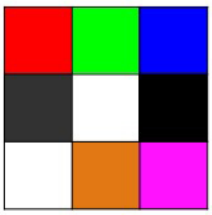

Image on screen

Matrix Red -plane

255	0	0
50	200	0
255	225	255

Matrix Green - plane

0	255	0
50	200	0
255	120	20

Matrix Blue - plane

0	0	255
50	200	0
255	20	255

Figure 2-1: How a digital image is build up in RGB
On the left hand side, it shows how the image would be seen on the screen. The right hand side shows the three matrix planes, red, green and blue. For example, the red box is built up by R:255 G:0 and B:0, while the grey colour below the red box is built up from the values R:50, G:50 and B:50.

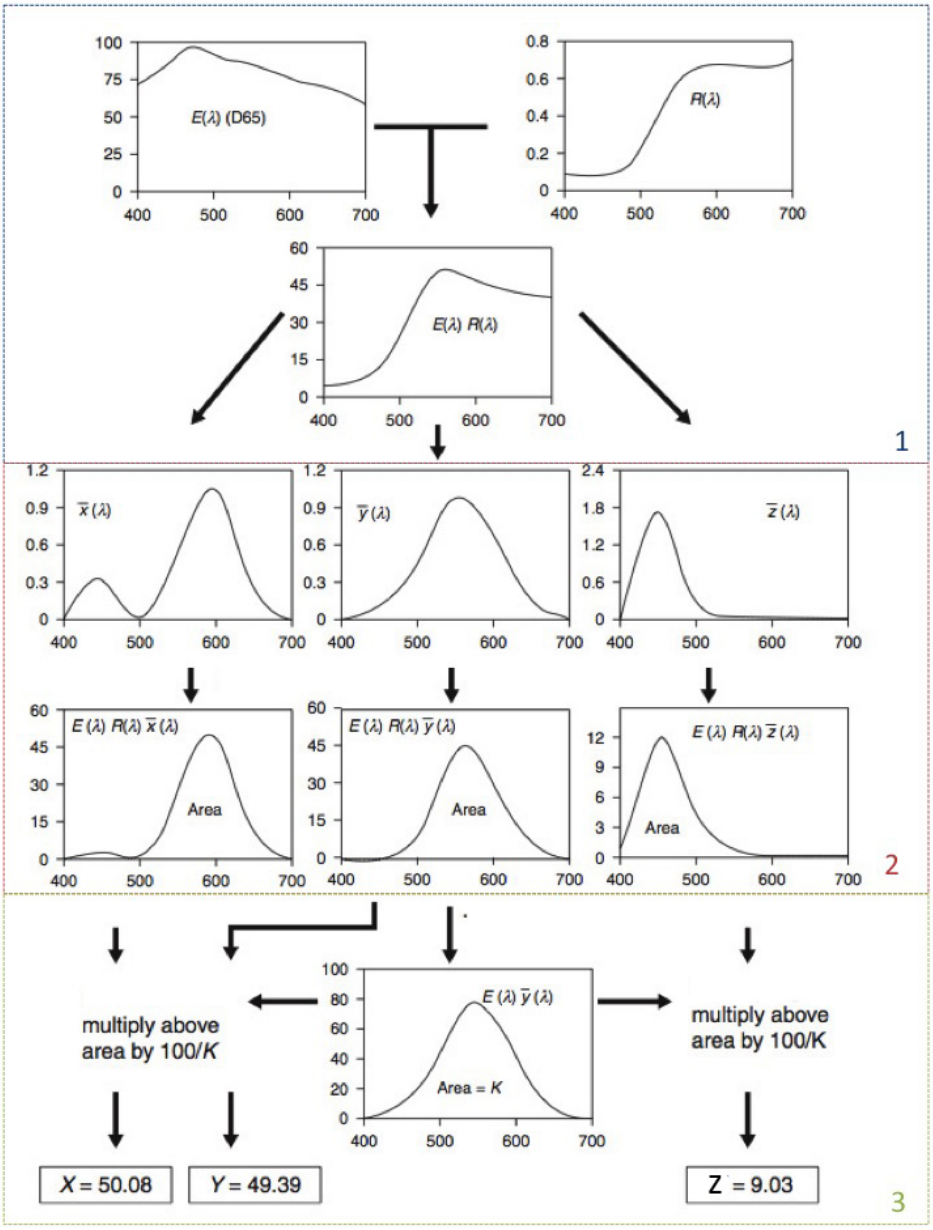

Figure 2-2: Method reflectance curve to XYZ [3]
First the spectral reflectance curve R(λ), will be multiplied with the D65 light, E(λ)(65), normal daylight; see panel number 1. I. It is then multiplied with the light sensitive curves of the eye ($\bar{x}$, $\bar{y}$ and $\bar{z}$),; see panel number 2. The area beneath the curve is calculated, which gives three values X, Y, and Z; see panel number 3. X, Y, and Z are then converted to R, G, and B values with a matrix.

2-2-2 Previous work

In this section, three paintings will be discussed in which pigment degradation has been digitally reconstructed. These are *The Conversion of the Magdalen* (1562) by Pedro Campaña (1503-1580), *The Evangelist Luke* (1622) by Hendrick ter Brugghen(1588-1629) and *The Bedroom* (1888) by Vincent van Gogh (1853-1890).

2-2-2-1 *The Conversion of the Magdalen*

Figure 2-3a shows the *The Conversion of the Magdalen* before the digital reconstruction.[27] The colour reconstruction was carried out by Clare Richardson (Conservation, Victoria and Albert Museum, London) for the National Gallery of London in 2001. The colour changes were noticed, since there is a copy of the painting that was made by Luca Longhi (1507-1580) with stable pigments; see Figure 2-3b. It this painting, *Christ preaching before the Magdalen*, the original colours are still visible, and it is clear there is a discrepancy between the two paintings.
To make this digital reconstruction, samples were taken from some of the deteriorated areas of Pedro Campaña's painting. The sample locations are the robe of Christ (the man sitting below the canopy), the brown drapery of the figure crouching in the bottom left corner, the brown drapery of the standing bearded man with the yellow robe, and a white highlight on the red cloak of the large figure at the extreme left edge.
The cross-sections gave an insight into which pigments were used and the concentration of pigments in those areas. The pigments that had deteriorated are smalt, red lake and copper containing glazes. Paint-outs were made based on those samples with non-degraded pigments. The colours of the paint-outs were measured and placed back on the deteriorated areas. The results are seen in Figure 2-3c.
The method which was used to placed the colour back in the deteriorated areas was never published. Most likely it was done with Photoshop and based on RGB values. Compared with the original painting by Pedro Campaña , it is clear that the fading of the colours has had an effect on the pictorial aspect of the painting.



(a) Pedro Campaña, *The Conversion of the Magdalen*, 1562, National Gallery, London[27]. This shows the present-day image of the painting. By comparing against a copy of the painting, see **(b)**, it shows that the blue and red in the painting has faded.



(b) Luca Longhi, *Christ preaching before the Magdalen*, Villa Borghese, Rome[27]. This shows a copy of painting, Figure 2-3a. From the comparison between the two paintings **(a)** and **(b)**, it became appeared that the blue and red had faded in the Pedro Campaña painting, see **(a)**.



(c) Reconstruction of Pedro Campaña, *The Conversion of the Magdalen* by Clare Richardson (Conservation, Victoria and Albert Museum, London) in 2001 for the National Gallery of London in 2001 [27]. In this image the blue and the red colours were digital colour reconstructed.

Figure 2-3: Three versions of *The conversion of the Magdalen*

2-2-2-2 *The Evangelist Luke*



Figure 2-4: Hendrick ter Brugghen, *The Evangelist Luke*, 1622, Museum De Waag, Deventer - Reconstruction of smalt in the cloak is shown on the left side, the right side isnot reconstructed[4].This reconstruction was carried out by Joris Dik (Antoni van Leeuwenhoek chair Materials in Art and Archaeology, TU Delft)[5] in 2002. It shows the effect of the smalt degradation and the effect on the pictorial image.

Figure 2-4 shows a partly digital reconstruction of smalt in the cloak of Luke. The left side of the cloak has been reconstructed to its original colour, while the right side shows the original image. This reconstruction was carried out by Joris Dik (Antoni van Leeuwenhoek chair Materials in Art and Archaeology, TU Delft)[5] in 2002 [4]. The reconstruction was created by looking at how the smalt was distributed in the painting. Through neutron activation autoradiography, the distribution of arsenic could be measured. The arsenic distribution could be directly linked to the distribution of smalt, since arsenic is one of the main impurities in smalt. The RGB value was taken from non-degraded smalt and the saturation level was changed according to the distribution level. Through this method the details of the folds are still clear. The only disadvantage is that the RGB colour space is non-linear, and therefore it cannot be used when the colour is in a mixture. Nevertheless, it provides a representation of what the image could look like and how much it might have changed over time.[4]

2-2-2-3 *The Bedroom*



Figure 2-5: Van Gogh, *The Bedroom*, 1888, Van Gogh Museum, Amsterdam - On the left side original painting and on the right side the reconstruction done by prof.dr. Roy Berns (Richard S. Hunter chair Color Science, Rochester Institute Of Technology) in 2016 [6]. There were two red lakes reconstructed eosin and cochineal, especially on the wall this had a great effect. In the present-day they appear blue, while in the digital reconstruction they became purple.

Figure 2-5 shows the painting before and after the reconstruction. This reconstruction was conducted by Roy Berns (Richard S. Hunter chair Color Science, Rochester Institute Of Technology) in 2016. Here two red pigments have faded: eosin and cochineal lake. The art institute have provided 8 areas of interest where there used to be eosin and cochineal. It is not stated how the art institute achieved this data, most likely through cross-section paint samples analysis. The areas and lake used are shown in Table 2-2. It is stated that

Table 2-2: Image areas of Figure 2-5 and lake used on those locations

Image Area	Lake used
Landscape Sky	Eosin
Dark Brown Floor	Eosin
Overall Brown	Eosin
Green Floor	Eosin
Blue Doors	Cochineal
Left Gray Door	50% Eosin and 50% Cochineal
Right Gray Door	67% Eosin and 33% Cochineal
Blue Wall	Cochineal
Gray Wall	50% Eosin and 50% Cochineal

the distribution of the lake pigment is homogeneous for that particular area. Through the Kubelka-Munk theory (this theory will be discussed in the next section), a concentration of these pigments is added back in the painting per area. Through this the painting has changed in appearance drastically, the walls are purple instead of blue and the floor more red. Also, the green patch beneath the left chair turned the same colour as the rest of the floor. [28]

This method can be used for paint mixtures and shows clearly the difference between the original image and the digital colour reconstruction.

2-2-2-4 Requirements for a digital reconstruction

As stated that in the introduction, there are certain requirements were the method is tested against:
It must have a scientific basis.
The method must be easy to use.
The method must be applicable to paint mixtures.
It should have the possibility of being extrapolated to the whole painting.
The method should also be applicable for other paintings.

When evaluating *The Conversion of the Magdalen*, it is unsure how the reconstruction was done, most likely by adding back the colour based on the paint-outs through Photoshop. Since this is done via RGB values, it is not compliant with paint mixtures. Although this method gives a fast and easy indication of what a painting might have looked like, the method is not suitable for *The Jewish Bride*, since pigment mixtures are used in the background.
The reconstruction of *The Evangelist Luke* Luke is also based on the RGB colour space, although the distribution of arsenic in the painting is used as a guideline, which gives a more accurate account of the smalt distribution. On the whole, it gives a clear representation, but is also not suitable for *The Jewish Bride* for the same reason as stated above.
The Bedroom reconstruction does takes paint mixtures into account, although the pigments are set to be homogeneously distributed for a certain area. Previous research of *The Jewish Bride* has shown that the distribution of the pigments is not homogeneously spread in the background. Therefore, this method cannot be used for *The Jewish Bride*.

To digitally colour reconstruct *The Jewish Bride*, a new method must be developed. In that method the idea of using the distribution of an element and linking it to a pigment concentration, as is done in *The Evangelist Luke*, should be used.. Also, the method of using the aspect of the digital colour reconstruction of*The Bedroom* , where pigment mixtures are taken into account, is needed. By combining these two methods, it is possible to digitally colour reconstruct the complex paint mixtures made by Rembrandt.

2-3 Colour prediction methods

Before the 19th century, the only method to match colour or predict a colour recipe was through trial and error. Today there are different methods that can be used to predict a colour.
First the physical part of colours will be discussed followed by the different colour prediction methods.

2-3-1 Physical background of colour appearance

Visible light has the wavelengths between 380 nm and 750 nm. A wavelength consists of a large amount of photon particles, all having the same amount of energy. Table 2-3, shows the connection between wavelengths and colours.
When light falls on a surface it interacts with it. The main interactions with pigment parti-

Table 2-3: Colour and wavelength [12]

Colour	Wavelength
Violet	380-450 nm
Blue	450-480 nm
Blue-green	480-510 nm
Green	510-550 nm
Yellow-green	550-570 nm
Yellow	570-590 nm
Orange	590-630 nm
Red	630-750 nm

cles can be seen in Figure 2-6.
When a wavelength hits the object, part of that wavelength can be reflected from the surface

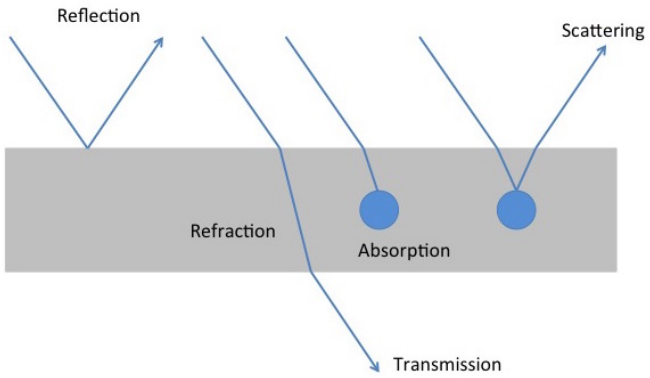

Figure 2-6: Different visible light interactions with an object.

without interaction. This creates the texture and the gloss of a surface, see Figure 2-6. When

a wavelength penetrates the surface the angle changes. This is called refraction; see Figure 2-6. This is due to the difference in index of refraction between two mediums, in this case that of air and substrate.
If the wavelength goes through the substrate without interacting with pigment particles (indicated as a blue circle in Figure 2-6), it is called transmission. The lack of interaction between a wavelength and pigment particles influences transparency of the substrate. If there is more transmission it is more transparent and less transmission makes the substrate more opaque. The colour appears when certain wavelengths are absorbed, and others are scattered. The scattered wavelengths create the colour. For instance, if only the blue wavelength is scattered and the rest are absorbed, the substrate appears blue. The scattered light can go in many directions, not necessarily straight back towards the surface. It can scatter in every direction depending on the angle of the pigment particle, Figure2-6 only show the light being scattered in one direction, which is a simplification. The incoming and outgoing light can be measured by visible light spectroscopic technique. This can be plotted in a spectral curve, such as in Figure 2-7.Here D65, standard sunlight, is plotted. It can be seen that it is not a straight horizontal line, but that there is a difference in the relative amount of power per wavelength.
Reflectance imaging spectroscopy (RIS) can also be used to define the colour of a substrate.

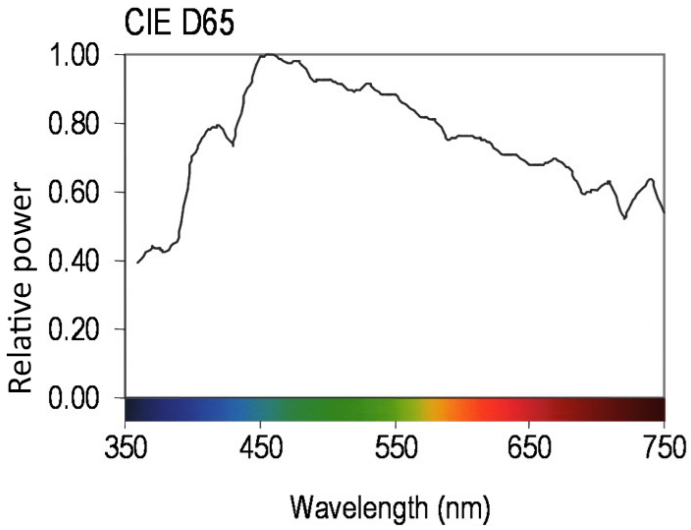

Figure 2-7: Spectral curve of D65 (sun light) [7]. It shows that the relative power per wavelength differs.

It measures how much of a wavelength is reflected back by scattering and reflections. This is called the spectral reflection or the reflectance curve. The reflectance curve is only based on the light that has interacted with the substrate. The reflection from the top of the surface should be corrected for.

To get a more in-depth view, the two volumes of Principles of Colour Appearance and Measurement by Asim Kumar Roy Choudhury (2014) can be used, as they touch upon all aspects of colour appearance and different measurement techniques and different aspects of colour perception.

2-3-1-1 Paint

Paint is a mixture of pigment particles and binder. A pigment is a fine powder of an organic or inorganic material. The binder is used to disperse the pigment particles and to spread the pigment evenly on the surface. When the binder dries it becomes a stable paint film, which traps the pigment particles. Drying oils can be used as a binder. They create a film that is durable and water-resistant. Rembrandt used linseed oil as binder. Also, a diluent could be used. This is a liquid that makes it easier to spread out the paint mixture made out of pigment particles and binder. In the case of oil, turpentine or petroleum could be used. [29]
A common paint layer creates colour as is seen in Figure 2-8. Here white light goes through the surface and interacts with the pigment particles. In the yellow particles all the light except yellow light is absorbed, and the same goes for the blue pigment particles where only the blue light is not absorbed. The yellow light is scattered by the yellow pigments and the blue light is scattered by blue pigments. Out of the surface comes blue and yellow light, and together it creates a green colour.
A different way of mixing colour is by applying a transparent layer of paint on top of an opaque layer of paint; see Figure 2-9. The transparent layer scatters some of the yellow light back towards the surface, while part of the incoming white light goes through the transparent layer without interaction. This light reacts with the blue opaque layer after scattering the blue light towards the surface without interacting with the transparent yellow layer. The two coloured lights, blue and yellow, are mixed into green.

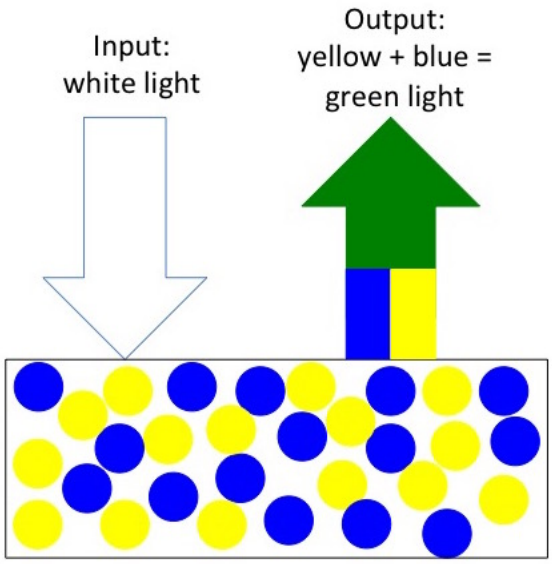

Figure 2-8: Colour from a paint layer
Here white light goes through the surface and interacts with the pigment particles. In the yellow particles all the light except yellow light is absorbed, and the same goes for the blue pigment particles where only the blue light is not absorbed. The yellow light is scattered by the yellow pigments and the blue light is scattered by blue pigments. Out of the surface comes blue and yellow light, and together it creates a green colour.

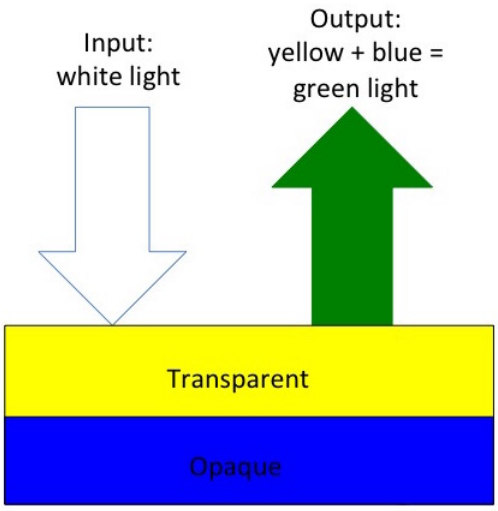

Figure 2-9: Colour from a transparent layer on top of a opaque layer
The transparent layer scatters some of the yellow light back towards the surface, while part of the incoming white light goes through the transparent layer without interaction. This light reacts with the blue opaque layer after scattering the blue light towards the surface without interacting with the transparent yellow layer. The two coloured lights, blue and yellow, are mixed into green.

The amount of scattering depends on the difference between the refractive indices of the pigment itself and the binder. If these are close together, there will be less scattering. This will enhance the transparency of the pigment.
The amount of absorption is different per pigment per wavelength, also affects the transparency. For instance, ultramarine and smalt, both blue pigments, have roughly the same refraction index, but ultramarine absorps more of the light. Therefore, ultramarine has a higher hiding power and is more opaque than smalt. [8] [30] Besides the amount of absorption being dependent on the pigment particles, it also depends on the density of those pigments in the binder. If the pigment concentration is very high compared to binder, the amount of absorption is increased and the pigment will be more opaque.
As stated before, Rembrandt used mixtures of colours. The pigment used could differ from opaque to transparent. Also, he tended to build up his paintings using different layers on top of each other. This is the main reason why it is very difficult to accurately digitally colour reconstruct Rembrandt.

2-3-1-2 Other aspects involved in appearance of paint

Although colour plays an important part in the appearance attributed, it cannot predict appearance exclusively, as other factors are also involved. For instance, surface texture plays a role in the appearance of an object. The surface can be smooth, glossy, matt, or rough. Each surface gives a different colour. Rough texture for example will show two colour tones. The raised areas will be lighter while the depressed surface will become darker. By using a varnish, the surface can become smoother and more reflective. Hereby the appearance of an

object changes.
The scattering of pigment particles changes when they are mixed in with oil. The oil decreases the amount of scattering, and thus the pigment oil mixture is darker than the dry pigment. [8]
The opacity and transparency of a paint layer is an important appearance attribute. The opacity and transparency can be influenced by the thickness of the layer, the amount of pigment particles and the amount of scattering of light by pigment particles, and the difference between the refractive indices of and the refractive index between the binding medium and the pigment particles.
A change in the size of the pigment particles will influence the scattering of light. This can be seen in the Hunter experiment. Here pebbles of the same colour are used with decreasing size. The light scatters more on the smaller pebbles, which therefore appear lighter of colour.[8]
A colour can also be influenced by the colour surrounding it, see Figure 2-11. For instance,

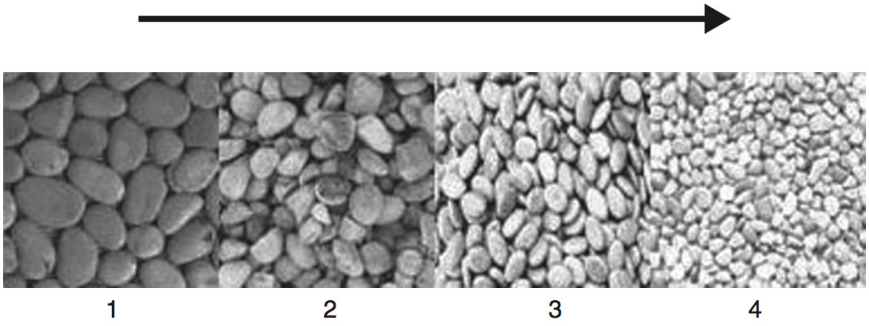

Figure 2-10: Hunter's experiment[8]. Here pebbles of the same colour are used with decreasing size. The light scatters more on the smaller pebbles, which therefore appear lighter of colour.

inside the white and black box all the colours appear the same grey tone, while placed side by side, they are actually a different colour. This phenomenon is called simultaneous colour contrast. The reason that the colours inside the coloured appear the same, while in fact they are different, is that our eyes cannot see colour in isolation. The colour our eyes register is influenced by the colours surrounding it. [8]
These are only a few aspects that influence the appearance of a substrate. The digital colour reconstruction will be a simplification of the reality and will only focus on the colour.

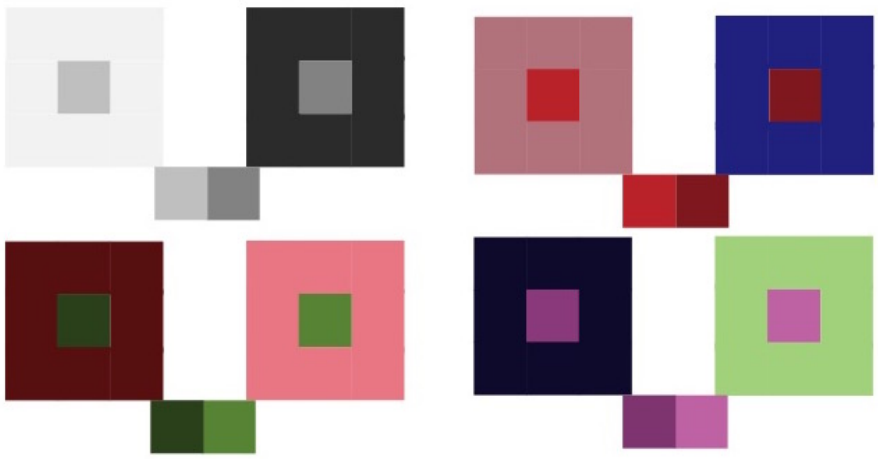

Figure 2-11: Simultaneous colour contrast
Colours can appear the same due to the colour surrounding them, while when placed side by side they differ. For instance, inside the white and black box the grey colour appear the same grey tone, while placed side by side, they are actually a different colour.

2-3-2 Colour prediction methods

To digital colour reconstruct the background of *The Jewish Bride*, a suitable colour prediction method is needed. There are different methods to digitally predict the colour of a surface. Four main methods of them will be discussed here.

2-3-2-1 Kubelka-Munk Theory

The Kubelka-Munk Theory is one of the most used theories on paint colour prediction.[31] [3] This colour prediction method is used in this thesis for the digital colour reconstruction. It is a very simplified method, as it takes into account only the light that comes in and out perpendicular to the surface and only focuses on the scattering and absorption properties per wavelength of a certain pigment. Spectral reflectance per wavelength, R, is translated into K for absorption and S for scattering.[32] This is done via the equation 2-1. To translate K/S to R, equation 2-2 is used.

$$\frac{K}{S} = \frac{(1-R)^2}{2R} \tag{2-1}$$

$$R = 1 + \frac{K}{S} - [(1+\frac{K}{S})^2 - 1]^{\frac{1}{2}} \tag{2-2}$$

Through thetranslation into K/S values, it is possible to add different K/S values in different concentration to achieve the K/S value of a mixture. This can be seen in equation 2-3.

$$(\frac{K}{S})_m = C_1(\frac{K_1}{S_1}) + C_2(\frac{K_2}{S_2}) + ... + C_n(\frac{K_n}{S_n}) \tag{2-3}$$

where m stands for mixture and C for the concentration of different pigments. For this equation the input should be the relative reflectance per wavelength or the K/S of the pigment. The output is the concentration of pigments, spectral curve of one of the pigment or the spectacular curve of a mixture. Since particle size influences the colour, it also influences the spectral reflection curve. Therefore it creates a different K/S value.
The limitation of the Kubelka-Munk Theory is that when working with transparent layers an extension of the theory is needed. The same goes for fluorescent pigments. The main advantage is that it is a simple equation. It is easy to add and subtract pigments from a mixture.
For more information two works are recommended. The first is by Ruth Johnston-Feller, Color Science in the Examination of Museum Objects: Nondestructive procedures (2001) published by the Getty museum. In chapter 4 the theory is discussed and how it can be used for museum objects.[24] For a better understanding of the theory, the book Colour Physics for Industry edited by Roderick McDonald could be used. In chapter 6 "colour-match prediction for pigmented materials" (1997) by James H Nobbs, the basis of this theory is explained.

2-3-2-2 Beer-Bouguer theory

The Beer-Bouguer theory works for transparent material, which can either be liquid or solid. The equation relates the transmitted radiant energy to the thickness and the absorption of

the material. In an extension of the theory, different absorbed components can be taken into account, and therefore their concentration is needed as well. The theory works per wavelength.

$$log(\frac{I_0}{I}) = X_1C_1A_1 + X_2C_2A_2 + ... \tag{2-4}$$

where I_0 is the incoming intensity, I is the outgoing intensity, X is the thickness, C is the concentration and A is the specific absorption per pigment.
The input for this is a certain wavelength, the specific absorption and concentrations. The outcome will be the amount of intensity left after passing through.
The limitation of the Beer-Bouguer theory is that it only works for transparent layers. Also, many factors can influence the outcome, such as solvent, pH and temperature. The main advantage is that it works very well on transparent layers, which are difficult to analyse with other theories. [32]
The above-mentioned book by Ruth Johnston-Feller provides a good insight into this theory.

2-3-2-3 Monte Carlo simulation

The Monte Carlo theory can be applied to get a deep understanding about how photons move in / interact with the substrate, as well as their reflection and transmission. This is used to understand, e.g., the working of sun screen. It is programmed to launch photons on the substrate and monitors their random walks through the substrate. There are many parameters needed to make the theory valid, among others the concentration of pigments, particle size, absorption coefficient, and inter particle scattering refractive index. As output, one can get a detailed understanding of how photons travel through the substrate.
The main limitation of the Monte Carlo theory is that exact knowledge is needed of all the parameters, as otherwise the output cannot be trusted. Much iteration is needed to get a reliable outcome, since not wavelengths but photons are the input. When the concentrations are different or for different particle sizes a new program and iteration must be done. Besides, it is mathematically challenging to program a complex paint substrate. The advantage of this theory is that it provides a detailed understanding of a complex substrate. [33]

2-3-2-4 Artificial Neural Networks

Artificial Neural Networks (ANNs) are one of the newest methods for colour prediction. Kubelka-Munk state that colour behaves linear, while in reality it might behave non-linear. ANNs, like the human brain, can learn by themselves. By giving them a sample set of input and output data, they can learn the non-linear relationship between those.[34][3] Through this relationship ANNs can make colour predictions and calculate colour concentrations.
The limitation is that the method is still developing and does not consistently give better results than the Kubelka-Munk theory.[3] The key advantage is that ANNs can be used on different substrates such as paper and fibres and complex paints.

2-3-2-5 Comparing Theories

Table 2-4 shows all the theories with their advantages and limitations. The goal of this thesis is to achieve an easy method for digitally reconstructing the background of *The Jewish*

Table 2-4: Overview of the Theories with there Advantages and Limitations

Theory	Advantages	Limitations
Kubelka-Munk	Based on paint and easy to use	Simplification of reality
Beer-Bouger	Works on transparent material	Many factors influence the outcome
Monte Carlo Simulation	Detailed understanding of photon interaction in the material	Exact knowledge needed for many parameters mathematically challenging
Artifical Neural Networks	Colour prediction for difficult substrates	Still developing

Bride, which contains a pigment mixture. Monte Carlo simulation and using Artificial Neural Networks do not apply for this instance.And as the theory must be used on paint, therefore the Beer-Bouguer theory cannot be used.
That leads towards the Kubelka-Munk theory, which is widely used for paint mixtures and is an easy-to-use theory.

2-4 Analytical techniques

Different methods are used for pigment identification and colour measurements. In this section, an overview is given of the different methods and how they are used. For this research four different imaging techniques have been used. Light microscopy, SEM-EDX, macro-XRF and hyperspectral imaging. They can be subdivided into micro and macro techniques. The micro techniques focus on small cross-sections of paint taken from a painting or a paint mock-up. The macro techniques can be used on areas of a painting or on the whole painting. Also, these techniques are non-invasive and non-destructive, as they do not require cross-section paint samples. For all data analysis MATLAB with the extension of *Image Processing and Computer Vision* is used.[35].

2-4-1 Micro analytical techniques

This section focuses on the micro analytical techniques, which are light microscopy and SEM-EDX.

2-4-1-1 Light microscopy

Light microscopes can be used to examine cross-sections of a painting. There are three different lighting conditions; bright field, dark field, and UV fluorescence.
The main reason for looking through a microscope is to see the layers of paints (stratigraphy). This gives an insight into how the painter built up his painting. It is also used to identify the

pigments used and to see the pigment distribution through the layers and size of the particles. In the case of the cross-section samples of *The Jewish Bride*, the UV lighting shows the layers best and the smalt particles. When using dark field or bright field the other coloured pigments, especially red earth, become better visible. Dark field tends to give the best contrast. The input for this measuring technique are six paint samples from *The Jewish Bride* taken in 1992 and 2011, as well as samples from paint mock-ups/reconstructions. Images can be taken with the microscope in RGB values (8-bit). By selecting the RGB values of a pigment, they can be filtered out. The amount of pigment in the sample can then be calculated. Limitations occur when the colours differ between two pigments or the binder is very small and therefore they have similar RGB values. In that case they cannot be filtered out with sufficient precision.

2-4-1-1-1 Experimental details on the light microscopy The embedded paint cross-sections were viewed under different lighting settings; Brightfield (BF) and Darkfield (DF) for visible light and ultraviolet radiation (UV 365 nm). In the DF setting the samples were saturated using Shellsol T. The visible light source is an LED lamp with the colour temperature of 5600 Kelvin. The UV light source is a colibiri.2 controller with LEDs in the wavelengths of 365 nm, 420 nm and 470 nm. The microscope used is Zeiss AXIO Imager.A2m (Carl Zeiss Microscopy, LLC, United States). All the images were recorded using the Axio Cam MRc5, which is mounted on top of the microscope. The camera captures 5 megapixel 12-bit images. Different magnifications can be used ranging from 25 - 1000 x. The images were obtained and processed using Zen 2 pro (blue edition) software, which also transforms the 12-bit images into 8-bit.
All the images of the cross-sections taken followed the protocol of the Paint Sample Database, which is developed at the Rijksmuseum.

2-4-1-2 SEM-EDX

SEM-EDX is an abbreviation for scanning electron microscopy - energy-dispersive X-ray spectroscopy. By using electrons instead of light, a higher depth of focus can be reached. This means that even if the surface is very rough, it appears to be all in focus. By using electrons, an SEM can produce backscattered electron images, which are in grey tones. Since heavier elements backscatter electrons better, they appear lighter in the image and vice versa for lighter elements. Also, the backscattered electron image can show difference in mixtures of elements. Besides imaging the surface, it can map the elements concentration of a small sample spot or the distribution of an element over the whole cross section. The different elements can be linked with different pigments. The input for this measuring technique are five paint samples from *The Jewish Bride* taken in 1992 and 2011, and a paint sample of the paint mock-up/reconstruction. For this thesis, the backscattered images and elemental maps are used. In the elemental map, the brightness of the coloured image indicates whether there is more or less of that element present. The limiting factor here is that some elements are not specific for one pigment, or the signal is too weak to make a correct estimation.

2-4-1-2-1 Experimental details on SEM-EDX The embedded cross-sections were analysed using the SEM-EDX at the FOM Institute AMOLF in Amsterdam. SEM-EDX is a FEI Verios 460 high-pressure electron microscope with an Oxford EDX system. The EDX spot analysis

was performed with a 20kV acceleration voltage and a 0.20 nA beam current. To improve the conductivity of the samples they were coated with gold (3 nm). This is done by SC7640 sputter coater (Quorum Technologies, Newhaven, East Sussex, UK). The experiments were performed by Annelies van Loon (Conservation scientist, Rijksmuseum/TU Delft) [15].

2-4-2 Macro analytical techniques

In this section, macro-XRF and hyperspectral imaging technique are discussed.

2-4-2-1 Macro-XRF

Marco-XRF is an abbreviation for macro-X-ray fluorescence imaging. It is a non-invasive and non-destructive technique. This is a recent technique developed through a collaboration between the University of Antwerp and the Delft University of Technology. The Macro-XRF scanner is a Bruker M6 Jetstream. The scanner is placed on a mobile stage. It scans an area of 80 cm by 60 cm. This is done line by line and pixel by pixel. Paintings of larger dimensions need to be scanned in sections that are than assembled/stitched together, which is the case with the *The Jewish Bride*. The macro-XRF sends out X-rays. Those X-rays can eject an electron close to the core of an atom. When the hole is filled by an electron of an outer orbital, an X-ray (XRF) that is specific for that element is sent out; see Figure 2-12.
The XRF cannot detect every element, only if the atom number of an element is high enough

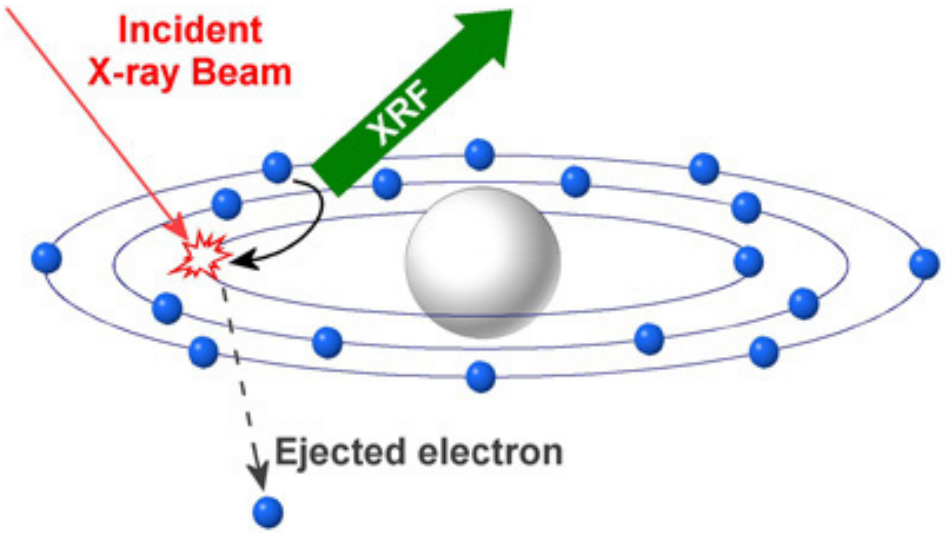

Figure 2-12: Working principle of XRF [9]
X-rays can eject an electron close to the core of an atom. When the hole is filled by an electron of an outer orbital, an X-ray (XRF) that is specific for that element is sent out.

can it be detected. In the case of *The Jewish Bride*, the lowest atom number that is detected is 19, potassium. Argon, 18, is also detected, but that came out of the air. Sometimes even phosphorus, atom number 15, can be detected if it is present in high quantities on the top surface of a painting. Phosphorus can indicate the presence of bone black. Light elements can

only be seen when they are present in the top layer of the painting, while heavier elements can be seen throughout the paint layers. The data is made manageable by plotting one element in grey tones. The lighter pixels show where there is a large amount of that element present and vice versa. The limitation of this technique is that it does not give stratigraphic information as to the layer in which the pigments are present. The X-ray signal from an element can come from the top layer as well as from the ground layer. Additional cross-section analyses can be helpful here to determine in which layer the pigment is present. In addition it is also possible to scan the back of the painting, which can also give extra information of the stratigraphic of the layers. The backside of *The Jewish Bride* is not scanned. The image created only gives relative proportions of the elements present. It shows where there is an element present, but not the particular amount of that element. The scanning time can be an issue, as it may take several days, which means that the painting cannot be on display during the period.

2-4-2-1-1 Experimental details on Macro-XRF Macro X-Ray Fluorescence (XRF) scanning has been done on *The Jewish Bride* in 2013 in the honour gallery before the opening of the new Rijksmuseum. The scanning was executed by Geert van der Snickt (Cultural heritage scientist, University of Antwerp), Anna Krekelaar (Paintings conservator, Rijksmuseum) and Lisette Vos (Paintings conservator, Rijksmuseum).
The X-ray tube is a 50 W molybdenum with a fixed polycapillary lens and four energy dispersive X-ray detectors mounted on an XZ-motor stage. [36] The dwell tie for *The Jewish Bride* was 70 ms and the pixel size 0.950 mm. Four scans were stitched together to form in total 1625 x 1199 pixel. The acquired spectra were processed by the Datamuncher software, PyMCA and other in-house software. [36] The elements that were detected in *The Jewish Bride* are: lead, calcium, mercury, arsenic, nickel, bismuth, iron, manganese, copper, potassium, tin, chrome, barium, zinc, cobalt, and titanium. As stated before, the data was made manageable by transforming it into grey scale images (8-bit).

2-4-2-2 Hyperspectral imaging

Hyperspectral imaging shows the spectral reflection of a spot/area or whole painting. This can be used for pigment identification or to create a digital colour. It is a non-invasive and non-destructive technique.
For this thesis only the range of 400 nm to 1000 nm is investigated. Below 400 nm there will be varnish interference. [37]
Hyperspectral imaging plots the amount of light reflected against the wavelengths. The reflected light values can range between 0-1. 0 means that all the light is absorbed, while 1 shows that all the light is reflected. An example of how different colours have different spectral reflection curves can be seen in Figure 2-13. Each box has its own colour; white, black, red, or green. Looking at the spectral reflection of the coloured boxes, it shows that in the case of white all the light is reflected back, with the line very close to 1, while for black almost all of the light is absorbed. The line is around 0.005. Comparing the red and green spectral reflection shows that red colour reflection is increasing to 0.2 around 600 nm which are the wavelengths that are considered to have a red colour. The green colour reflection is increasing to 0.2 around 530 nm, so that those wavelengths have a greenish colour.
The limitation is that the technique works only with different use of lighting. This is because there is specular reflection. This contains no colour information and influences the outcome

and affects with the precious of the measurement.
The main limitation is that of the data itself. The data volume after a scanning is very large and fast computers are needed to analyse the data. [37]

2-4-2-2-1 Experimental details on hyperspectral imaging The hyperspectral imaging was done using a Visible Near Infrared (VNIR) whiskbroom scanning hyperspectral camera (surface Optics Company, USA). The scanning was executed by John Delaney (Senior Scientist, National Gallery of Art in Washington D.C.)[17]. The spectral range was from 400 to 1000 nm, in steps of 2.54 nm. The scans are 1024 pixels by 1024 pixels. The incoming light goes through a vertical slit, where after going trough a transmission grating spectrometer. This were the light is split into the different wavelength This was recorded by an Electron Multiplying Charge Coupled Device (EM-CCD, EMV-VGA, Illunis). The whiskbroom scan mirror goes into step to scan, line by line. The scan data was corrected for dark offset and aligned with software. The image processing was done using ENVI 5 (Exelis, USA) and Matlab (2016a, MathWorks, MA).

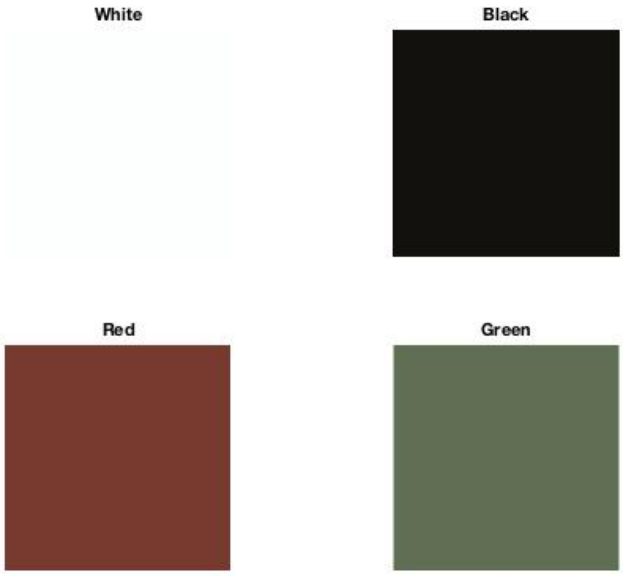

(a) Colours in RGB
These RGB values are created from the hyperspectral

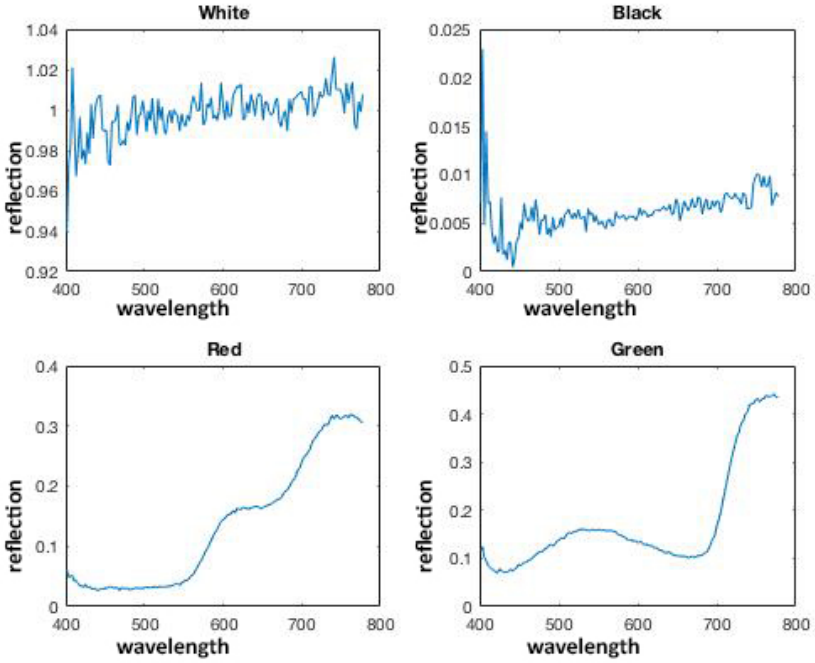

(b) Colours in RGB and spectral reflection plots
It shows that in the case of white all the light is reflected back, with the line very close to 1, while for black almost all of the light is absorbed. The line is around 0.005. Comparing the red and green spectral reflection shows that red colour reflection is increasing to 0.2 around 600 nm which are the wavelengths that are considered to have a red colour. The green colour reflection is increasing to 0.2 around 530 nm, so that those wavelengths have a greenish colour.

Figure 2-13: Different Representation of Colours

2-4-3 Combination of outputs of measuring techniques

Table 2-5: Overview of the Theories with their advantages and limitations

Analytical Technique	Advantages	Limitations
Microscopy	Shows stratigraphy and pigment distribution/size	Paint cross-section needed and colour not pigment specific
SEM-EDX	Can be used on rough surfaces and shows elemental concentration of spot/area	Paint cross-section needed and elements not pigment specific
XRF	non-invasive and non-destructive and shows element distribution for an area	Not all elements detected and some elements not pigment specific
Hyperspectral Imaging	non-invasive and non-destructive and measures reflectance/colour	Specular reflection and large amount of data storage needed

Table 2-5 shows the different analytical techniques and their main advantages and limitations. The key difference is that for the micro techniques cross-sections are needed and that only a very small percentage of the painting can be investigated. The limitation of the macro techniques is that no stratigraphic information is given. Therefore, there is uncertainty as to which depth the measured element/colour originates from. By combining the micro and macro techniques, the data from micro techniques can be extrapolated using the macro analytical data. By integrating the outcomes of the micro and macro analytical techniques, they can complement each other.
Microscopy and SEM-EDX can also benefit from each other, especially for pigment analysis, distribution, and concentration. By combining Macro-XRF and hyperspectral imaging, better pigment identification can take place. Where Macro-XRF uses elements for pigment identification, hyperspectral imaging uses colour. For instance, for red earth and yellow earth the distinctions cannot be made with Macro-XRF, since they both have the same main element iron, but it is possible to separate them using hyperspectral imaging.

2-5 Conclusion

Rembrandt used complex mixtures of bone black, red earth, smalt, yellow earth, and yellow lake in the background of *The Jewish Bride*. Smalt and yellow lake are unstable and change colour over time.
The digital reconstruction focus must be on the paint mixtures as well as on the distribution/concentration of the pigments per location. By combining two previous digital colour reconstruction approaches, this can be realised.
The colour prediction method will be Kubelka-Munk theory, which uses spectral reflection as input, which can be given by hyperspectral imaging.
The analytical techniques used can be subdivided as micro and macro techniques. The micro techniques, microscopy and SEM-EDX, use paint cross-sections, whereas the macro techniques, XRF and hyperspectral, are non-invasive and non-destructive. When the macro and the micro analytical techniques are combined, they provide a greater insight into the pigment distribution/concentration in the painting.

Chapter 3

Method

In this chapter, the method for digital colour reconstruction will be discussed. There are 4 different routes proposed, named A, B, C, and D. These are walked through simultaneously. This can be seen in the overview of methods in figure 3-1. The different routes A, B, C, and D are boxed and lettered. The outcomes of routes A, B, C, and D are used in the new routes named E 1-4, as shown in figure 3-2. Section E 1-4 will focus on the digital colour reconstruction. Each section of A, B, C, D, and E 1-4 will be discussed individually.

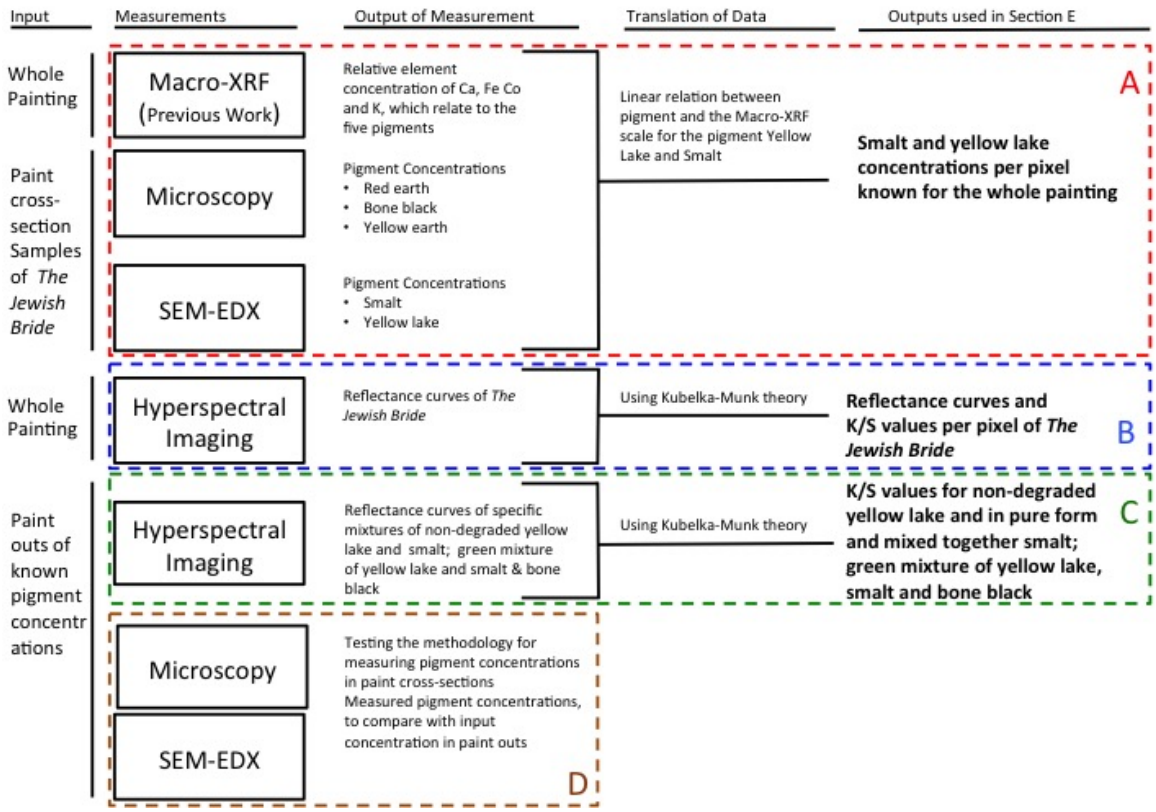

Figure 3-1: Method sections A, B, C, and D
Section A Paragraph 4-1 page 44
Section B Paragraph 4-2 page 78
Section C Paragraph 4-3 page 83
Section D Paragraph 4-4 page 94

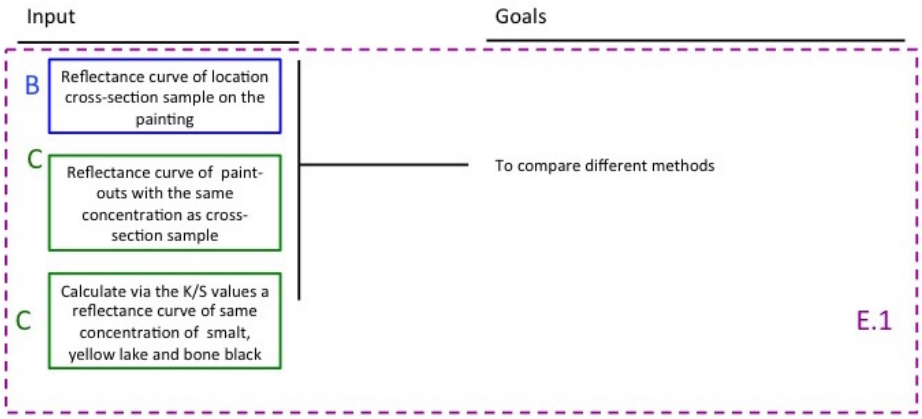

(a) Section E.1

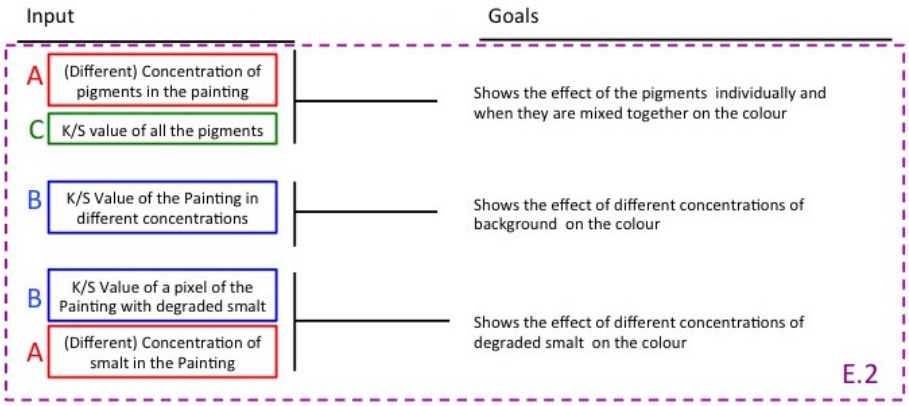

(b) Section E.2

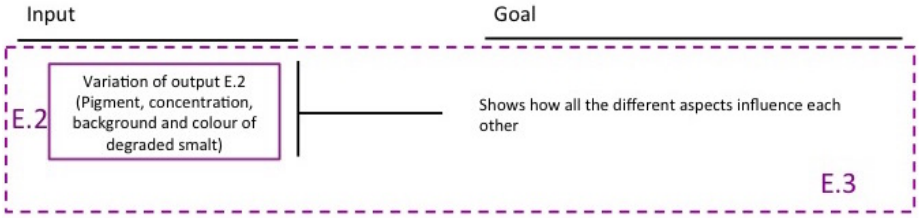

(c) Section E.3

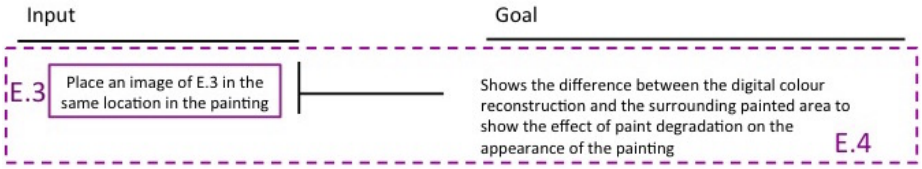

(d) Section E.4

Figure 3-2: Section E
Section E Paragraph 4-5 page 98
Section E.1 Paragraph 4-5-2 page 101, Section E.2 Paragraph 4-5-3 page 105, Section E.3 Paragraph 4-5-4 page 111, Section E.4 Paragraph 4-5-5 page 115

3-1 Section A

For method A, Paragraph 4-1 page 44, the input is the previous measurement of the Macro-XRF of *The Jewish Bride* and 5 existing cross-section samples taken from the background of the painting in early research. The limitation of Macro-XRF is that it does not provide any insight into the actual concentration of pigment, but only offers a relative scale for the element distribution by linking the grey value of the sample spots with the pigment concentrations of those sample spots. Therefore it is possible to quantify the Macro-XRF data, as there is a linear link between pigment concentration and the Macro-XRF value.

3-1-1 Macro-XRF

Originally, the Macro-XRF data received is in grey scale RGB values (8-bit). In the image, the highest amount of a certain element is indicated with a white pixel and the lowest amount with a black pixel. Since the images are in grey scale, they can be translated into values between 0-1 with 1 being the highest and white. This is done without losing information. There are 4 element maps that provide the pigment concentration in the background. Calcium for bone black, iron for red and yellow earth, potassium for yellow lake and cobalt for smalt. Calcium can also indicate the presence of yellow lake and potassium is also linked to smalt. This should be taken into consideration when analysing these maps.

3-1-2 Pigment concentrations calculated from cross-sections of *The Jewish Bride*

The cross-section samples of *The Jewish Bride* were used to calculate the pigment concentration of the top layers. This was done by examining the cross-sections under the microscope and analysing them with SEM-EDX. Through the examination, it was possible to identify and show the distribution of the five pigments, bone black, red earth, smalt, yellow earth and yellow lake.
The microscopic, backscattered electron images and the elemental maps were linked together. So they all portrayed the same area of the sample, also the images have the same dimension and pixel size.
The pigment concentrations of bone black, red earth and yellow earth were calculated from the microscope images. Their concentrations (vol%) were measured by using the pigments' RGB values. By selecting a range around the pigment RGB values, the pigments could be filtered out. After that it was possible to calculate the concentration of the pigment in the sample. Elemental maps were not used, since the calcium maps, which indicate bone black, were too noisy to make a clear calculation. Red earth and yellow earth both contain iron as the main component. Therefore, it is impossible to make a distinction between the two pigments solely based on their main element.
Smalt and yellow lake concentrations were measured using the elemental maps. These two pigments have degraded, and are no longer clearly distinguishable under the microscope. The main elements however still remain in the sample, and can be seen in the elemental maps. For smalt the silicon map is used, while for yellow lake three maps are used; potassium, sulphur and calcium. Spot analysis showed that yellow lake contains potassium, sulphur, and calcium. The noise of all the elemental maps was filtered out. Through this, clusters of elements

became visible. By calculating the area of the silicon clusters from the elemental map the amount of smalt present in the paint layer (in vol%) is known.
To calculate the volume percentage of yellow lake an extra step is needed. The clustered map of potassium was placed on top of the sulphur cluster map. If the clusters overlap, it is stated to be yellow lake cluster. The same was done using the calcium and the sulphur cluster map. The two yellow lake cluster maps were merged into one and from that the volume percentage was calculated.

3-1-3 Linking the Macro-XRF data with the pigment concentrations of smalt and yellow lake of the samples

In the Macro-XRF images, the location of the cross-section samples was identified. This gives five data points between 0–1 of the elements cobalt and potassium. Cobalt indicates the presence of smalt and potassium shows the presence of yellow lake. These data points were set against pigment concentrations of smalt and yellow lake of the cross-section samples. A relationship could then be found between the Macro-XRF data and the concentrations of yellow lake and smalt in the samples. This information could then be extrapolated to the whole painting, which gave the pigment concentration for the entire painting.

3-2 Section B

In section B, Paragraph 4-2 page 78, John Delaney (Senior Scientist, National Gallery of Art in Washington D.C.)[17] scanned *The Jewish Bride* with a hyperspectral imaging instrument. This gives the spectral reflection curve of the whole painting. He corrected the data for reflection from the top surface and that did not interact with the paint pigments. After that the curves show only the amount of light particles that penetrated the paint layer and interacted with the pigments. The dataset was subsequently transferred with the Kubelka-Munk theory to K/S per wavelength per pixel. This was also executed by him.

3-3 Section C

In section C, Paragraph 4-3 page 83, the paint-outs were made with a mixture of known concentrations of pigmented paint. The pigments used were bone black, red earth, non-degraded smalt, yellow earth, and non-degraded yellow lake. Four sets were made. The first set is based on the cross-section of the painting and what their colour would be when the pigments were not degraded. The second set shows how the colour of the cross-sections might be if there was no smalt present. The third set focuses on one of the cross-sections. Here the concentrations of bone black, red earth, yellow earth, and yellow lake are individually changed, while the rest of the pigments' percentages stay the same. This is to show how the colour of mixture is influenced per pigment. The fourth set focuses on how the pigments, bone black, red earth, yellow earth, and yellow lake behave with smalt. Smalt was mixed with one other pigment in set concentrations. How the paint-outs were made can be seen in Appendix D.

John Delaney[17] measured the paint-outs with the hyperspectral imaging instrument. As stated before, the reflective data must be corrected. The K/S values of the paint-outs can then be calculated from smalt, yellow lake, and bone black using the Kubelka-Munk theory.

3-4 Section D

In section D, Paragraph 4-4 page 94, determined the precision of these paint-outs. A cross-section was taken from one of the paint- outs, which was based on one of the cross-sections samples. This paint-out cross-section was examined under the microscope and analysed using SEM-EDX. Through the same method as in section A the pigment concentration was calculated. This gave an insight into the reliability of the paint-outs, and the method used to determine the pigment concentrations from cross-sections from the background of *The Jewish Bride*.

3-5 Section E

Different routes were proposed for section E, Paragraph 4-5 page 98. Although the whole painting was scanned by John Delaney[17], a focus area was chosen. This is the potted plant beside Rebecca on the right side. The exact location of this area is seen here in figure 3-3.

The area is interesting due to the fact that the amount of bone black, earth pigments, smalt, and yellow lake is heterogeneously distributed, which means there are likely to be some different shades of colour present.

3-5-1 Section E.1

In section E.1, Paragraph 4-5-2 page 101, the colour difference between a mixture with degraded pigments and non-degraded pigment was analysed and also the accuracy of the methods used for the digital colour reconstruction were compared.
Four different hyperspectral data sets, all based on the same paint cross-section were reviewed. The data sets were translated into RGB values, so they could be easily compared. The colour differences between the four data sets give an indication of how accurate the method proposed is.
The first hyperspectral data set was from the sample location in the painting. The second hyperspectral data set was that of the paint-out reconstruction of that cross-section. The third hyperspectral data set was based on the sample concentration and the K/S value of bone black, smalt and yellow lake. The fourth hyperspectral data set was also based on the K/S value of the pigments, but different in concentrations.

First the colour differences between the sample location and the paint-out were compared. Since for the paint-out non-degraded smalt and yellow lake were used, placing them side by side with the colour from the sample location where there is degraded smalt and yellow lake showed the colour difference between degraded and non-degraded pigments in a mixture.
Secondly, the paint-out colour was compared with digital mixtures made with hyperspectral



Figure 3-3: Focus Area of *The Jewish Bride*, the plant beside Rebecca

data of smalt, yellow lake, and bone black in two different concentrations. The first concentration was solely based on the concentration of the cross-section of the painting, while in the second the concentration of smalt was lowered, while the bone black and yellow lake concentrations were raised. This was done to take the transparency of smalt into account. The colour difference between the paint-out and the digital mixture indicated where and what would be the margin of error in the final digital colour reconstruction.

3-5-2 Section E.2

In section E.2, Paragraph 4-5-3 page 105, the focus was on three main aspects that influence the digital colour colour reconstruction.
The first aspect was the concentration of smalt, yellow lake. By using the Macro-XRF maps, it showed the distribution of smalt and yellow lake, also it showed the effect of the concentration of the colour. By digitally mixing the colour it became visible how they affect each other.
The second aspect is, the concentration of the background of the painting can be different. When adding the 'extra' colour, the concentration of background decreases and the colour of the background play less of a role. The goal was to see how different concentrations influence

the appearance, and whether this should be done in the digital colour reconstruction.
The third aspect is the oil matrix and the top paint layer turning monochrome brown due to the potassium leaking out of the smalt particles. Since there was no hyperspectral data of a degraded smalt matrix, the painting itself was used to achieve this data. Through the Macro-XRF data a location was found where there was a small amount of other elements, but a very high concentration of cobalt and therefore smalt. From that location the K/S value was taken and used as the colour of a degraded smalt matrix. Using the Macro-XRF map, the K/S value of degraded smalt was subtracted from the focus area in different concentrations. This gave a new insight on how much the painting has turned brown, but also it showed more colour differences. The goal of this was to see if and in what concentration the colour of the degraded smalt matrix should be subtracted from the focus area.

3-5-3 Section E.3

In section E.3, Paragraph 4-5-4 page 111, the information of section E.2 was used to make digital colour reconstructions. This showed how the different aspects influence each other. The goal was to show certain trends in the digital colour reconstructions instead of one outcome. This is because there are many uncertainties in the method created.

3-5-4 Section E.4

In section E.4, Paragraph 4-5-5 page 115, two of the outcomes of section E.3 wer placed back into the painting gave a notion, as to how much the painting has changed over time and what it may have looked like.

Chapter 4

Results & Discussion

In this chapter, all the results will be discussed in five different sections, A, B, C, D and E. The sections correspond with the sections A, B, C, D, and E of chapter 3, where the method was discussed. (see Figure 3-1 and Figure 3-2)
Every section has its own outcome and gives insights into the proposed method which is used in the final digital colour reconstructions.
Section A focuses on the Macro-XRF image of the whole painting and the paint cross-section sample of the background of *The Jewish Bride*. By calculating the pigment concentration of all the samples and plotting it against the values of the sample location of the Macro-XRF image, a relationship between the two can be established. Through this relationship, it is possible to estimate the concentration of smalt and yellow lake per Macro-XRF pixel for the whole painting.
Section B will focus on the hyperspectral analysis of the painting.
Section C will focus on the different paint-outs made and the hyperspectral analysis will emphasize on smalt and yellow lake.
Section D shows the accuracy of the method of pigment concentration calculation and the creation of the paint-outs. This is done by taking a cross-section sample of one of the paint-outs and analysing the same way as is done in section A.
Section E solely focuses on the digital colour reconstructions and their main parameters. The digital colour reconstruction can only be made by combining the outcome and insights from the previous sections A, B, C and D. Section E is split up into five different sub-paragraphs. At first, the focus area will be discussed in detail and a prediction will be made of what the focus areas could have looked like. This is done using the information of sections A and C.
Section E.1: here the accuracy of the suggested method is given through comparison of four different sets of hyperspectral data. The data is all based on the cross-section paint sample. The outcomes of sections A, B and C will be used for this.
Section E.2: the different parameters that influence the digital colour reconstruction are discussed individually. For this not only section A, B and C will be used, but also section E.1.
Section E.3: the digital colour reconstructions are made, they show the trend of colour changes and also what the focus area could have looked like. Here all the previous outcomes and insights will be used.

Section E.4: two reconstructions of section E.3 are placed back inside the painting. This shows the colour differences between them. Here the effect on the pictorial image will also be discussed, if the whole background of *The Jewish Bride* were to be digitally colour reconstructed.

The aim is to give an insight into how the background of *The Jewish Bride* could have looked liked when Rembrandt painted it using digital colour reconstruction.

4-1 Section A

The focus of this section will be to show the correlation between the concentration of pigments of the cross-section samples and the values of the Macro-XRF image.

This section is split up into four sub-paragraphs. Figure 4-1 shows a schematic overview

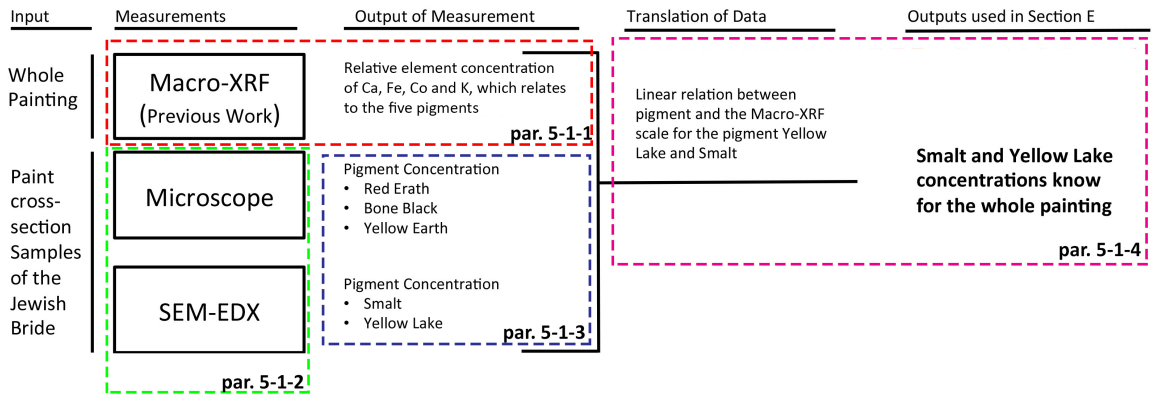

Figure 4-1: A schematic overview of section A
It also shows the different paragraphs containing section A.

of this section and indicates the different sub-paragraphs.
Paragraph 4-1-1: the Macro-XRF images (values between 0–1) are discussed. The images that will be studied are on calcium, cobalt, iron, and potassium. These elements are present in high quantities in the background of *The Jewish Bride* and can be related to the presence of pigments: bone black, earth pigments, smalt and lake pigments.
Paragraph 4-1-2: the cross-section samples from the background of the sample will be discussed, using the images taken by the microscope and SEM-EDX. The images shows the build-up of the paint layers and can lead to pigment detection and distribution of the pigments inside the layers.
Paragraph 4-1-3: by combining the microscope and SEM-EDX images, it is possible to calculate the concentration (between 0–100 vol%) of pigment present per sample for bone black, red earth, smalt, yellow earth and yellow lake.
Paragraph 4-1-4: the concentration of the pigment smalt (0–100 vol %) was set against the data of the cobalt Macro-XRF image (between 0–1) of the sample location. The same is done for yellow lake against the potassium Macro-XRF image values. The main reason of

Paragraph 4-1-4 focuses on smalt and yellow lake because these are the only two elements in the background that degrade overtime.
Through the relationship between the two pigment concentrations and their corresponding Macro-XRF image value, it is possible to estimate the concentrations of smalt and yellow lake for every pixel of *The Jewish Bride*.
This correlation will play a main role in sections E.2 and E.3. In those sections, the Macro-XRF images of cobalt and yellow lake will be used as a guide for the different concentrations when digitaly 'mixing' back smalt and yellow lake in the focus area.

4-1-1 Macro-XRF images of *The Jewish Bride* - previous work

Macro-XRF imaging shows the relative distribution of elements that are used in *The Jewish Bride*. Certain elements can be related back to the different pigments that Rembrandt used in his paintings. This gives an insight in the paint mixtures Rembrandt used.
Figure 4-2 shows the areas scanned by the Macro-XRF. The scanning was executed in 2013.

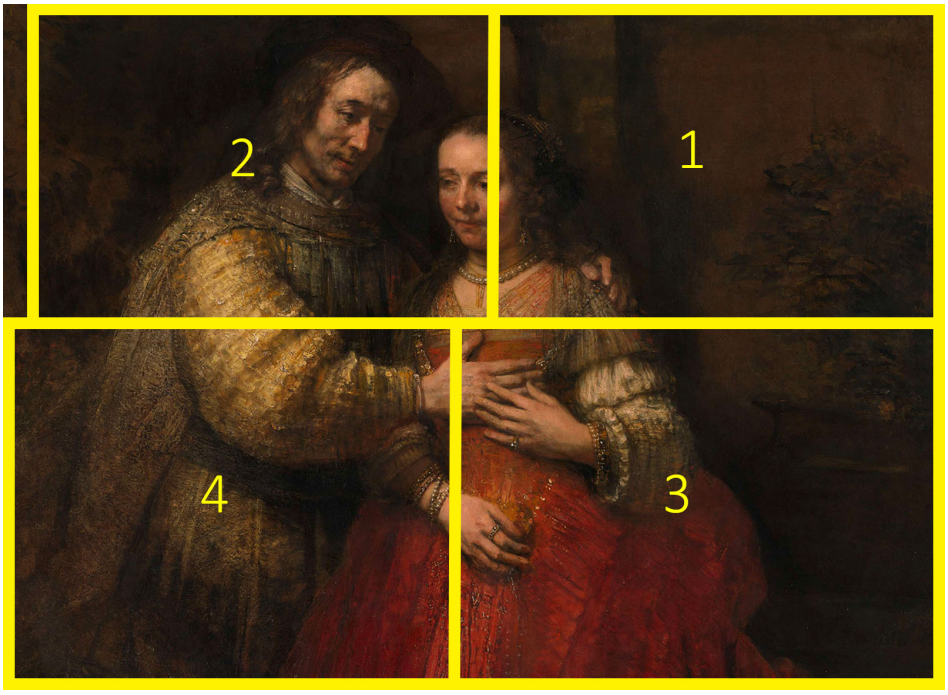

Figure 4-2: *The Jewish Bride* is scanned in four sessions (1–4) using the Macro-XRF scanner.

The four scans are stitched together; as can be seen a small section on the left side is not scanned.

The elements that were detected in *The Jewish Bride* are: lead, calcium, mercury, arsenic, nickel, bismuth, iron, manganese, copper, potassium, tin, chrome, barium, zinc, cobalt, and titanium. The Macro-XRF images are grey scale images, which show the relative intensity of the element concentration. White indicates a relatively high concentration, black indicates a relatively low concentration. Note that these distribution images are relative distribution maps and do not reflect absolute elemental concentrations.

Only the calcium, iron, potassium, and cobalt Macro-XRF images will be individually discussed. These elements are present in the background in relatively high amounts, and can be linked to the pigments that are this research focus of: bone black, red earth, smalt, yellow earth and yellow lake.

Every sub-paragraph will show two images. On the left, it shows the Macro-XRF images of a certain element in grey scale, showing the relative concentration of the element. White indicates a relatively high concentration, black indicates a relatively low concentration.
The right image shows the painting of *The Jewish Bride*, but only of the areas where there is a relatively high amount of the element present. On the locations where there is a relatively low amount of the element present, the pixels appear grey. Therefore it is possible to see, what the colour of those high intensities areas of the element have inside *The Jewish bride*. This is process is also explained in Figure 4-3. As was explained in Paragraph 2-3-1-2, the naked eye has difficulties discriminating between different intensities. Using digital intensities this problem can be mitigated as can be seen in the right images.

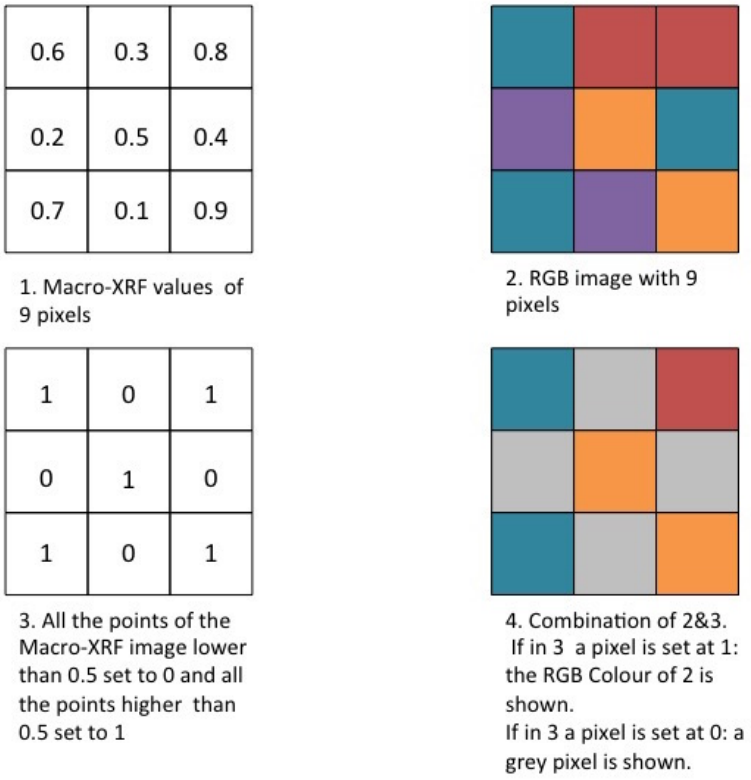

Figure 4-3: Schematic representation of the steps taken to achieve Figures 5-4b, 5-5b, 5-6b and 5-7b

After discussing the Macro-XRF image overall, the focus will be on the distribution of elements of the plant on the right side of Rebecca in the painting. All the Macro-XRF images will be shown in appendix A.

4-1-1-1 Calcium



(a) Calcium Macro-XRF image in grey scale, showing the relative concentration of the element



(b) Areas show original colour of *The Jewish Bride* where there is a high amount of calcium present.

Figure 4-4: Distribution of Calcium in the Painting
(a) White indicates a relatively high concentration, black indicates a relatively low concentration.
(b) Grey areas indicate areas where there is a low amount of the element. Areas show original colour when there is a high concentration of the element present. The figure shows that the dark areas in background of the original painting correspond with high amounts of calcium. This element is linked in the background to bone black.

The distribution of calcium is made visible in two figures; see Figure 4-4. On the left side, Figure 4-4a, the calcium Macro-XRF image is visible in grey scale. On the right side, Figure 4-4b shows the painting of *The Jewish Bride* where only the pixels with relatively high amounts of calcium, pixels with a value higher than 0.4 in the Macro-XRF, are presented in the RGB colour of the *The Jewish Bride*. The same figure shows where relatively low amounts of calcium are present, those pixels are set to grey.
The Figure 4-4 shows that high intensities of calcium are around the figures of Isaac and Rebecca in the background and in shadow of the cloak of Isaac. Looking at Figure 4-4b, only dark areas are visible in the background of *The Jewish Bride*. Therefore, it can be assumed that high intensities of calcium are related to the darker and shadowed areas of the background of the painting.
Calcium can be linked with the pigment bone black and lake pigments. This is, since bone black consists largely out of calcium phosphate. Lake pigments on the other hand use the element chalk or other calcium salts to precipitate dyestuff on.
Combining the colour information of figure 4-4b with the fact that calcium can be related to bone black, it can be said that relatively high intensities of calcium are mostly related to the pigment bone black in the background of *The Jewish Bride*.

4-1-1-2 Iron

The distribution of iron is made visible in two figures; see Figure 4-5. On the left side, Figure 4-5a, the iron Macro-XRF image is visible in grey scale. On the right side, only pixels with a value higher than 0.5 of the Macro-XRF are presented in the RGB colour of *The Jewish Bride* in Figure 4-5b.
Figures 4-5a and 4-5b show that iron is mostly present in the background and in the middle of



(a) Iron Macro-XRF image in grey scale in grey scale, showing the relative concentration of the element.



(b) Areas show original colour of *The Jewish Bride* where there is a high amount of iron present.

Figure 4-5: Distribution of iron in the painting
(a) White indicates a relatively high concentration, black indicates a relatively low concentration.
(b) Grey areas indicate areas where there is a low amount of the element. Areas show original colour when there is a high concentration of the element present. The figure shows that the iron distribution is homogeneous in the whole background, apart from some areas in the plant on the right side of Rebecca. This element is linked to earth pigments.

Rebecca's dress. They also show that various parts of the plant on the right side of Rebecca have some areas with significantly less iron. Those are seen as grey areas in Figure 4-5b.
Iron can be linked with the earth pigments, but is also an impurity of smalt. However, iron is the main element of earth pigment and therefore the Macro-XRF image can be related to that pigment. The earth pigments can differ in colour, ranging from yellow to brown.

4-1-1-3 Cobalt

The distribution of cobalt is made visible in two figures; see Figure 4-6. On the left side, Figure 4-6a, the cobalt Macro-XRF image is visible in grey scale. On the right side, only pixels with a value higher than 0.3 of the Macro-XRF are presented in the RGB colour of *The Jewish Bride* in Figure 4-6b.
Figure 4-6b shows that cobalt is mainly present in the background. There is only a small amount of cobalt present around the hat of Isaac and above the plant. This has most likely to do with previous restorations: the hat of Isaac has been altered and the paint has been removed in the area above the plant, where the ground layer is visible. This information comes from Petria Noble's[16] ongoing post-doctoral research.
Cobalt is linked with the pigment smalt. As discussed before, smalt is an unstable glassy blue pigment in oil, over time smalt particles turn grey and colourless, while the oil matrix and top layer have turned monochrome brown. Due to this smalt degradation the coloured locations in Figure 4-6b might have looked very different.



(a) Cobalt Macro-XRF image, showing the relative concentration of the element.



(b) Areas show original colour of *The Jewish Bride* where there is a high amount of cobalt present.

Figure 4-6: Distribution of cobalt in the painting
(a) White indicates a relatively high concentration, black indicates a relatively low concentration.
(b) Grey areas indicate areas where there is a low amount of the element. Areas show original colour when there is a high concentration of the element present. The figure shows that cobalt is used extensively in the whole background. This element is linked to smalt.



(a) Potassium Macro-XRF Image in grey scale, showing the relative concentration of the element



(b) Areas show original colour of *The Jewish Bride* where there is a high amount of potassium present.

Figure 4-7: Distribution of potassium in the painting
(a) White indicates a relatively high concentration, black indicates a relatively low concentration.
(b) Grey areas indicate areas where there is a low amount of the element. Areas show original colour when there is a high concentration of the element present. The figure shows that in the background potassium is not homogeneously distributed, especially in the plant on the right side of Rebecca. The element is linked to lake pigments.

4-1-1-4 Potassium

The distribution of potassium is made visible in two figures; see Figure 4-7. On the left side, Figure 4-7a, the potassium Macro-XRF image is visible in grey scale. On the right side, only pixels with a value higher than 0.33 of the Macro-XRF are presented in the RGB colour of *The Jewish Bride* in Figure 4-7b.
Figure 4-7 shows that relatively high concentrations of potassium are present in the background and also in the robe of Isaac. In the plant on the right side of Rebecca, there is an interesting distribution, which could indicate a highlight was placed with a certain pigment.

Potassium is linked to lake pigments, but is also a main component of smalt. Looking at the colours of Figure 4-7b, the yellow robe of Isaac appears that was painted with yellow lake. The dress of Rebecca is painted with a final red glaze consisting of an organic red lake pigment, which explains high amounts of potassium in the red dress. It is unsure to say, if the background is painted in smalt or a lake pigment.
Visually comparing the background of Macro-XRF image of potassium with the Macro-XRF image of cobalt, which indicates the presence of smalt shows, they do not correspond; see Figures 4-7a and 4-6a. One would expect that potassium has roughly the same distribution pattern as cobalt, if all the potassium was from smalt. For instance, the high element distribution of potassium in the plant does not correspond with that of the cobalt distribution.
From the different distributions, it can be assumed that high intensity potassium is most likely linked with lake pigments, rather than smalt.

Potassium is a integral part of smalt, therefore a link between the smalt distribution and potassium distribution is expected, but in the current dataset a correlation between the two distributions is not found.
Most likely, the lack of a link is due to the fact that every elemental distribution image is stretched independently between 0–1 to cover all colours between white and black, and by doing so the relative link between two elemental maps is lost between the Macro-XRF data set of cobalt and potassium. More research on the raw dataset of potassium and cobalt might give an insight why, there is no correlation between the cobalt Macro-XRF image and potassium Macro-XRF image.

4-1-1-5 Distribution of the elements in the Plant

The plant on the right side of the painting has been painted using various mixtures. This becomes apparent when looking at the different Macro-XRF images side by side and linking that to the different pigments; see Figure 4-8.

Figure 4-8 shows that the calcium map corresponds with the shading of the leafs of the plant, and this corresponds with the link between calcium and bone black.
Potassium has some distinct areas in the plant, which can indicate higher intensities of lake pigments.
The iron Macro-XRF shows a very homogeneous distribution of earth pigments, although some particular areas in the leaves have a low intensity of iron. However, those low intensity iron areas correspond with the high potassium areas.
Cobalt is distributed throughout the plant. This indicates that smalt is present in the whole plant.
Also, Figure 4-8 shows that elemental maps of potassium and cobalt are very high in the leaves of the plant. This could indicate a mixture of yellow lake and smalt. Since both of those pigments have lost their colour, it could imply that in the painting in its original state a different colour was present in these locations.
The variation and distribution of elements, and therefore the pigments, is the main reason for choosing the plant as focus area.

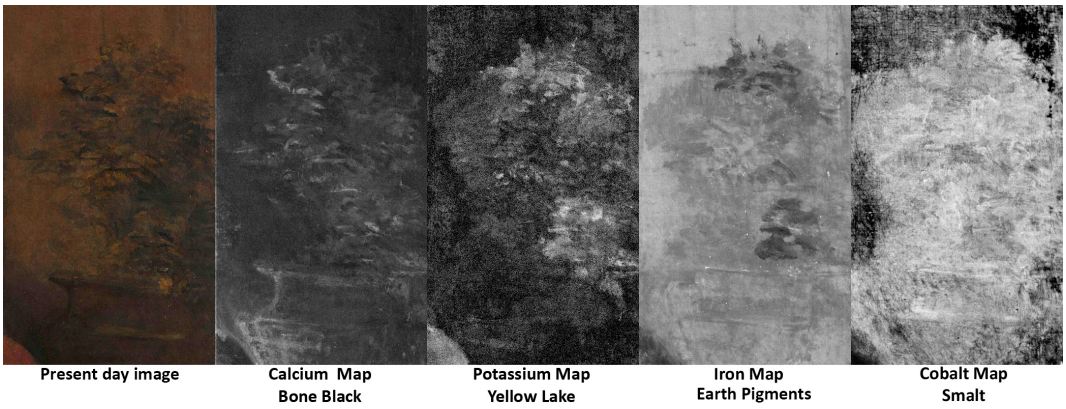

Figure 4-8: Close-up of the different elemental maps of the plant, in grey scale. White indicates a relatively high concentration of the element, black indicates a relatively low concentration. Each element can be linked to specific pigment(s). Notice that the painting is build-up by using different pigment mixtures.

4-1-1-6 Conclusion and discussion of the Macro-XRF images

To conclude, calcium, iron, cobalt and potassium are all linked to different pigments. It appears that high values of calcium are connected with the high amounts of bone black and high values of the potassium Macro-XRF appears to be linked with lake pigments. The Macro-XRF image of iron can almost be completely linked with earth pigments. The whole of the Macro-XRF image of cobalt is related to smalt.

The main limitation of the dataset is that the Macro-XRF images give data on a relative scale per element. The exact concentration of the different elements is therefore unknown, and it is not possible to link it to pigment concentration. The dataset only shows that more of an element is present in one spot compared to another. Another limitation is that potassium, iron, and calcium are also an impurity or integral part of other pigments. Therefore, the distribution of these elements cannot be exclusively linked with one pigment.
Although the Macro-XRF dataset has these limitations, it does give insight into element distribution and therefore pigment distribution. As already stated in chapter 2, Rembrandt is famous for his paint mixing. This can be seen in the heterogeneous distribution of all the discussed elements. This shows that no paint mixture in the background was the same and there were subtle colour differences throughout the background.

These outcomes will be used in paragraph 4-1-4 of this section. Further, the Macro-XRF images of cobalt and potassium will be used in sections E.2 and E.3. Here they will be used as a guide for the concentration of the 'mixing' back of pigments in the focus area of *The Jewish Bride*.

4-1-2 Pigment detection of five cross-section samples of *The Jewish Bride*'s background

In this section, the five cross-section samples from the background of *The Jewish Bride* will be discussed. This is split up into three sub-paragraphs.
In the first sub-paragraph, the different sample locations will be shown and discussed.
In the second sub-paragraph, the samples will be reviewed individually. This is done by different microscope images and SEM-EDX images. This will show the distribution of the pigments in the samples and the combined information will show which pigments are present.
In the third sub-paragraph, the EDX spot analysis of all the different smalt particles will be discussed.
Through this, the pigments used in the background can be discriminated.

4-1-2-1 Location of the cross-section samples

The five existing cross-section samples of the background were taken in 2 sets. The first set is that of dr. Karin Groen (chemist & research technician, Rembrandt Research Project) [13] in 1992, which are numbered, 40_7, 40_12, and 40_15. The second set is that of prof.dr. Arie Wallert (chair Atelier Practice, University of Amsterdam/Rijksmuseum)[14] in 2011 and are numbered 215/2 and 215/3.
Figure 4-9 shows the sample locations and Table 4-1 state the dimension of the sample spot in the painting and the description. Sample 215/2 is taken from the hat of Isaac, while sample 215/3 is taken above the head of Rebecca in the shadow of the beam. Sample 40_7 is taken from a smalt region in the leaves of the flower pot. Sample 40_12 is in the brown background, left of the head of Isaac. Sample 40_15 is taken from beside the beam in the background.

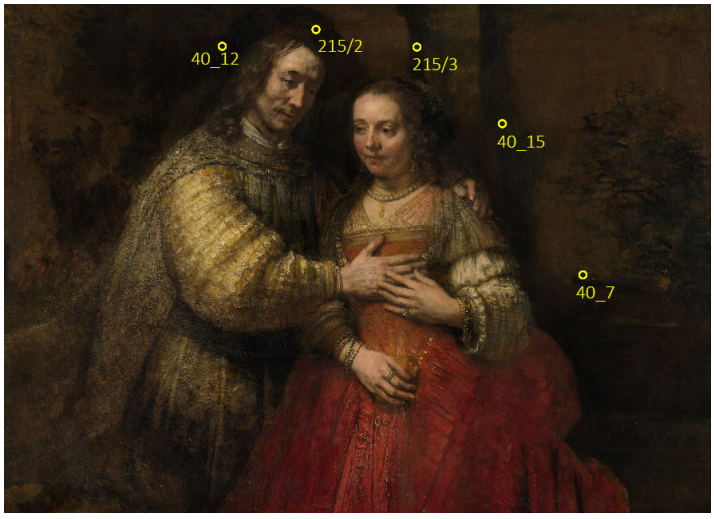

Figure 4-9: Cross-section sample locations, descriptions can be found in Table 4-1.

Table 4-1: Cross-section sample spots and description

Sample	Sample spot	Description
215/2	73.6 cm from the left, 7.9 cm from the top	Black hat
215/3	69.1 cm from the right, 12 cm from the top	Above the head of *The Jewish Bride*
40_7	30 cm from the right, 56 cm from the bottom	Leaves above the flower pot
40_12	51.5 cm from the left, 12.5 from the top	Left of the hat
40_15	49 cm from the right, 30 cm from the top	Right of the dark beam

4-1-2-2 Images of the cross-section samples

In this paragraph the images per sample (215/2, 215/3, 40_ 7, 40_ 12 and 40_ 15) of the microscope will be discussed, as well as the images and elemental map of the SEM-EDX.
The description and discussion of the samples in the following paragraphs 4-1-2-3 – 4-1-2-7 was done by Annelies van Loon (Conservation scientist, Rijksmuseum/TU Delft)[15] and Petria Noble (Head of Paintings Conservation, Rijksmuseum)[16]. All the overview images of the samples can be seen in appendix B
From the SEM-EDX, the backscattered electron image is shown and only the elemental maps of silicon, potassium, sulphur, and calcium are shown, since in the next sub-paragraph these are used to calculate the different pigment concentrations.
Silicon can indicate the glass particles of smalt.
Cobalt also indicates smalt, but since less is present in the particles the images showed less pronounced particles and therefore it is inferior to that of the silicon map.
To identify yellow lake a combination of different elemental maps should be used. Spot analysis of yellow lake particles, which can be seen in appendix C, showed the presence of calcium, potassium, and sulphur in yellow lake clusters. Therefore, to identify yellow lake the elemental maps of potassium, sulphur, and calcium are combined.
All the different elemental maps and sample spot analyses will be shown in the appendix C.

4-1-2-3 Sample 215/2 - Hat of Isaac

Sample 215/2 can be seen in Figure 4-10. This sample location was that of the hat of Isaac. Here 3 layers are visible and numbered accordingly.
Layer 1 is the background layer with smalt particles. Some accumulation of yellow pigment is visible, which is yellow lake.
Layer 2 is a compact layer of smalt (visible as angular glassy particles) with some red specks, which is red earth. This is part of the red hat, which was previously painted and is covered now by the black hat.
Layer 3 is a very compact black layer of bone black with organic yellow and red lake particles. This layer is shown in the painting as the black hat.

Figure 4-11 shows the backscattered electron image and element maps. In the silicon map, the distribution of smalt particles is clearly visible. These correspond with the angular

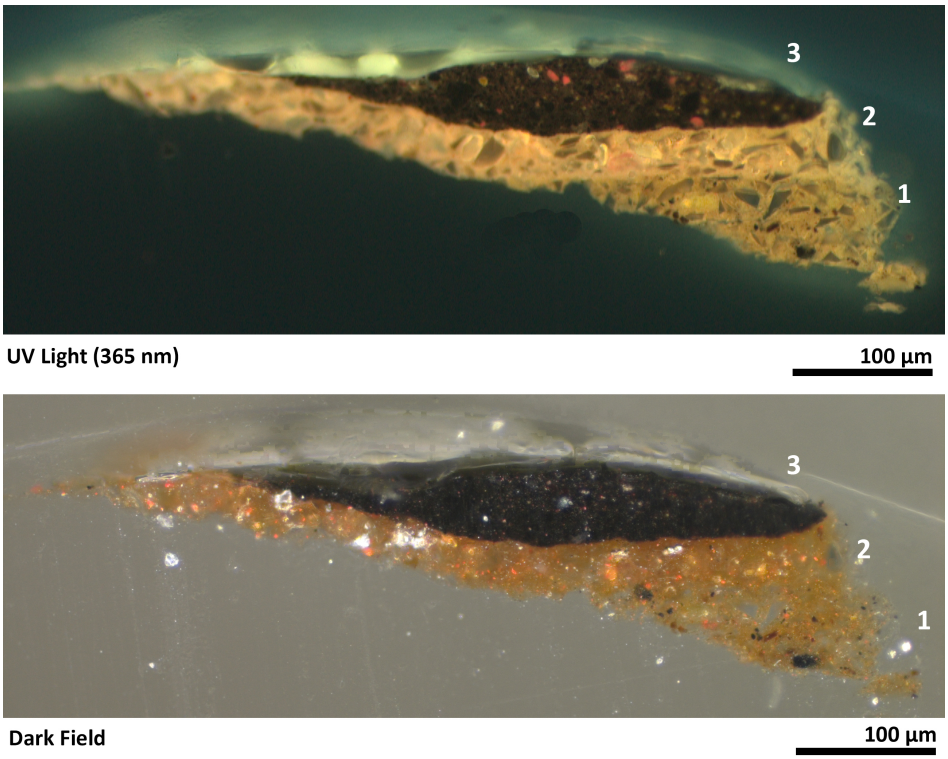

Figure 4-10: Microscope images of cross-section of sample 215/2 depicting the three layers. In layer 1 and 2 smalt particles are visible, as angular particles.

particles in the electron image. In the sulphur map and potassium map there are multiple yellow lake particles visible. These correspond with the lighter clusters in the backscattered electron image. The reason that those clusters appear to be lighter is that besides sulphur, potassium, and chalk, lead also is presented. This is seen in the spot spectrum taken in those locations; appendix C. This is the common degradation product of yellow lake.
Calcium is mostly present in the top layer of the sample. This is due to the fact that calcium can be related to bone black.

4-1-2-4 Sample 215/3 - the shadow of the beam

Sample 215/3 can be seen in Figure 4-12. The sample location is that of the shadow area beside the beam above Rebecca. Here 3 layers are visible and numbered accordingly.
Layer 1 is the quartz ground layer, containing a homogeneous layer of quartz. Quartz ground layer are unique for Rembrandt and are researched by Karin Groen [13] for Art Matters. It is a partial layer.
Layer 2 has some red specks, which is red earth. Some yellow is visible, which can be either yellow earth or yellow lake.
Layer 3 differs from layer 2 only in that a large quantity of black pigment, bone black, is used.

Figure 4-13 shows the backscattered electron image and element maps. The smalt particles are clearly visible in the silicon map. In the ground layer also silicon is visible. The

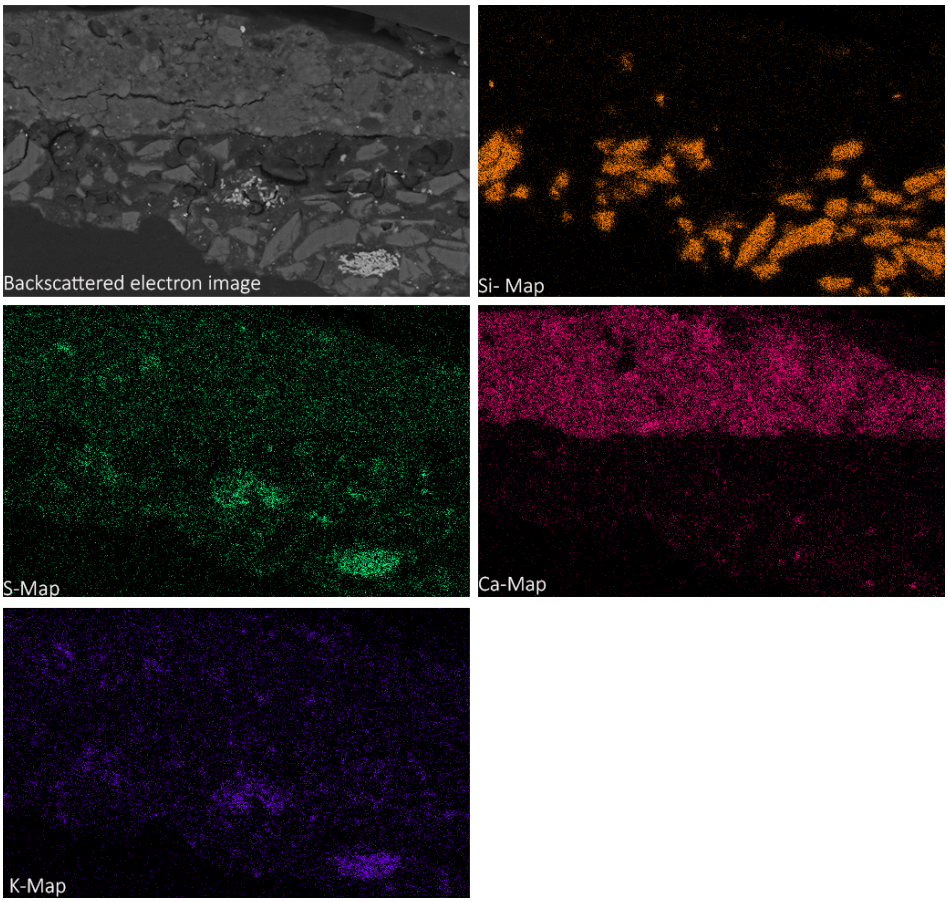

Figure 4-11: Cross-section of sample 215/2 scanned by SEM-EDX. It shows the backscattered electron image and elemental maps. Silicon shows the smalt particles, while the combination of maps of sulphur and potassium show yellow lake particles.

sulphur, potassium, and calcium maps only show small specks that completely overlap, which can be related to yellow lake.

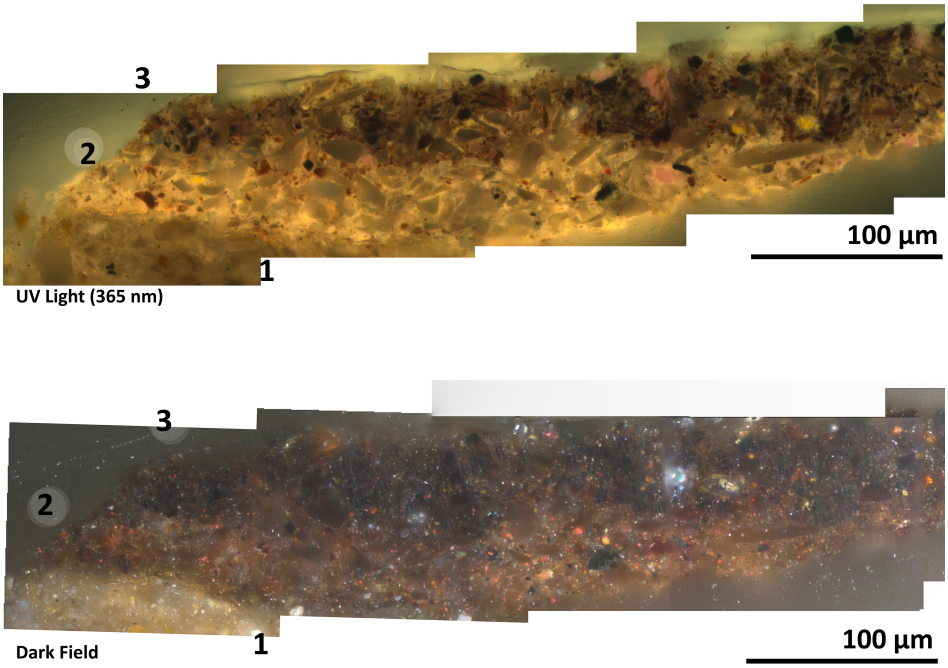

Figure 4-12: Microscope images of cross-section of sample 215/3 depicting the three layers. In layer 2 & 3 smalt particles are visible in UV as angular particles.

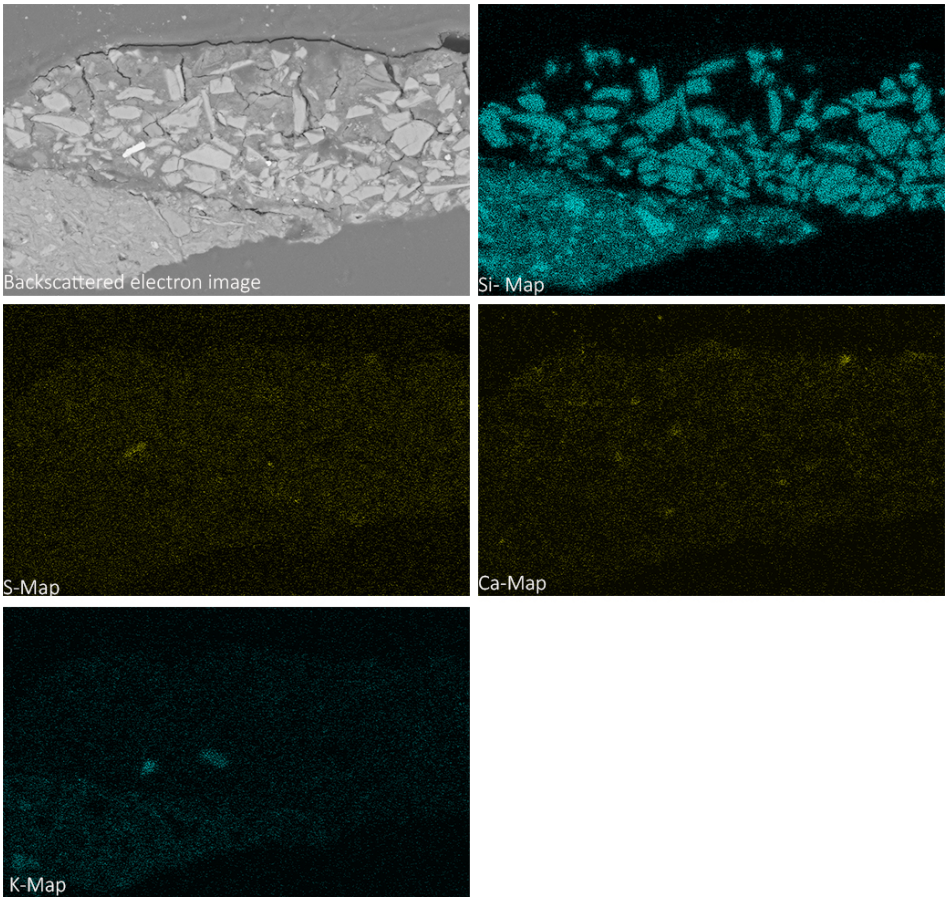

Figure 4-13: Cross-section of sample 215/3 scanned by SEM-EDX. It shows the backscattered electron image and elemental maps. Silicon shows the smalt particles as angular particles, while the combination of sulphur, potassium and calcium show yellow lake particles.

4-1-2-5 Sample 40_7 - leaves above the flower pot

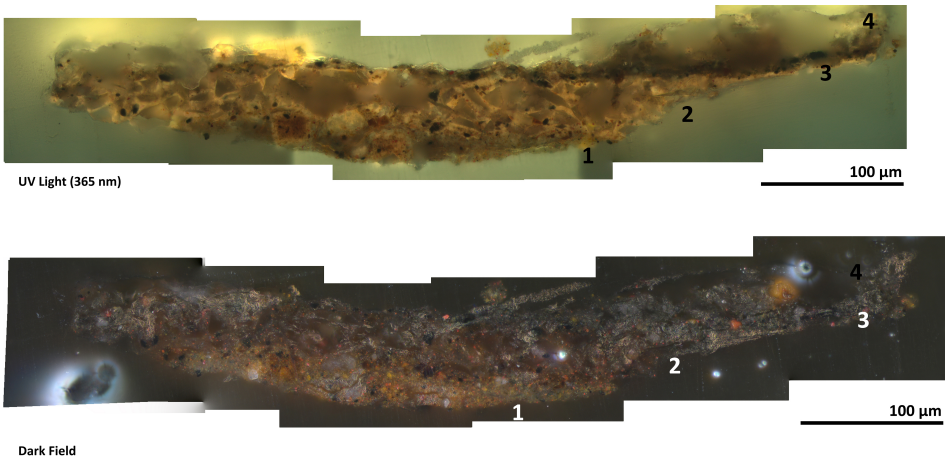

Figure 4-14: Microscope images of cross-section of sample 40_7 depicting the three layers. In layer 2 & 3 smalt particles are visible in UV as angular particles.

Sample 40_7 can be seen in Figure 4-14. The sample is taken from the bottom of the plant on the right side.
There are 4 layers and they are numbered accordingly.
Layer 1 is the ground, it has yellow earth, bone black, lead white, and some red particles, which can either be red lake or red earth.
Layer 2 is made up of compact smalt, with yellow lake particles. There are tiny red particles throughout the layer, that is red earth.
Layer 3 is an incomplete layer of smalt with black pigment, bone black.
In layer 4, where the number is placed, some varnish is visible.

Figure 4-15 shows the backscattered electron image and element maps. The backscattered electron image shows the roughness of the sample, especially on the left side of the sample. There is also no clear distinction between the layers visible. The smalt particles are only visible in the silicon map. In the sulphur, calcium and potassium map there is a clear accumulation of yellow lake. The spot spectrum of that region also indicates that it is a yellow lake particle.

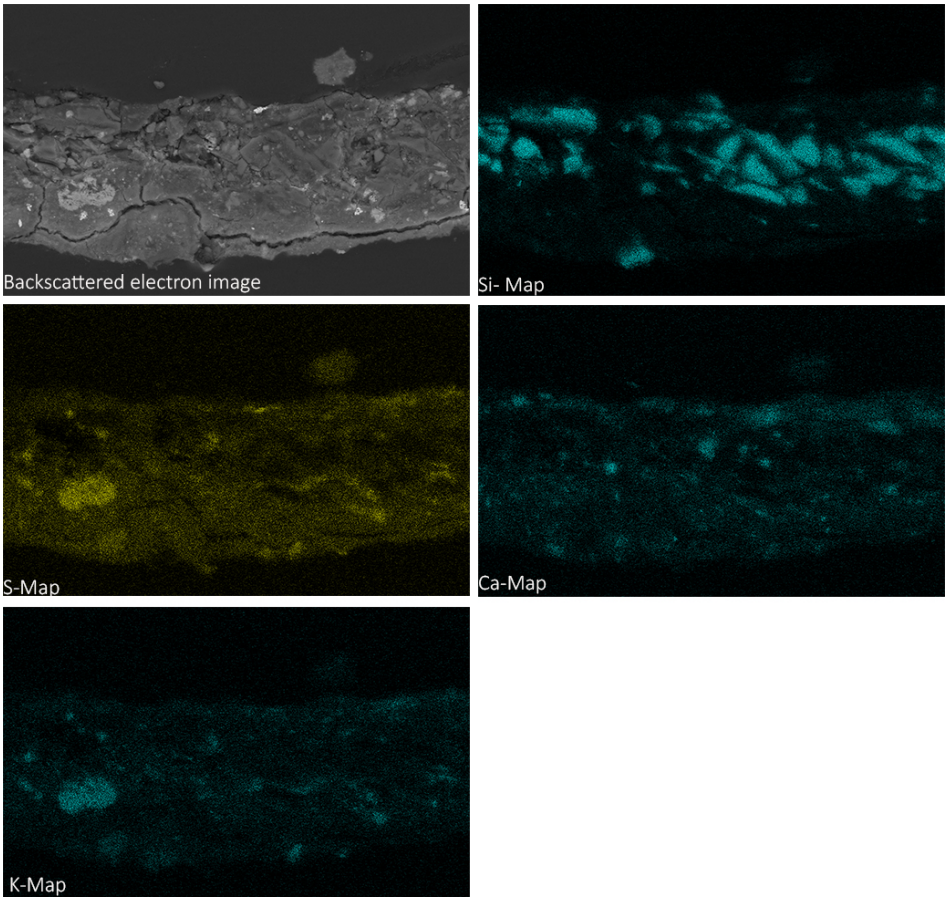

Figure 4-15: Cross-section of sample 40_7 scanned by SEM-EDX. It shows the backscattered electron image and elemental maps. Silicon shows the smalt particles as angular particles, while the combination of sulphur, potassium and calcium show yellow lake particles.

4-1-2-6 Sample 40_12 - left of the head of Isaac

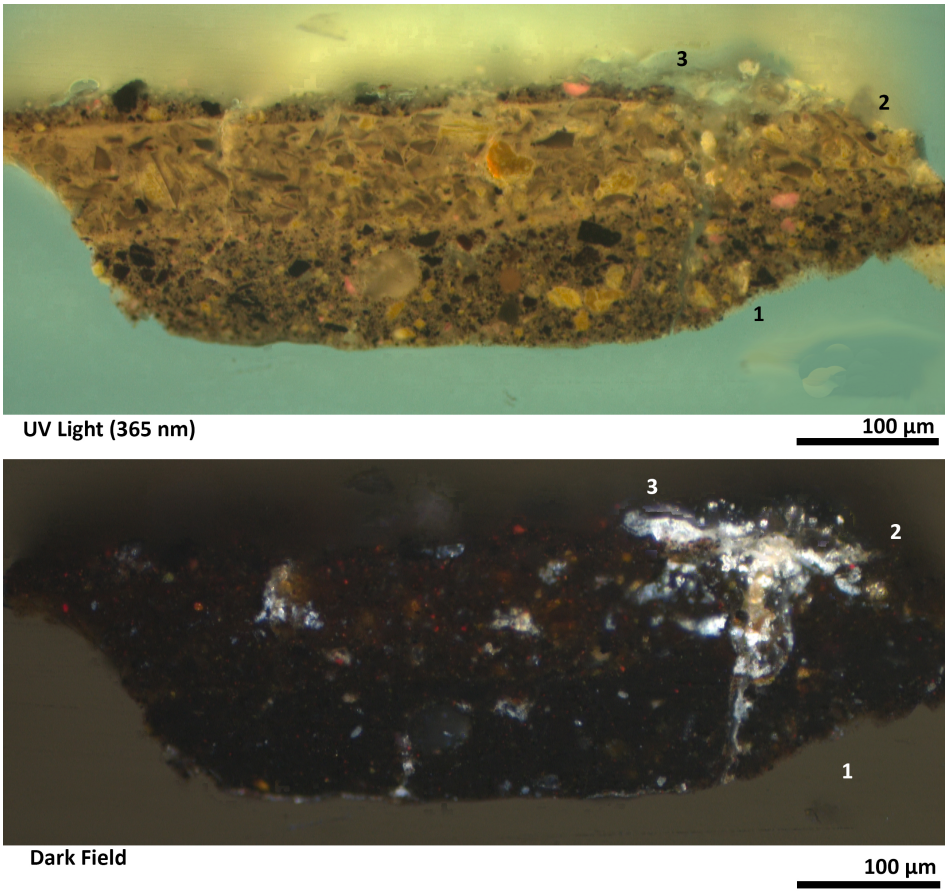

Figure 4-16: Microscope images of cross-section of sample 40_12 depicting the three layers. In layer 2 & 3 smalt particles are visible in UV as angular particles.

Sample 40_12 can be seen in Figure 4-16. The sample is taken from beside the head of Isaac. There are 3 layers visible and they are numbered accordingly.
Layer 1 is a dark layer with reddish particles and yellow particles throughout the layer. Those are bone black, red earth, and yellow lake/earth. Layer 2 is made up mostly of smalt with some accumulation of yellow lake. Layer 3 is a partial dark layer with some red specks, probably bone black and red earth/lake.

Figure 4-17 shows the backscattered electron image and element maps. Layers 1 and 2 are clearly visible in the electron image. The silicon map does not show an even distribution of smalt particles. On the right side, there is empty space. This corresponds with a cracked area. The sulphur, potassium, and calcium maps show some overlap, so there is a presence of yellow lake specks.

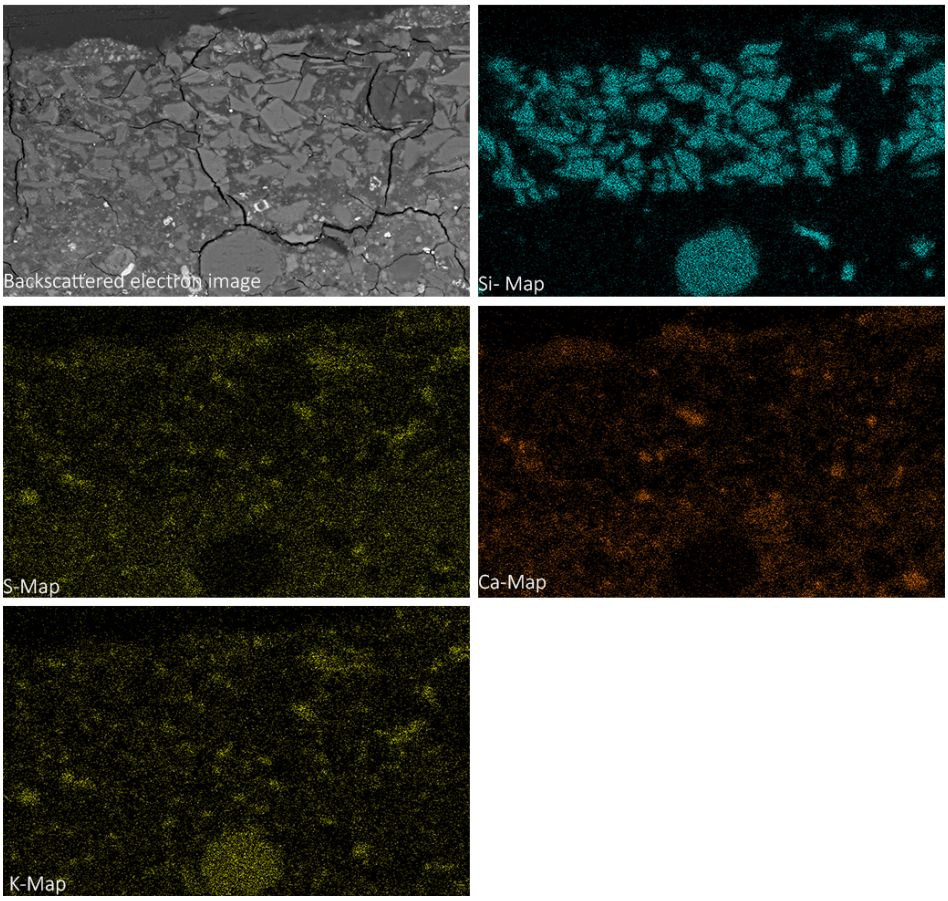

Figure 4-17: Cross-section of sample 40_12 scanned by SEM-EDX. It shows the backscattered electron image and elemental maps. Silicon shows the smalt particles as angular particles, while the combination of sulphur, potassium and calcium show yellow lake particles.

4-1-2-7 Sample 40_15 - shadow area of the beam

Sample 40_15 can be seen in Figure 4-18. The sample is taken from the shadow area of the beam. There are 3 layers visible and they are numbered accordingly. Layer 1 is the ground, which is made up of quartz and is only partial. This layer is the same as Layer 1 in Figure 4-12 and Figure 4-18.
Layer 2 is dark and similar to layer 2 in Figure 4-18. It consists of bone black, yellow lake and red earth and there might be some smalt particles. Between layer 2 and 3 there might be an extra layer. Layer 3 is a compact layer of smalt, with some particles that are still blueish. At the top of the sample, above layer 3, an air bubble can be seen.

Figure 4-19 shows the backscattered electron image and element maps. This is the largest area scanned of any of the samples. The air pocket above the sample is visible in the electron image. The different smalt particles are visible and are evenly distributed in the layer. The sulphur, calcium, and potassium maps show some yellow lake particles.

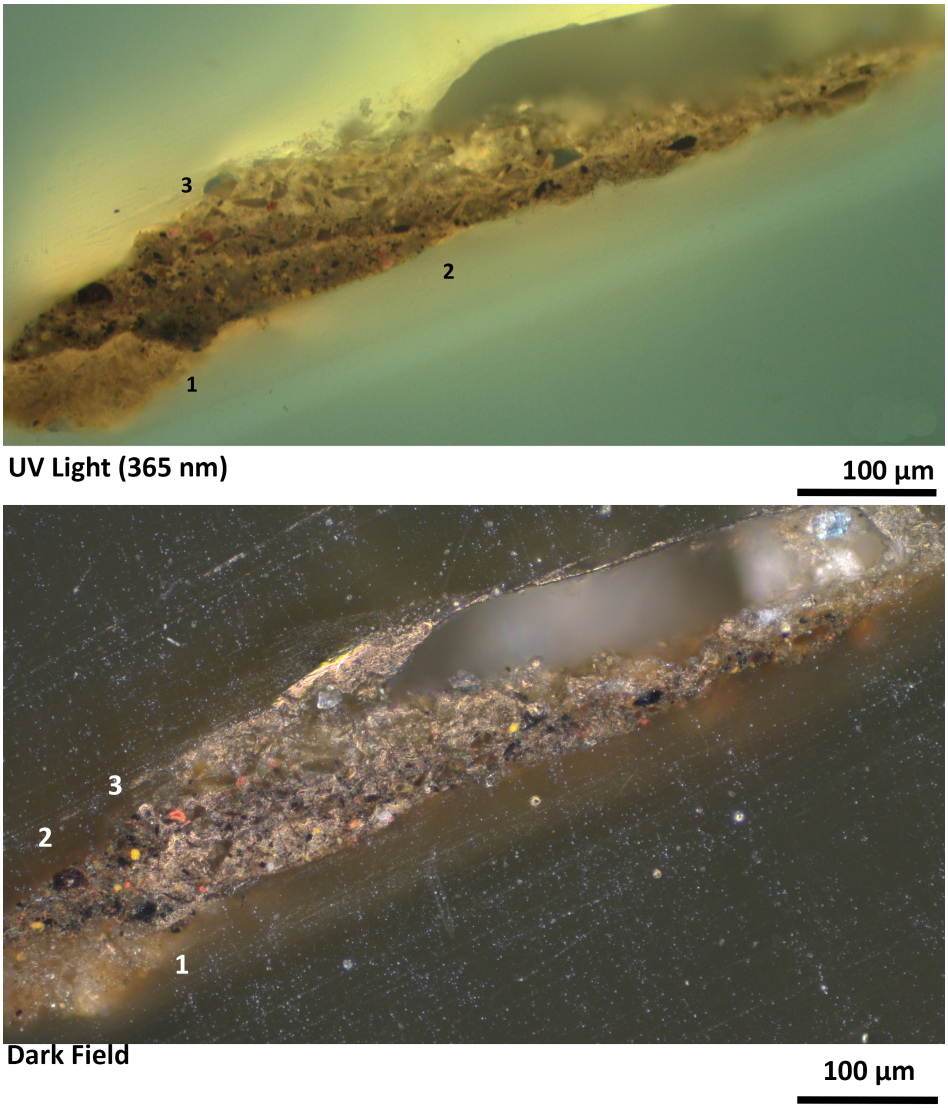

Figure 4-18: Microscope images of cross-section of sample 40_15 depicting the three layers. In layer 3 smalt particles are visible in UV as angular particles.

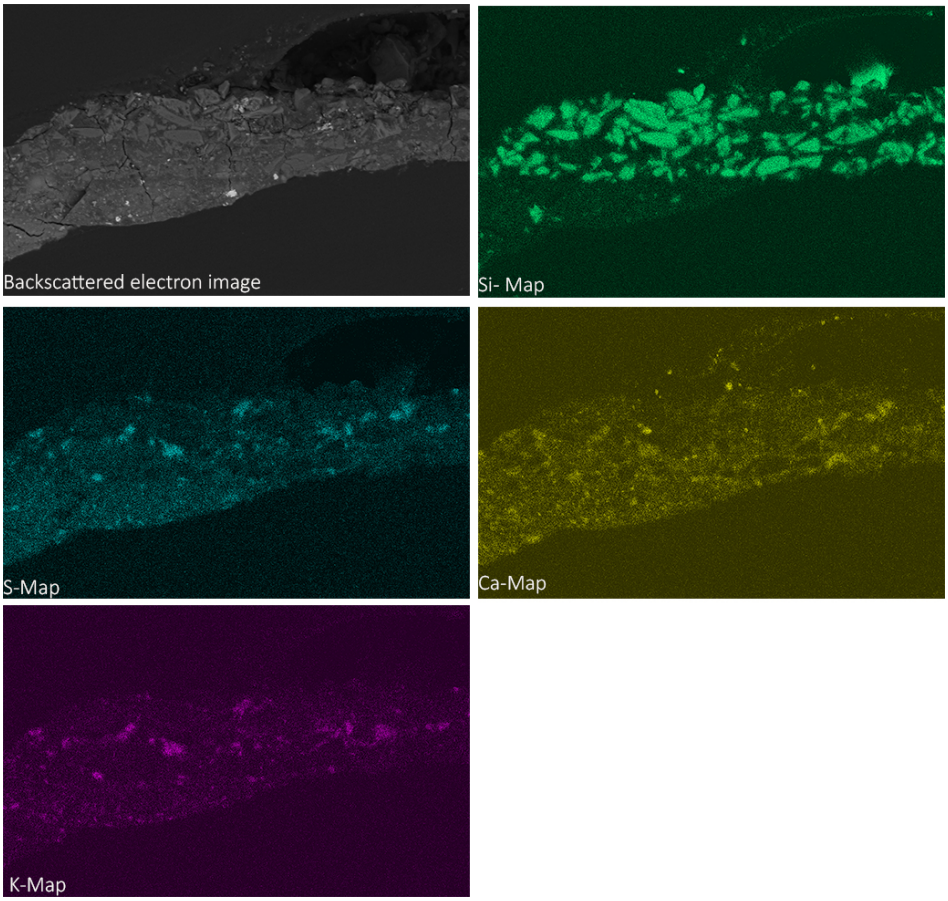

Figure 4-19: Cross-section of sample 40_15 scanned by SEM-EDX. It shows the backscattered electron image and elemental maps. Silicon shows the smalt particles as angular particles, while the combination of sulphur, potassium and calcium show yellow lake particles.

4-1-2-8 EDX spot analysis of the smalt particles

Here the EDX data of the smalt particles will be discussed. Table 4-2 shows averages of all the spot spectra of the smalt particles. The main elements of the particles are silicon, cobalt, and iron. The table shows that most of the potassium (K_2O) as leached out; in non-degraded smalt its concentration would be much higher around 16 wt% - 21 wt%.[10] Also it shows that all the smalt particles have roughly the same amount of cobalt throughout the particles, which is around 3.61%.
All the individual spot analysis per sample can be seen in appendix C.

Table 4-2: Comparison of the smalt particles in wt% using EDX spot analysis

	215/2	215/3	40_7	40_12	40_15	Average	Standard Deviation
Al_2O_3	1.00	2.09	1.41	0.89	1.38	1.35	0.42
SiO_2	86.46	81.41	85.5	79.24	84.99	83.52	2.74
K_2O	0.71	1.84	1.19	0.88	0.79	1.08	0.41
CaO	0.73	1.44	1.14	0.48	1.13	0.98	0.34
FeO	2.97	3.20	2.88	3.04	3.16	3.05	0.12
CoO	3.68	3.59	3.09	4.02	3.67	3.61	0.30
NiO	0.84	0.77	0.58	0.6	1.09	0.78	0.19
As_2O_3	3.50	3.92	4.2	3.96	3.4	3.80	0.30
MgO	0.05	0.00	0.00	0.00	0.00	0.01	0.02
PbO	0.00	1.67	0.00	0.00	0.40	0.41	0.65
Bi_2O_3	0.00	0.00	0.00	0.44	0.00	0.09	0.18
SO_3	0.00	0.00	0.00	0.11	0.00	0.02	0.04

4-1-2-9 Conclusion and discussion of the samples

To conclude, there are five pigments present in the top layer of paint of the background, namely bone black, red earth, smalt, and yellow earth and yellow lake. Smalt particles can be seen in the silicon elemental map, and yellow lake substrate is a mixture of calcium, potassium, and sulphur. The smalt particles consist of around 3.61 wt% of cobalt.

By visually comparing the different samples, it is clear that the quantities of these five pigments vary across the samples. The heterogeneous distribution of pigments was already suggested from the Macro-XRF images in a previous paragraph.
The different pigment distributions suggested from the Macro-XRF match with the pigments used in the cross-sections of the background of *The Jewish Bride*. The distribution of iron in the Macro-XRF map, which indicates earth pigment, is split into red earth and yellow earth. The lake pigment distribution, which could be seen in the background of the potassium Macro-XRF, is yellow lake.

It is difficult to get an extensive insight into pigment mixture of the whole background from five small samples, which are all taken from dark areas of the background of the painting, also some layers are only partially present. It does show which pigments are used and how they are distributed in that particular sample. It also shows how Rembrandt built up *The Jewish Bride*.

In the next paragraph, the focus will be on calculating the concentrations of the detected pigments of the samples. The sample size will considerably impact the accuracy of the outcome of the calculation. The microscope image will be used to calculate bone black, red earth and yellow earth. The SEM-EDX elemental maps of silicon will be used for smalt and the combined elemental maps of potassium calcium and sulphur will be used for yellow lake, as only yellow lake contains all three elements. Bone black is linked to calcium and earth pigments to iron, but due to the noisiness of the calcium and iron maps, these could not be used for calculating the volume fraction.

4-1-3 Calculating the volume fractions of the pigments in the five different cross-section samples

This paragraph will focus on how the pigment concentration of the smalt top layer of the different samples is calculated and the outcome of the calculation. With this knowledge, the pigment concentration can be linked to the Macro-XRF values of that sample location.
The paragraph can be sub-divided into four sub-paragraphs. In the first three paragraphs sample 40_15 will serve as an example to make the steps of the pigment calculation visible. In the final sub-paragraph, the calculated concentrations of all the different samples will be discussed.
The first sub-paragraph will focus on linking the different images of the same sample together. The images are of the different lighting settings of the microscope and that of the SEM-EDX. This is done, so that all input images show the same area and have the same pixel size. From that a region of interest is selected. The region of interest of each sample is the smalt containing paint layers.
The second sub-paragraph will focus on the process of calculating the pigment concentration from EDX elemental map. Only smalt and yellow lake can be calculated by using elemental maps. The elemental maps used for this process are silicon for smalt and potassium, sulphur and calcium for yellow lake. As shown in the previous paragraph 4-1-2, these maps can be used as indicators of smalt and yellow lake. As explained in the previous paragraph 4-1-2 bone black, red earth and yellow earth could not be calculated using elemental maps.
The third sub-paragraph will focus on the process of calculating the pigment concentration from microscope images. These calculations are based on the pigments' RGB values. The concentrations of bone black, red earth, and yellow earth were calculated. The pigments smalt and yellow lake could not be measured accordingly, since the pigment particles have become colourless.
From the calculated data, the conclusions and the outcome will be discussed.

To get more insight about the mathematical process of the different MATLAB functions used, the book 'Digital Image Processing' by Gonzales and Woods (2008) is recommended. A short description of relevant functions is also given in Appendix F.

4-1-3-1 Relating the different inputs and choosing an area of focus

To calculate the pigment concentration of the samples, first the input images (different microscope images and elemental maps) must be related to each other. This is required to ensure that the microscope image and SEM-EDX image of the same sample can be compared. Each of the images should show the same location of the sample, have the same dimension, and have the same number of pixels. The pixel size should be the same, because from the amount of pixel the concentrations will be calculated.
The region of interest is selected: the smalt containing layer, which is indicated as the black boundary around the samples image, Figure 4-20. This process is not only done for the UV microscope image and backscattered images, but for all the input images. By doing this, multiple inputs can help determine the pigment concentration.



(a) Region of Interest selected in the UV microsope image of cross-section of sample 40_15

(b) Region of Interest selected in the Backscattered electron image of cross-section of sample 40_15 Backscattered electron image

Figure 4-20: Cross-section image of sample 40_15 in UV and scanned by SEM-EDX. **(a)** and **(b)** depict the same area and have the same pixel size. The region of interest is selected: the smalt containing layer, which is indicated as the black boundary around the cross-section sample images.

4-1-3-2 SEM-EDX images - Volume fractions of smalt and yellow lake

This sub-paragraph explains the calculation of the area percentages of the pigments smalt and yellow lake in the samples. This calculation is based on the elemental maps. Smalt can be calculated from the silicon elemental map, while the amount of yellow lake is calculated from three different elemental maps, potassium, calcium, and sulphur.
Figures 4-21 and 4-22 give a high level overview of the steps that lead to an volume fraction of smalt and yellow lake.
The amounts of bone black, red earth, and yellow earth are not calculated from elemental maps. There is a calcium elemental map, which can indicate bone black and iron elemental map that can indicate earth pigments. However, the pigment particles were too small and the elemental maps too noisy to make a clear distinction. Bone black, red earth and yellow earth are therefore calculated in the next sub-paragraph 4-1-3-3 using microscope images.

4-1-3-2-1 Smalt Figure 4-21 shows all the steps taken to discriminate the smalt particles out of the silicon map.
Figure 4-21a shows the silicon elemental map. As can be seen there is noise, and stray pixels are surrounding the outline of the smalt particles. Therefore the image is processed to filter out noise and stray pixels. Subsequently the back scattered electron image is used to bring back detail. To calculate the volume fraction, the white pixels of figure 4-21b are summed

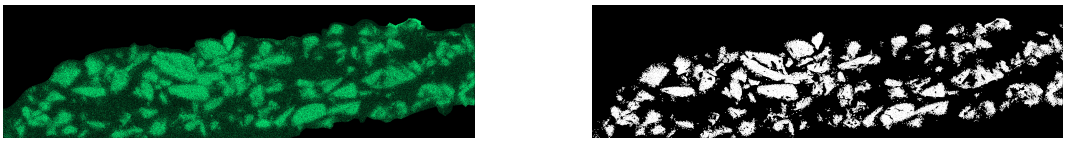

(a) Silicon map of cross-section of sample 40_15 **(b)** Smalt particles are filtered out

Figure 4-21: Process of filtering out smalt particles.
(a) shows the input image
(b) shows the output, where the white pixels represent the smalt particles

up and divided by the area of the region of interest, which leads towards an area fraction of smalt with sample 40_15.

4-1-3-2-2 Yellow lake To calculate yellow lake pigment particles three EDX images are used, potassium, calcium and sulper; see Figure 4-22. These three maps are used, since spot spectrum analysis showed in section 5-1 that yellow lake substrates have three main elements, potassium, calcium, and sulphur.

To begin with all the maps individually undergo the same steps as the silicon map to reduce noise and filter out stray pixels. This results in the black and white maps of potassium, calcium and sulphur.
The black and white potassium map is multiplied with the black and white sulphur map. This will create a new black and white image. In the new image, the white pixels will appear on the places where in both maps that pixel was white. Those white clusters in the new image are seen as yellow lake particles. The same is done with the calcium and sulphur maps. All the yellow lake pixels are placed in one figure. This is seen in the black and white Figure 4-22d. Here all the white clusters are yellow lake particles. Comparing the white pixel clusters of Figure 4-22d with the high intensity of the potassium, calcium and sulphur map, it shows that it overlaps. The yellow lake white pixels are summed up and divided by the region of interest to create an area percentage.
However, as can be seen that the elemental maps are noisy, which influence the accuracy. This means that some white pixel clusters that are seen as yellow lake might not be, and other yellow lake particles might not be taken into the equation.

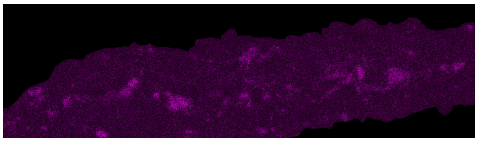

(a) Potassium map of cross-section of sample 40_15

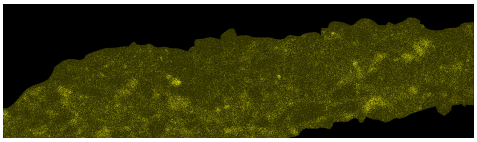

(b) Calcium map of cross-section of sample 40_15

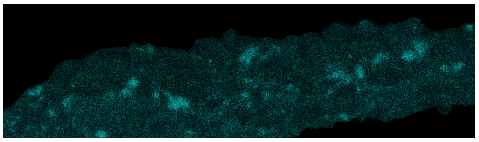

(c) Sulphur map of cross-section of sample 40_15



(d) Filtered out yellow lake

Figure 4-22: Process of filtering out yellow lake.
Figures **(a)**, **(b)** and **(c)** shows the input elemental maps.
(d) shows the output, where **(a)**, **(b)** and **(c)** are combined. White pixels represent the yellow lake clusters.

4-1-3-3 Microscope images -volume fractions of bone black, red earth and yellow earth

The focus of this chapter is to show the steps taken to filter out the pigments, bone black, red earth and yellow earth. This is based on the microscope images and uses the fact that every pigment, bone black, red earth and yellow earth has a different RGB value.
To start the microscope images are enhanced to show more detail and make the colours more vivid. The images are sharpened and stretched. By stretching the image the RGB range of the image is increased, so the colours are more vivid. By sharpening the image there is more distinction between the different pigments particles. This is done on all the microscope images (UV, bright field and dark field).

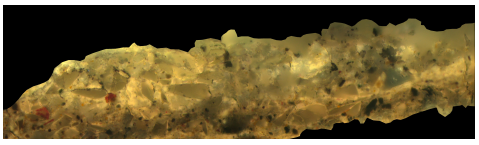

(a) Microscope image of cross-section of sample 40-15 in UV showing the region of interest.

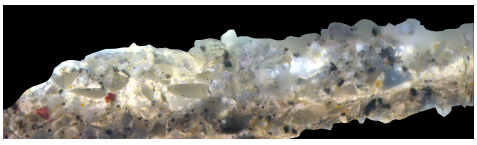

(b) Microscope image of cross-section of sample 40-15 in UV showing the region of interest. The figure is stretched and sharpened.

Figure 4-23: UV images with different mutations
(a) is the input image.
(b) shows **(a)** with a larger range of RGB values (stretched) and more distinct transitions between the pigment particles and the oil matrix (sharpened).

4-1-3-3-1 Bone black The focus of this sub-paragrarh is to show the step taken to filter out the pigment particles of bone black.
Bone black is best visible in sharpened and stretched UV image; see Figure 4-24a. Through the Colour Thresholder in the UV image RGB values were selected that were only present in the bone black particles. The result of that is Figure 4-24b. Here, the black particles are filtered out of the Figure 4-24a and the rest of the pixels are set to grey. This method works well, but might be that not all bone black particles are filtered out due to the fact some particles have a slightly different RGB value than selected. To visual check that the bone black particles are filtered out, the last image in Figure 4-24 shows the UV image without bone black particles.
The area of the bone black particles is summed and divided by the region of interest to come to a volume fraction.

4-1-3-3-2 Red earth The focus of this sub-paragraph is to show the steps taken to filter red earth out of the samples. The same method is used as for bone black and it is based on RGB value or red earth. Red earth is visible in all the three different microscopic lighting settings, as seen on the left side of Figure 4-25. For that reason, the choice is made to use all three lightings, bright field, dark field, and UV.
From all the three images, see Figure 4-25, red earth was filtered out using the Colour Thresholder. Per image more than one range of RGB value was used, since the colour of red earth can vary from bright red to a more pinkish colour. The pixel clusters were dilated to match the red earth particles as precisely as possible. The outcome can be seen in Figure 4-25b.

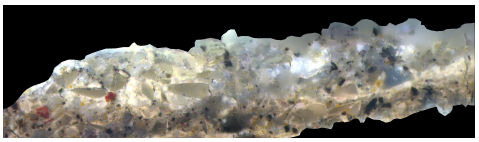

(a) Microscope image of cross-section of sample 40-15 in UV showing the region of interest and stretched and sharpened.



(b) The same as **a**, but only the bone black particles of the cross-section are visible.

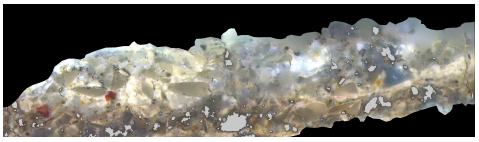

(c) The inverse of **(b)**, showing the cross-section sample **(a)** without bone black particles.

Figure 4-24: Steps of filtering out bone black

Here the red particles from the different input images are filtered out.
The difficulty with red earth is that the colour can vary. Therefore it is possible that not all the red earth particles are taken into account, even though a range was taken into account when using the Colour Thresholder. To visual check that the red earth particles are filtered out the last image in Figure 4-25 shows the UV image without red earth particles. The area of the red earth particles is summed up and divided by the area of interest, which results in the volume percentage of red earth.

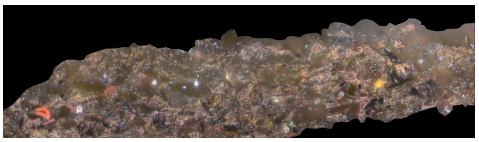

(a) Microscope image of cross-section of sample 40_15 in dark field showing the region of interest.



(b) The same as **(a)**, but only the red earth particles of the cross-section are visible.

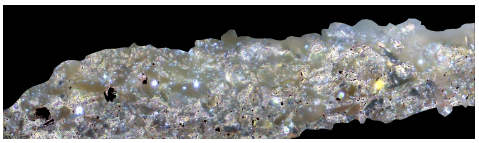

(c) The inverse of **(b)**, showing the cross-section sample **(a)** without red earth particles.

Figure 4-25: Steps of filtering out red earth

4-1-3-3-3 Yellow earth The focus of the sub-paragraph is to show the steps taken to achieve the volume percentage of yellow earth. It uses the same method as bone black and red earth, also the filtered out yellow lake image, Figure 4-22d is used. This is, because some of the yellow lake particles appear yellow. Yellow earth is best visible in the stretched and sharpened image. Through the use of Colour Thresholder an RGB range is chosen, which filter out the yellow coloured particles. Figure 4-26 shows on the left side the input UV

image, while on the right side it shows the yellow earth filtered out particles. Since some of the yellow lake particles still show some yellow colouring, the yellow lake map was placed on top of the yellow earth map and only the yellow pigments, which were not visible in the yellow lake map, were stated to be yellow earth. As can be seen in Figure 4-23a of the UV image of the sample, it shows that the oil matrix has a yellow colour. It is difficult in that image to make out the yellow earth particles. The stretched image make it easier, but still is hard to distinguishes between yellow earth and the oil matrix. That means that some of the yellow particles might not be filtered out. To visual check that the yellow earth particles are filtered out the last image in Figure 4-26 shows the UV image without yellow earth particles. The yellow earth particle areas were summed together and divided by the area of interest, so the volume fraction could be calculated.

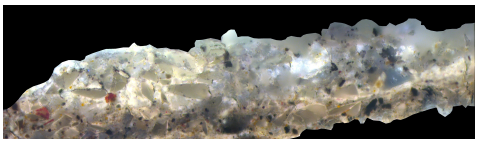

(a) Microscope image of cross-section of sample 40_15 in UV showing the region of interest.



(b) The same as **(a)**, but only the yellow earth particles of the cross-section are visible.

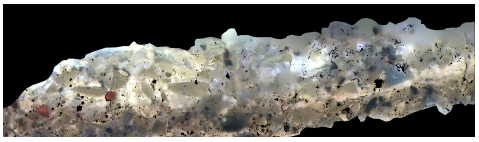

(c) The inverse of **(b)**, showing the cross-section sample **(a)** without yellow earth particles.

Figure 4-26: Steps of filtering out yellow earth

4-1-3-4 Concentration of pigments per sample

The concentration of pigments is calculated following the steps shown in the previous paragraphs. The samples calculated are 215/2, 215/3, 40_7, 40_12 and 40_15. Table 4-3 shows the non-normalised fractions. This means the calculated fraction of pigments. Table 4-4 show normalised fraction, here each fraction is the calculated fraction of pigments plus the oil binder.

Table 4-3: Non-normalised fraction of pigments in samples 215/2, 215/3, 40_7, 40_12 and 40_15

Sample	Bone black	Red earth	Smalt	Yellow earth	Yellow lake	Yellow pigments	Total	Oil
215/2	-	-	24.63	-	9.27	-	-	-
215/3	6.74	3.12	30.23	5.29	6.21	-	51.59	48.41
40_7	1.85	1.44	32.7	3.42	2.8	-	42.21	57.79
40_12	3.12	5.76	41.12	-	-	3.26	53.26	46.74
40_15	4.07	2.22	30.56	3.81	5.41	-	46.07	53.93

Table 4-4: Normalised fraction of pigments in the samples 215/3, 40_7, 40_12 and 40_15

Sample	Bone black	Red earth	Smalt	Yellow earth	Yellow lake	Yellow pigments	Total
215/3	13.06	6.05	58.6	10.25	12.04		100
40_7	4.39	3.41	77.45	8.11	6.64		100
40_12	5.85	10.81	77.21			6.12	100
40_15	8.89	4.85	66.73	8.31	11.22		100

4-1-3-4-1 Fraction of pigments in sample 215/2 Table 4-3 shows the fraction of smalt and yellow lake. Looking at the SEM-EDX image of the sample (Figure 4-11), it shows that only a very small part of the smalt layer is captured. This was subsequently linked to the microscope images (Figure 4-10). Since smalt is densely packed in the area and the yellow lake clusters are also in that area, those could be easily calculated. For the other pigments, they were more heterogeneously distributed throughout the smalt layer and therefore the region of interest was not a good representation of the distribution of the other three pigments. What was already seen in the microscope image was that there is a compact layer of smalt and a few yellow lake clusters, which translated into a high fraction of smalt and a lower fraction of yellow lake.
Since not all the volume percentage of the five pigments are calculated it is impossible to normalize the data.

4-1-3-4-2 Fraction of pigments in sample 215/3 Tables 4-3 and 4-4 show the pigment concentration of sample 215/3. As suggested from Figure 4-12, smalt is the main pigment, which is verified when calculating the pigment fractions. There is also a high amount of bone black in the sample. This correlates back to the sample location, which is in the shadow of the pillar. Since the pigment fractions add up to 51.59%, the rest of sample consists of the oil matrix.

4-1-3-4-3 Fraction of pigments in sample 40_7 Tables 4-3 and 4-4 show the fraction of pigments of sample 40_7.
The biggest difference between sample 215/3 and 40_7 is that there is less bone black in sample 40_7. Comparing the sample locations, sample 40_7 is a less dark area than the area of sample 215/3. Smalt is still the main element of the sample and over 50% of the sample consists of the oil matrix.

4-1-3-4-4 Concentration sample 40_12 Tables 4-3 and 4-4 show the pigment concentration of sample 40_12. As can be seen there is no distinction between yellow earth and yellow lake pigments. This is due to the fact that the scan time of the sample was very short, therefore the noise could not be filtered out from the potassium, calcium, and sulphur maps. Therefore, all the yellow coloured pigments were filtered without making a distinction between yellow earth and yellow lake.
As suspected from the microscope and SEM images, the smalt layer is very compact. It has the highest amount of smalt compared to the other samples.

4-1-3-4-5 Concentration sample 40_15 Tables 4-3 and 4-4 show the pigment percentages of sample 40_15. In this sample, the amount of bone black is closer to that of sample 215/3; Table 4-4. When comparing the calcium XRF image and the painting, we can explain this since both of the samls are taken in shadow areas of the pillar. Smalt is again the main pigment in sample 40_15. In this sample, roughly the same amount of yellow lake is present as in the other samples.

4-1-3-5 Conclusion and discussion

To conclude, by using the SEM-EDX and the microscope images, it was possible to estimate the pigment volume concentration of the smalt layer in samples 215/2, 215/3, 40_7, 40_12 and 40_15. It also shows that smalt was the main pigment throughout the samples. The rest of the pigments were bone black, red earth, yellow earth and yellow lake.

As was already seen in the Macro-XRF images, the pigment concentration is not homogeneously spread in the background, but varies from location to location, most likely creating interesting subtle colour differences.
The outcome of the pigment concentrations per sample will be used in the next paragraph, where it will be plotted against the value of the Macro-XRF image.

It should be taken into account that there are three factors limiting the accuracy of the volume calculations . As seen in sample 215/2 the smalt layer exists only partially. Therefore, it was impossible to make an accurate estimation of the pigments that were present in smaller quantities. The EDX images of sample 40_12 are very noisy and therefore it was impossible to calculate the concentration of yellow lake.
The surface areas of all the samples are very small and therefore cannot represent correctly that particular section of the background.
Also, discriminating the pigments by colour may lead to errors. The pigment particles might look as if they have the same colour red, but in reality one might look lighter/darker or have a different shade. Therefore, it is possible that not all the pigment particles present were measured.
To make sure that the amount of error is limited, an image of the sample without the particles is consulted to see if all the pigment particles are filtered out.

4-1-4 Smalt and yellow lake concentration in *The Jewish Bride*

The volume fraction per sample for smalt and yellow lake are set against the Macro-XRF intensity (between values 0–1) of that sample location and a relationship for smalt and yellow lake can be found.
The sample locations were measured on the painting itself. This transferred to a pixel location in the Macro-XRF image. Between the pixel location there can be some small fluctuations, therefore the average value of 9 pixels around the sample locations was taken.
The Macro-XRF values for cobalt and potassium on the sample locations are plotted against the pigment concentrations of the non-normalised smalt and yellow lake calculated out of the samples, Table 4-3. The reason for using the non-normalised concentration is that for sample 215/2 is not normalised.
Figure 4-27 shows the correlation. Looking at Figures 4-27, they show that the cobalt Macro-XRF value and the amount of smalt seems to have a relationship, as does potassium Macro-XRF value and the amount of yellow lake.
A linear relationship can be found and is stated in two formulas, here the R^2 also is given.

$$Smalt\ percentage = 45\ x\ Intensity\ of\ Cobalt \tag{4-1}$$

The R^2 value is 0.43.

$$Yellow\ Lake\ percentage = 11\ x\ Intensity\ of\ Potassium \tag{4-2}$$

The R^2 value is 0.60.
This formula can be extrapolated to the whole painting, giving the amount of smalt and yellow lake in every pixel of the Macro-XRF image using the formulas.
Since roughly half of the sample is the oil matrix, the formula can be normalised by multiplying by two.

4-1-4-1 Conclusion and discussion

To conclude, from analysing the limited number of available samples, it shows, in Figure 4-27, that it does not give a high accuracy. Therefore the only conclusion that can be stated is that low amount of cobalt means low amount of smalt and vice versa. The same conclusion holds for yellow lake and potassium.

The main limitation of the relationship as shown above is the number of samples present. Only 4 of 5 samples are used. Therefore the R^2 is very low, since the fluctuation in measuring data of the Macro-XRF and the calculation of the pigment concentration cannot be accounted for. This would even out if more samples were available. The Figure 4-27 can only suggest that there exists a linearity between the pigment concentration and the ratio of that relation might change, if more samples were taken into account.
An error is made when linking the potassium Macro-XRF map absolutely to yellow lake, since potassium is also an element of smalt, although, looking at the Macro-XRF map in paragraph 4-1-1, no link between the images could be found. Nevertheless, this does influence

the accuracy of the linear relation between potassium and yellow lake.
A link between the Macro-XRF of calcium and bone black and the Macro-XRF of iron and earth pigments was not found. This is due to the limited amount of samples that could be used.
The link between smalt and the Macro-XRF image of cobalt and the link between yellow lake and the Macro-XRF image of potassium will play a role in section E of this chapter. Here it will function as a guide for the concentration of yellow lake and smalt that will be digitally 'mixed' back in the focus area.

4-1-5 Conclusion section A and discussion

To conclude, the Macro-XRF images show the heterogeneous distribution of the pigments; bone black, earth pigments, smalt, and yellow lake.
The cross-section samples of the background of *The Jewish Bride* show that between the five samples the distribution of pigments also varies. Here the five pigments were present, bone black, red earth, smalt, yellow earth, and yellow lake, but smalt was the main pigment used throughout. This was quantified by calculating the pigments volume fraction. By plotting the Macro-XRF values of cobalt and potassium against the percentages of smalt and yellow lake of the samples, a relationship was found, from which showed that low amount of cobalt means low amount of smalt and vice versa. The same goes for yellow lake and potassium.
The main limitation for section A is the size and the amount of the paint cross-sections. This influences the accuracy of the calculated pigments. In addition, it influences the accuracy of the relationship between the amount of smalt and yellow lake and the Macro-XRF value.

In section E this relationship will be used as a guide for the digital colour reconstruction. Through this link, the different concentrations of pigment per location can be taken estimated. This will show the highlights and lowlights of smalt and yellow lake as Rembrandt may have intended it to.

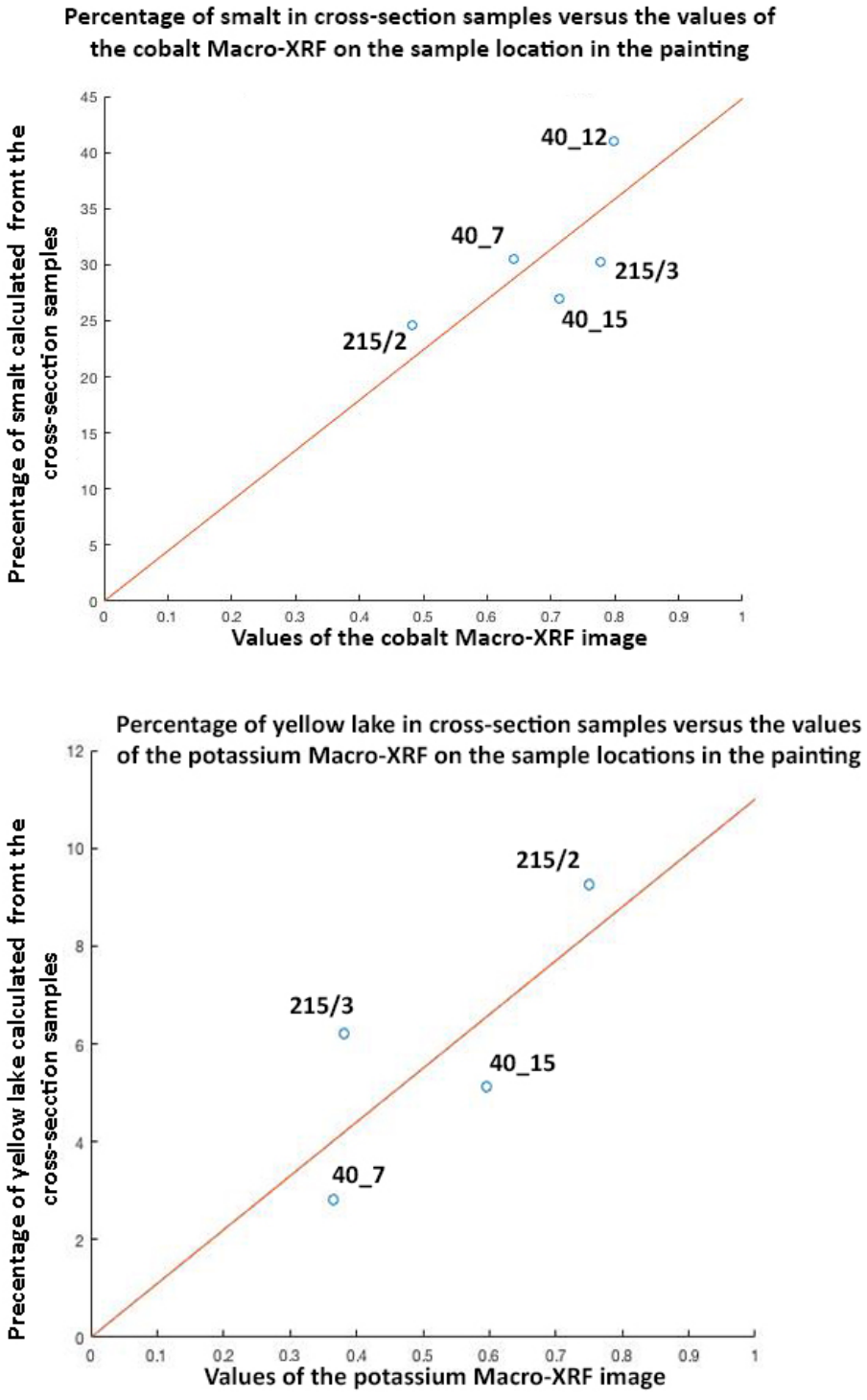

Figure 4-27: The Macro-XRF values for cobalt and potassium on the sample locations are plotted against the pigment concentrations of the non-normalised smalt and yellow lake calculated out of the samples, Table 4-3. The relationship that appears is that that low amount of cobalt means low amount of smalt and vice versa. The same holds for yellow lake and potassium.

4-2 Section B - Reflectance curves of *The Jewish Bride*

The focus of this section is on the translation of the hyperspectral data into RGB values and the translation of the hyperspectral data into K/S values using the Kubelka-Munk theory. The hyperspectral imaging of *The Jewish Bride* was executed by John Delaney (Senior Scientist, National Gallery of Art in Washington D.C.) [17].

By translating hyperspectral data into K/S values, it is possible to digitally 'mix' paint and also to 'un-mix' paint pigments. This is done by adding and subtracting K/S values of paint colours in different concentrations. This makes the K/S value very suitable for digital colour reconstruction and the K/S data set will be used in section E, when the focus is on digital colour reconstructions. The formulas used for the translation are shown in Chapter 2.

John Delaney[17] translated the scanned data into hyperspectral data. The hyperspectral data of *The Jewish Bride* is transferred into K/S values and RGB values. The RGB image is shown in Figure 4-29.
The focus area hyperspectral data is also transferred into RGB value and can be seen in Figure 4-30. The translations from the hyperspectral data to K/S values for the focus area was done by John Delaney[17].
Figure 4-28 shows the format of the dataset of the focus area: it is a matrix of 255 rows by 243 columns and has 217 layers. The row and columns give the location of the scanned area, while the layers show the reflection per wavelength.
Figures 4-29 and 4-30 show specular reflection. This is seen as white glare in the figures. This is where light reflects back without interaction with the paint layer. Therefore, it contains no colour information. This is due to the lighting of the painting, while scanning. Specular reflection also appears when there is a rough surface, therefore it appears around cracks in the painting.

There were negative values in the reflectance curves. Reflection itself cannot be negative, so negative values are errors in the dataset. The negative values were set to the closest positive value. There were also negative values in the K/S dataset and those were also set to the closest positive value.

To give an insight in the hyperspectral data, four pixels are chosen in the focus area; see Figure 4-31. Figure 4-32 shows the three different representations of the four pixels. The top image shows the pixels in RGB values. The middle image shows the pixels as hyperspectral data. The bottom image shows the pixels as K/S values. As can be seen, even though the pixels appear to have the same colour in Figure 4-31, they differ. The yellow colour appears to be lighter than the other colours. When looking at the reflectance curve, it shows that it has the highest reflection, while the shadow area is darker and shows in the reflectance curve the lowest values. Between the leaves and below the leaves, in the reflectance spectra, they appear to have the same curve, but the pixel below the leaves has a higher reflectance. This is why in the RGB values the leaves appear darker and the background of lighter colour. The K/S value shows as peak were the reflectance spectra are low and very low were they are high.

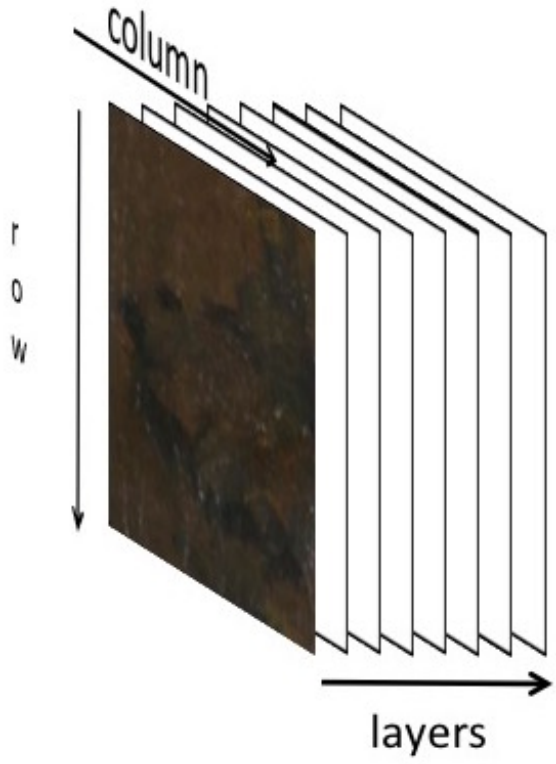

Figure 4-28: Schematic representation hyperspectral data set of the focus area. The row and columns give the location of the scanned area, while the layers show the reflection per wavelength.

4-2-1 Conclusion of section B and discussion

To conclude, the hyperspectral data is transformed into RGB values as well as K/S values. Figures 4-29 and 4-30 show specular reflection. Specular reflection contains no colour information and effects the accuracy of the scan.

The transition from hyperspectral data to RGB value of the whole painting is used in section E.1, when the colour of a sample location is compared with the paint-out based on the concentration of that sample.
The RGB image of the focus area will be used throughout section E, since it shows the present day colour of the focus area.
The K/S value of the area of interest are used in sections E.2 and E.3, where they will function as the basis for the digital colour reconstruction.
The main limitation is shown in Figure 4-29, where there are many areas where specular reflection is visible. It also shows in Figure 4-30, but less prominently. The specular reflection

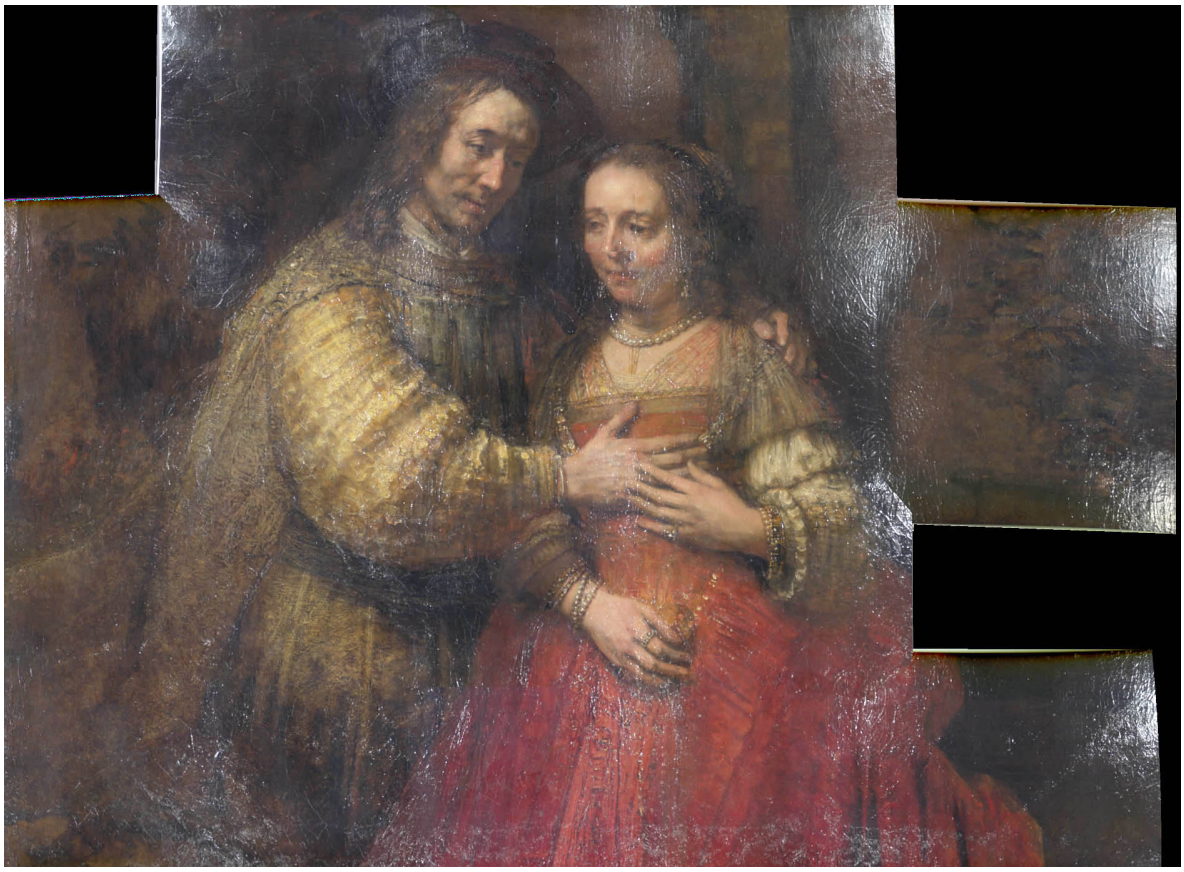

Figure 4-29: Hyperspectral scan in RGB of *The Jewish Bride*



Figure 4-30: The focus area in RGB based on the hyperspectral scan



Figure 4-31: Different pixels in the painting, which in Figure 4-32 are shown in RGB, hyperspectral curves and K/S curves

appears to come from the craquelé of the painting and the lighting while scanning. As stated in the previous chapter, the specular reflection highly influences the accuracy of the reflection curves and therefore K/S curves. Specular reflection has no colour information, since it is white coloured. The specular reflection is little in the focus area and will have a limited effect when the focus area undergoes digital colour reconstruction. The negative measurements also affect the accuracy of the outcome, but all the points were set to the closest positive value.
For future research it will be interesting to investigate hyperspectral data more to analyse pigment concentrations. In order to do this additional scans of the individual paint pigments samples are required, as well as additional scans of the painting itself to minimize specular reflection.



(a) Pixels from hyperspectral data translated into RGB.

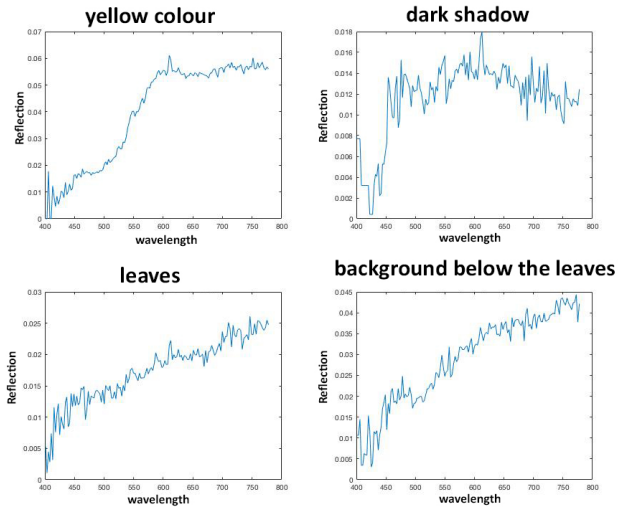

(b) Pixels in reflection curves. Locations in the focus area are shown in Figure 5-31

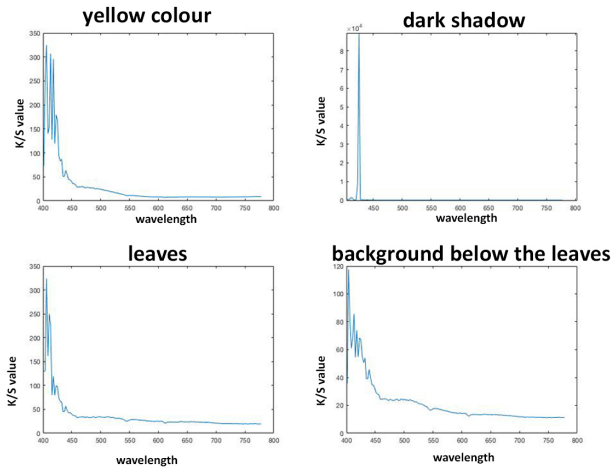

(c) Pixels from hyperspectral data translated into K/S values.

Figure 4-32: Pixels, from locations shown in Figure 5-31, represented in RGB, reflection curves and K/S values.

4-3 Section C - Paint-outs

The focus of section C is to determine the effect of non degraded smalt and yellow lake on the colour in paint mixtures and to scan these paint mixtures through hyperspectral imaging. This is to determine the K/S value of non-degraded smalt and yellow lake.

To get to this insight, four different sets of paint-outs are made. Paint-outs are paint swatches. All the mixtures use non-degraded smalt and yellow lake made by Diana de Man (MA Conservation and Restoration of Paintings, University of Amsterdam)[11]. The amount of cobalt in the smalt used is 4%, which is a good estimation of the amount of cobalt used by Rembrandt as described in section 5-1-2-8. EDX spot analysis of the smalt particles showed that Rembrandt smalt had 3.6% cobalt.

This paragraph is sub-divided into the four different sets of paint-outs and in hyperspectral analysis, with the focus on the scans of non-degraded smalt and yellow lake.
The first set of paint-outs is based on the concentrations of pigment found in the cross-section of *The Jewish Bride* samples (based on section 4-1-3). This is to see how these samples originally look liked with non-degraded smalt and yellow lake.
The second set is based on the same cross-section samples as the first set, but are made without smalt to see the difference between using smalt and not using smalt.
The third set is based on cross-section sample 40_15 (shadow area of the beam). Here the concentration of bone black, red earth, yellow earth, and yellow lake is changed individually from the other pigments. This is to see how the colour of the mixture is influenced by the changing concentration of one pigment, while the rest of the mixture stays the same.
The fourth set focuses on mixtures of smalt with one other pigment in different concentrations. This is to see how smalt influences the colour of the pigment mixture.
From all the sets of paint-outs, the reflectance curve was measured and preliminary analysed by John Delaney[17]. Besides the paint-outs stated above, the smalt paint-outs made by Diana de Man[11] were scanned. The hyperspectral data was then transferred into RGB values and K/S values.
The making of the paint-outs is detailed and all the images of the tiles can be seen in Appendix D.

4-3-1 First set of paint-outs

The first set of paint-outs are based on the calculated pigment concentrations of 40_7, 40_15 and 215/3; Figure 4-33. The pigment fractions are shown in Table 4-5.
There is some colour difference between the different paint-outs, but not as much suggested by the difference in pigment concentration. This is most likely due to the fact that they are all very dark mixtures, which corresponds with the sample locations. Those locations are all in the shadow area of the background. To create a significant colour change in a dark mixture, larger differences in pigment concentrations are needed.
The hyperspectral data is tempered by specular reflection and therefore could not be used. The specular reflection appears because the paint mixture is very rough, because of the glass particles.

Table 4-5: Amount of pigment without oil in percentages on which paint-outs seen in Figure 4-33 are made

Pigment	40_7	40_15	215/3
Bone Black	4.4	8.9	13.1
Red Earth	3.4	4.8	6.0
Smalt	77.5	66.7	58.6
Yellow Earth	8.1	8.3	10.3
Yellow Lake	6.6	11.2	12.0

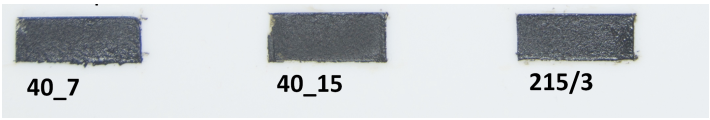

Figure 4-33: First set of paint-outs using pigment mixture described in Table 4-5 using no-degreaded smalt. The paint-outs based on the calculated pigment concentrations of 40_7, 40_15 and 215/3 and showing little colour difference between them. They all appear dark and cool of colour.

4-3-2 Second set of paint-outs

Figure 4-34 shows the same samples as in the previous sub-paragraph 4-3-1, but without the use of smalt. The pigment concentration can be seen in Table 4-6. Comparing Figure 4-34

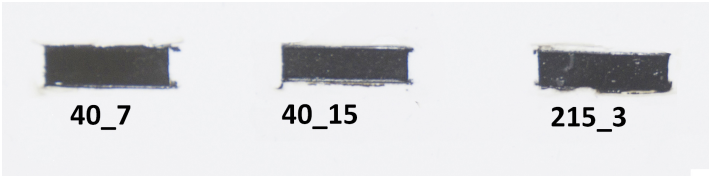

Figure 4-34: Second set of paint-outs using pigment mixture described in Table 4-6. The paint-outs shows the same samples as in the previous sub-paragraph 4-3-1, but without the use of non-degraded smalt. There is more colour difference between the samples and they appear browner than Figure 4-33.

to the first set of paint-outs, Figure 4-33, they have a difference in colour appearance. The first paint-out set with smalt appear very dark and has a cool colour. The second paint-out set without smalt has a warmer colour and appears to have a brownish colour. By adding large quantities of smalt, it makes the mixtures appear to have a cooler and darker colour, which is visible in the first paint-out. Also a colour change appears due to the loss of texture that smalt glass particles gives.
In the second paint-out set, a colour difference between the pigments is visible, Figure 4-35. Still the paint-outs are very dark, this is also visible in the reflection curves, where the reflection is around 0.03. The little difference in the reflection curves do lead to colour differences, Figure 4-35.

Table 4-6: Amount of oil per pigment and fraction on which paint-outs seen in Figure 4-34 are made

Pigment	40_7	40_15	215/3
Bone Black	19.5	26.7	31.6
Red Earth	15.1	14.6	14.6
Smalt	0.0	0.0	0.0
Yellow Earth	35.9	25.0	24.8
Yellow Lake	29.5	33.7	29.1

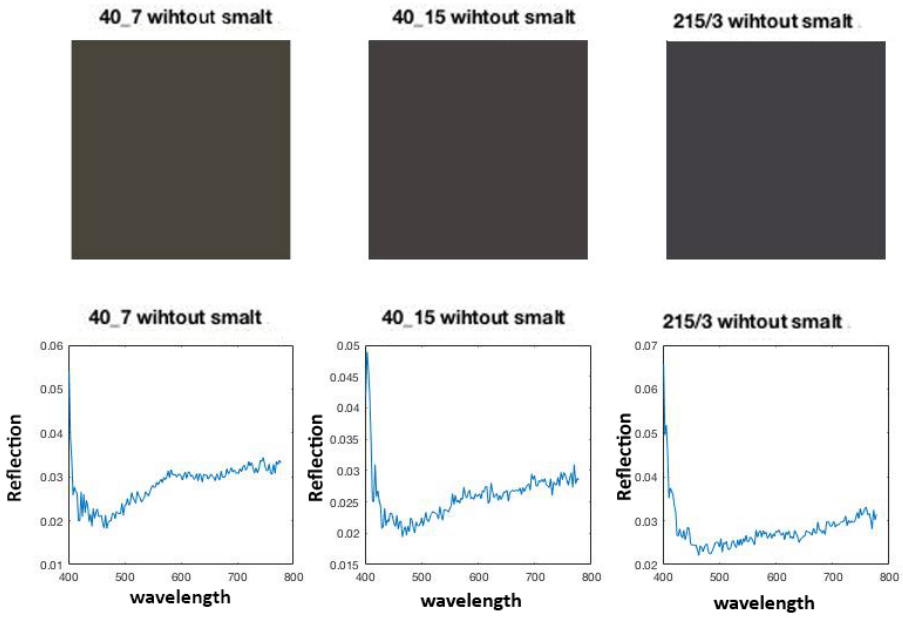

Figure 4-35: RGB values of the three paint-outs based on the reflection curves.
The paint-outs are very dark, this is also visible in the reflection curves, where the reflection is around 0.03. The little difference in the reflection curves do lead to colour differences.

4-3-3 Third set of paint-outs

Figure 4-36 shows the third set of paint-outs based on sample 40_15. The difference in percentages per pigment from sample 40_15 are shown in the figure, with only one pigment percentage changed per paint-out. The pigment concentrations that have changed are; bone black (BB), red earth (RE), yellow earth (YE), and yellow lake (YL). As can be seen in Figure 4-33, the colour change is quite small between the different paint-outs, although there is a large difference in concentration. This is most likely because the basis of the paint mixture of sample 40_15 is very dark. Changing the different pigment concentrations of a very dark mixture does not affect it as much as a lighter paint mixture is affected. Therefore, it is impossible to get an insight about how the different pigments affect the paint mixture.
The hyperspectral data is tempered by specular reflection and therefore could not be used.

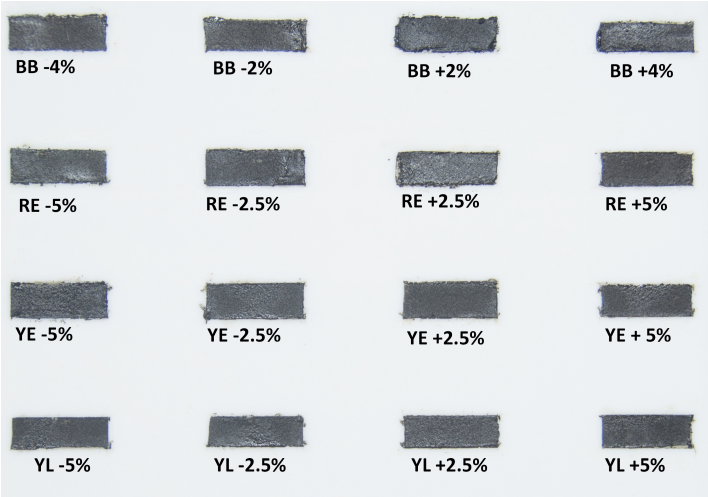

Figure 4-36: Third set of paint-outs. The paint-outs are based on sample 40_15. The difference in percentages per pigment from sample 40_15 are shown in the figure, with only one pigment percentage changed per paint-out. There is no real colour difference between the different paint-outs.

The specular reflection appears because the paint mixture is very rough, because of the glass particles.

4-3-4 Fourth set of paint-outs

Figures 4-37 and Figure 4-38 show the fourth set of paint-outs. Figure 4-38 shows the paint-out of non-degraded smalt, which is made by Diana de Man[11]. Looking at Figure 4-37, it is seen that every pigment has its own interaction with smalt, starting on the left with a mixture of bone black and smalt. Every mixture between the two pigments appears dark. This has to do with the fact that bone black is a very absorbent pigment, while smalt is transparent pigment. When mixed together it always appears the same colour as the bone black pigment, even when only 25% is bone black. A small colour difference does appear using the hyperspectral data, Figure 4-39. Here it shows that the mixtures do get darker.
The second mixture is that of red earth and smalt. When mixing red earth with smalt in different concentrations, there is a colour difference between the mixtures. The top mixture has a purplish colour, while the third mixture is clearly red. This colour difference is even better observed in the hyperspectral data, Figure 4-40. Here is shows that the red colour is created through the intensification of the reflection from around 600 nm to 750 nm. This is also seen in, Table 2-3, in Chapter 2. Here it is shown that the red colour is between wavelength 630 nm – 750 nm.
The third mixtures is that of yellow earth and smalt. When changing the concentration between them they appear from a greenish colour to a more yellow colour. These steps are also seen in the hyperspectral data, Figure 4-41. Here it is shown that the yellow colour comes from an intesification of the reflection from around wavelength 550 nm – 650 nm. This is also supported in, Table 2-3. Here it shows that yellow colour is around 570 nm – 590 nm.
The fourth mixture is that of yellow lake and smalt. The mixtures go also from dark brown-

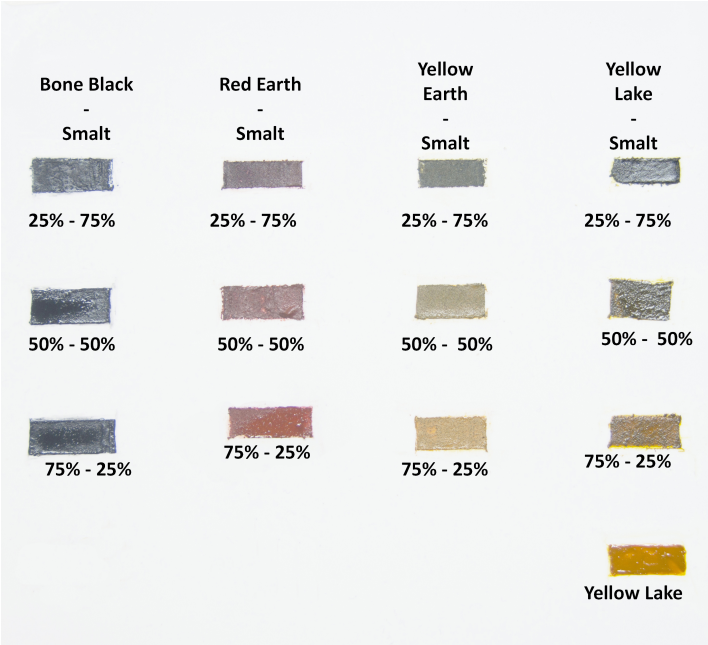

Figure 4-37: Fourth set of paint-outs
Here mixtures of non-degraded smalt and another pigments are shown. It is seen that every pigment has its own interaction with non-degraded smalt

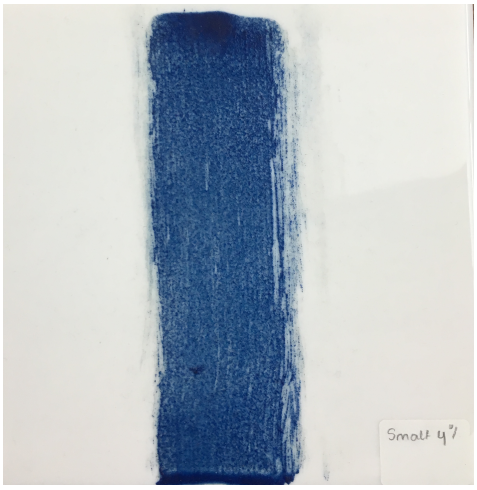

Figure 4-38: Paint-out Smalt 4% cobalt made by Diana de Man [10][11]
It shows that smalt is not evenly distributed over the surface.

ish/greenish to yellow, although compared to the yellow earth and yellow lake mixtures, they appear darker, especially the inside of the paint-out of 25% yellow lake and 75% smalt. This is most likely due to the fact that yellow lake has less colour strength than yellow earth and therefore the darker colour from the smalt is more dominant. Looking at the yellow lake paint-out at the bottom, it shows that the yellow lake has a reddish undertone. The colour

change is also visible in the hyperspectral data, Figure 4-42. Here it shows that around 550nm – 680 nm the reflection intensifies. Compared to the hyperspectral data of the yellow earth mixture it shows that the reflection is less apparent and that there is no dip in the reflection around 650 nm for the yellow lake mixture, see Figure 4-41. This means that the colour is a bit more reddish yellow, than bright yellow.
Focusing on the smalt paint-out, Figure 4-38 shows that smalt is not evenly distributed over the surface. This is because spreading glass particles evenly over a tile is very difficult, since it tends to scratch. On the top and bottom of the tile there is accumulation of smalt, there it is also visible that in large quantities it tends to be darker than expected from the middle part.

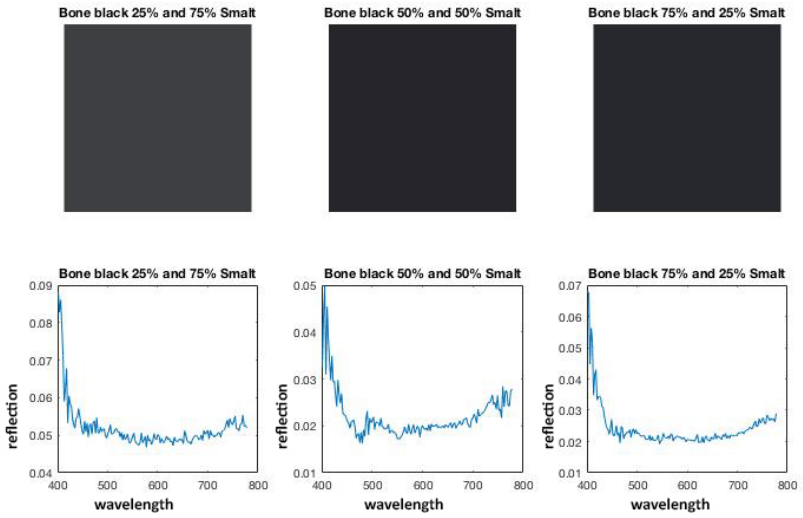

Figure 4-39: RGB and reflection curves of bone black and smalt mixtures. It shows that smalt has little effect on the colour of the mixtures.

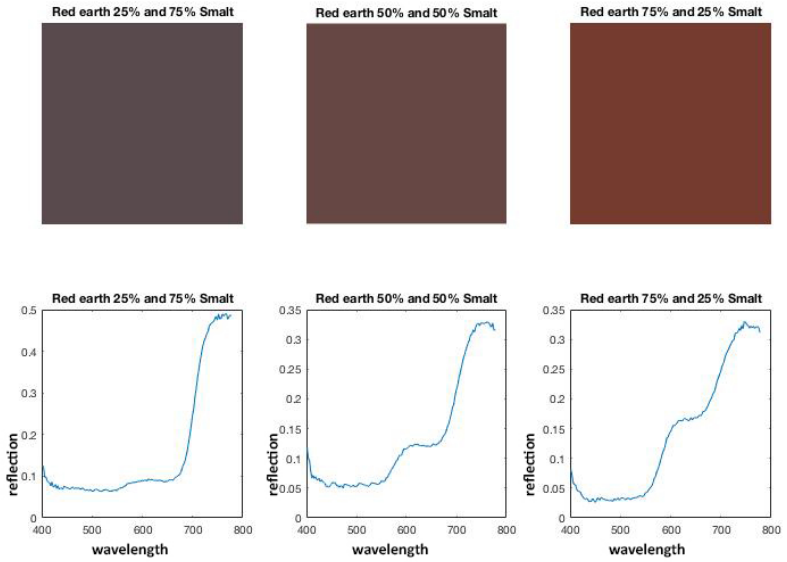

Figure 4-40: RGB and reflection curves of red earth and smalt mixtures. It shows that large amount of smalt make the colour more purple.

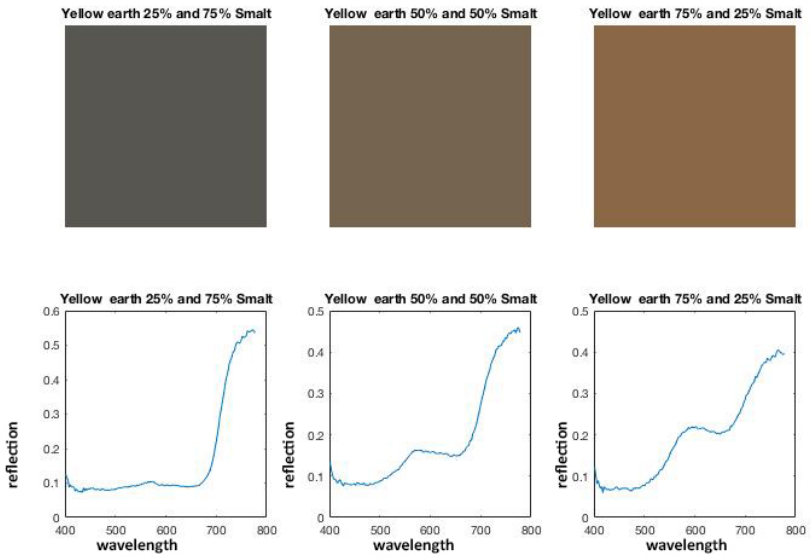

Figure 4-41: RGB and reflection curves of yellow earth and smalt mixtures. It shows that large amount of smalt make the colour more green.

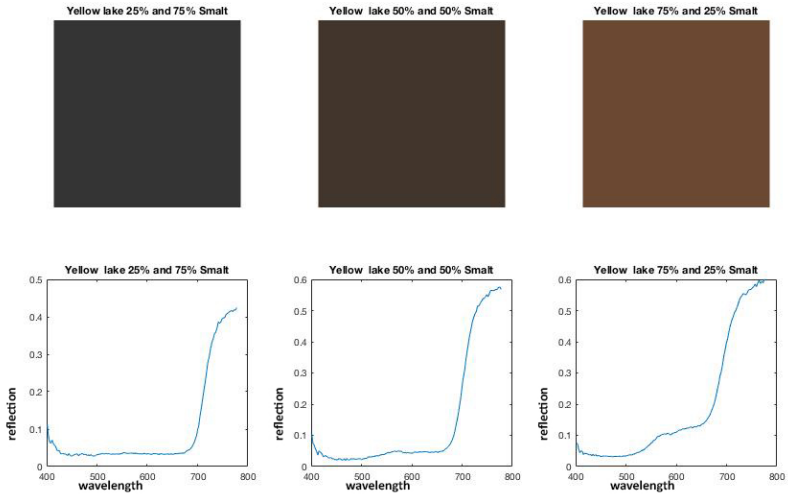

Figure 4-42: RGB and reflection curves of yellow lake and smalt mixtures. It shows that smalt makes the colour darker.

4-3-5 Hyperspectral analysis of smalt and yellow lake

All the tiles were scanned using hyperspectral imaging techniques, which was executed by John Delaney[17]. He also did the preliminary processing and analysis of the data. The hyperspectral data was changed into RGB values as well as K/S values. Both these values play a role in section E. The RGB value of one of the paint-outs will be used in section E.1, while the K/S of smalt and yellow lake will play a main role in section E.2 and in the final digital reconstruction of section E.3.

Figure 4-43 shows the different representations of smalt and yellow lake. At first the RGB values are shown. The colour of the yellow lake is a reddish yellow as was already seen from the paint-out. The blue of the smalt is a very dark and cool colour. As can be seen in the hyperspectral data, there is an increase in the yellow lake from 500 nm, while in the blue colour of smalt there is only a very small increase between 400 nm and 500nm. Due to the formula used to calculate K/S value the two graphs appear to be opposites of the hyperspectral curves.

4-3-5-1 Assumptions of the K/S value of the pigments

A few assumptions have been taken in calculating the K/S values of the paint-outs. The transparency of the pigments is not taken into account. The K/S values were calculated based on the paint-outs on the white tile.
Also, the K/S value is calculated and not the K and S separately, which is more precise.
As can be seen in the paint-outs, the thickness of the paint is uneven. Therefore only one hyperspectral pixel of smalt and yellow lake is used, instead of the average of the whole area.

4-3-6 Conclusion of section C and discussion

To conclude, the first and second set of paint-outs show that the blue colour of non-degraded smalt influences the colour of the mixtures. Smalt added in a mixture makes the colour darker and cooler of tone, also the paint-outs without smalt appear of browner colour.
Also from smalt and yellow lake, the RGB values, hyperspectral curves and K/S values were measured/calculated. It is visible that yellow lake has a reddish yellow colour.

The third set of paint-outs show that the colour difference by changing one of the pigments of a mixture does affect the colour marginally. Most likely this is due to the fact that the basis of the paint mixture is very dark and therefore it makes the difference in concentration less noticeable.
The fourth set of paint-outs shows the different effects of smalt on another pigment. It shows that it can be different per pigment.

From this set and the paint-out of smalt from Diana de Man [11], the RGB values, hyperspectral curves and K/S values were measured/calculated. In the Appendix D all the

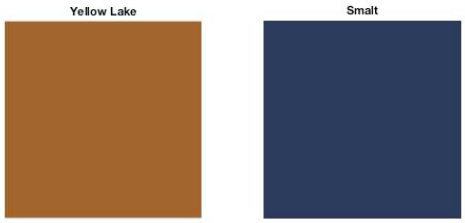

(a) Yellow Lake and Smalt in RGB. Calculated from the reflection curves of the paint-out as seen in **(b)**. Note that yellow lake has a reddish yellow colour.

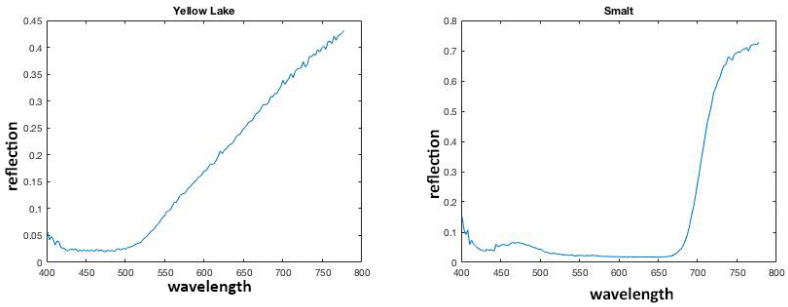

(b) Yellow Lake and Smalt in reflection curves of the paint-out.

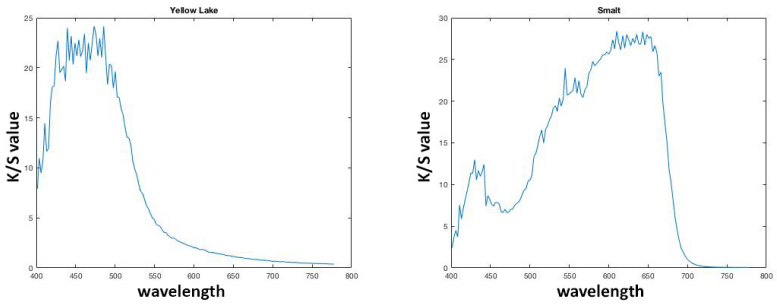

(c) Yellow Lake and Smalt in K/S values. Calculated from the reflection curves of the paint-out as seen in **(b)**.

Figure 4-43: Yellow lake and smalt represented in RGB, reflection curves and K/S values.

images of the tiles are visible and the method of creating the paint-outs is discussed.

In this chapter, all the paint-outs are compared based on interpretation of colour. As seen in Chapter 2, analysing colour based on sight is not an accurate tool for assessing. That said, the tiles do give an insight on how the mixture behaves, and large differences can be seen. The colour of smalt, as stated in Chapter 2, is not only affected by the amount of cobalt,

which in this case is very close to the smalt that Rembrandt used. It also depends on the particle size. It is very difficult to get exactly the same size and distribution of particles as Rembrandt. This could affect the colour.
The name 'yellow lake' can refer to a whole spectrum of yellow colours. The original colour of yellow lake is unknown in *The Jewish Bride*, only the elements where the dyestuff precipitated on. For this thesis only one colour of yellow lake, which has some reddish undertone, is taken into account, which might be a quite different shade.

Looking back at section A, the Macro-XRF showed the distribution of the amount of smalt in the background. From the cross-sections, it was calculated that smalt was the main pigment in the background mixtures. This would mean, looking at the first two paint-outs, that the whole background used to have a different colour, namely a darker and cooler colour.
In section E, from this insight a prediction will be made of what the focus area used to look like, which can help to verify the final digital colour reconstructions.
In section E.1 the RGB value of the first set will be used as comparison between the painting and the paint-out, and in sections E.2 and E.3 the K/S values of smalt and yellow lake will be 'mixed back' in the focus area to create the digital reconstruction.

In the next section, the method will be tested and discussed.

4-4 Section D - Cross-section analysis of paint-out reconstruction of sample 40_15

The focus of this paragraph is to determine the accuracy of the method used in this thesis to estimate the pigment concentration and to make the paint-out is.
A cross-section of paint-out reconstruction of sample 40_15 was taken.

This sample was analysed using the microscope and SEM-EDX. The SEM-EDX analysis was done by Annelies van Loon[15]. Figure 4-44 shows the difference between the paint-

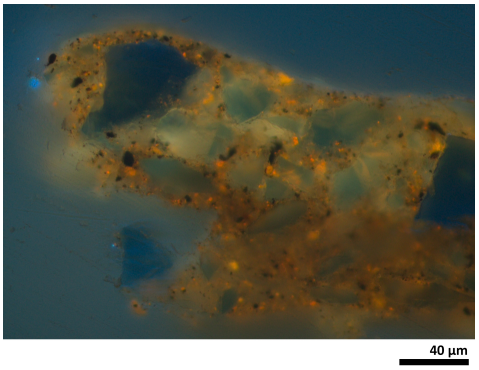

(a) Cross-section of paint-out reconstruction of sample 40_15. Microscope image under UV

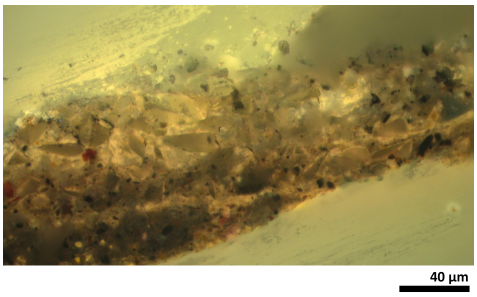

(b) Cross-section of sample 40_15. Microscope image under UV.

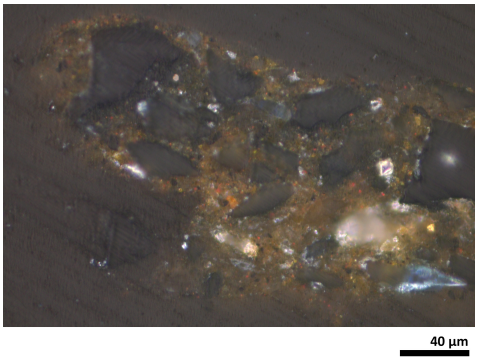

(c) Cross-section of paint-out reconstruction of sample 40_15. Microscope image under bright field

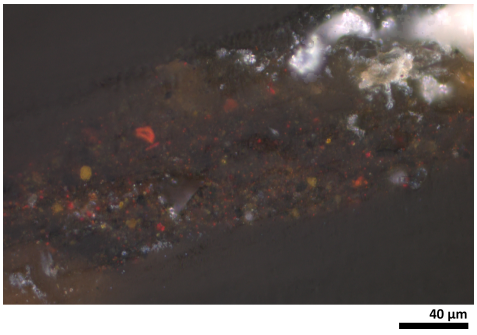

(d) Cross-section of sample 40_15. Microscope image under bright field.

Figure 4-44: Microscope images of cross-section paint-out reconstruction of sample 40_15 and cross-section of sample 40_15.
(a) the blue angular particles are non-degraded smalt. **(b)** shows degraded smalt as angular transparent particles. It shows that the smalt particles in **(a)** are bigger than in **(b)**. In both the smalt particles are evenly distributed.
All the images show that the thickness of the paint-out reconstruction cross-section sample is bigger than that of cross-section of sample 40_15.

out reconstruction of sample 40_15 and sample 40_15 using microscope images. The size of the layer differs. The paint-out reconstruction has a much thicker smalt containing layer compared to sample 40_15. As can be seen in the images, besides some very large smalt particles on the sides, smalt is very evenly distributed as is seen in Sample 40_15. Although

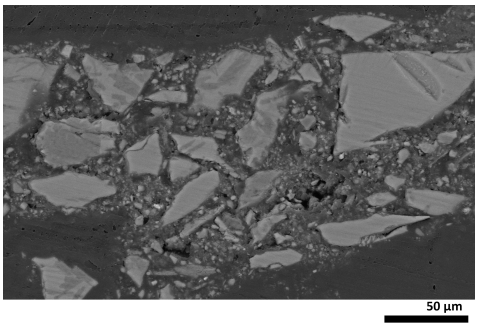

(a) Cross-section of paint-out reconstruction of sample 40_15 backscattered electron image

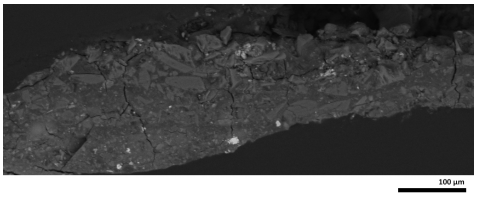

(b) Cross-section of sample 40_15 backscattered electron image

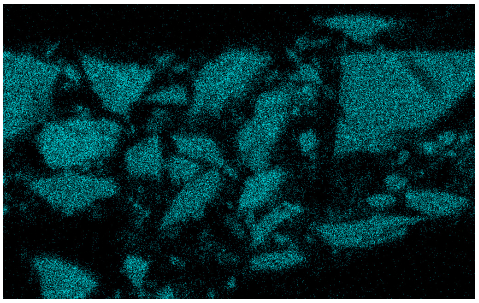

(c) Cross-section of paint-out reconstruction of sample 40_15 silicon map

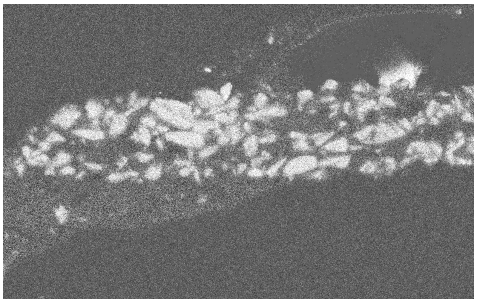

(d) Cross-section of sample 40_15 silicon map

Figure 4-45: Backscattered electron image and silicon map of cross-section paint-out reconstruction of sample 40_15 and cross-section of sample 40_15. It shows that in both the cross-section smalt is evenly distributed.

the smalt particles are smaller in sample 40_15. The distribution of bone black and yellow earth are also very homogeneous spread in the reconstruction of sample 40_15. In the bright field image, red earth is visible of the reconstruction of sample 40_15. The red earth particles do look less pronounced as is the bright field image of the sample 40_15.
Figure 4-44 shows the difference between the paint-out reconstruction of sample 40_15 and sample 40_15 using SEM-EDX images. Those images are very difficult to compare, since the reconstruction 40_15 images have a higher resolution than sample 40_15. Looking at the silicon map, Figure 4-45. the smalt particles are visible and very evenly distributed besides the bigger pigments. In the silcon map of sample 40_15 the smalt particles are also densely packed. In section A, the calcium, sulphur, and potassium maps were also included, but those were very noisy and no particles were visible there. The pigment concentration was calculated using images of Figure 4-45. The same method was used as in section A.
The differences in pigment concentrations are shown in tables 4-7 and 4-8. Table 4-8 shows the yellow pigment. The reason there is no distinction between the yellow pigments is that, as stated earlier, no clear spots were visible in the potassium, calcium, and sulphur maps. Therefore, it is impossible to calculate the amount of yellow lake. The total of the yellow lake and yellow earth pigment concentrations was calculated by RGB values instead.
Tables 4-7 and 4-8 show that there is some discrepancy between the paint-out and the cross-section paint sample, especially with bone black and red earth. Comparing this with the third

Table 4-7: Calculated pigment concentration of the cross-section of sample 40_15 and of paint-out reconstruction of 40_15

Pigments	sample 40_15	Paint-out reconstruction of sample 40_15
Bone Black	4.07	1.38
Red Earth	2.22	1.08
Smalt	30.56	33.68

Table 4-8: Calculated yellow pigment of the cross-section of sample 40_15 and of paint-out reconstruction of 40_15

Yellow Pigments	Sample 40_15	Paint-out reconstruction of sample 40_15
Yellow Earth	3.81	
Yellow Lake	5.14	
Total	8.95	10.37

set of paint-outs of the previous section, this will not have a large effect on the colour.

4-4-1 Conclusion of section D and discussion

To conclude, the paint layer itself and the calculated pigment concentration of the paint-out are not an exact replica of the cross-section samples of the painting.
Looking at the paint-out set 3 in section C, Figure 4-33, one can assume that even though there is a difference in pigment concentration in the sample, this most likely would have only a small effect on the colour perception.

Focusing on the microscope image, it shows that the pain-out reconstruction is much thicker than that of sample 40_15 and the smalt particles are bigger in the reconstruction, Figure4-44. The size of the smalt particles do have an effect the colour of smalt, as is stated in Chapter 2. However, it is very difficult to recreate the size distribution of smalt as Rembrandt used it.

The discrepancy between the paint-out and the sample pigment concentration can have two sources, the calculation of pigment concentration and the making of paint-out.
Looking at section A, it shows that in the method of calculating the pigment concentrations errors can occur. Since identical calculation are made, in section A and in this paragraph, the same amount of inaccuracy occurs in every calculation step.
In the method of making the paint-outs, the density of the dry pigment is calculated. This is done by measuring the volume of dry pigments and weighing that same amount of pigment. Measuring a volume of any powder is extremely difficult, since by tapping or pressing down

on the powder the volume changes drastically without any weight change.
Comparing the sources of the discrepancy, the calculation of pigment concentration and the making of paint-out, it is clear that the largest error occurs while making the paint-out. Due to the fact that the density of a dry pigments is very difficult to estimate.
This difference between stated pigment concentrations of the paint-outs and the actual pigment concentration does have an effect on the rest of the paint-out sets of section C. In the lighter paint-outs the colour effect can be quite large, while it has a smaller effect on the colour of the darker colour mixture is expected. Darker colour mixtures are less sensitive for different pigment concentrations as can be seen in the third set of paint-out in section C.

4-5 Section E

The focus of section E are the steps leading to the digital colour reconstructions of the focus area as well as the digital colour reconstruction itself. This section can be split into five paragraphs.
The first paragraph's goal is to explain the choice of the particular focus area. Also a prediction will be made of what the focus area would have looked like. To explain the choice of the focus area the Macro-XRF of section A will be used. For the prediction, the results of the paint-outs of section C will be used. The prediction will help to verify the colour of the final digital colour reconstructions of the focus area.
In the second paragraph, E.1, a colour comparison between four different representations of sample 40_7 is made all based on hyperspectral data. The first is the hyperspectral data of the sample location in the painting, section B. The second is the hyperspectral data of the paint-out reconstruction of sample 40_7. The third is a digital mixture of sample 40_7 based on Table 4-4 using the pigments bone black, smalt and yellow lake. The fourth is a digital mixture of sample 40_7 based on sample 40_7 in Table 4-4, but using half the amount of smalt. The goal of this section is to see how different concentrations of smalt affect the colour of the digital reconstruction. This will influence the concentrations of smalt and yellow lake 'mixed back' in the focus area, which is seen in sections E.2 and E.3.
The third paragraph, E.2, will focus on the different parameters that influence the digital colour reconstruction. The first parameter is the concentration of smalt, yellow lake and a mixture of the two. The second parameter is the concentration of the focus area itself. The third parameter is the colour and the concentration of degraded smalt. From this section knowledge is gathered, which indicates whether certain parameters should be taken into account and in what concentration they should be when making the digital colour reconstruction in section E.3. This section uses different aspects shown throughout this chapter; from section A the relationship between smalt and yellow lake concentration and Macro-XRF values of cobalt and potassium, from section B the K/S value of the focus area, and from section C the K/S value of smalt and yellow lake.
In the fourth paragraph, E.3, the digital reconstruction of the focus area will be made. The insight gathered in section E.2 will be used. The goal of this section is to show what the focus area of *The Jewish Bride* may have looked like. The digital reconstruction will be used in section E.4.
In the fifth paragraph, section E.4, the outcome of section E.3 will be placed back in the painting. The goal is to show how much the painting could have differed from the time Rembrandt painted it and how it looks now. Also, it is compared with the predictions made about the digital reconstruction.
All these different paragraphs give an overview of the steps required to make a digital colour reconstruction.

4-5-1 Focus Area of *The Jewish Bride*

In this paragraph, the reason for choosing the focus area is explained and also a prediction will be made of what the focus area would look like when digitally colour reconstructed. The focus area is seen in Figure 4-46 and is the top area of the plant on the right of Rebecca. As



Figure 4-46: Focus Area of *The Jewish Bride*. It shows the plant on the right side of Rebecca and the yellow border indicates the area of focus.

stated in section A, this area has a heterogeneous distribution of pigments. This is even better seen when the Macro-XRF image area is stretched. Stretching an image means that the whole range of pixel values, in this case between 0–1, are used. This gives a better indication of where the elements are present in high amounts and where they are present in lower amounts.



(a) Present-day image of the focus area.

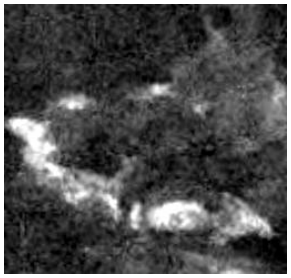

(b) Calcium Macro-XRF image showing the distribution of calcium in the focus area.

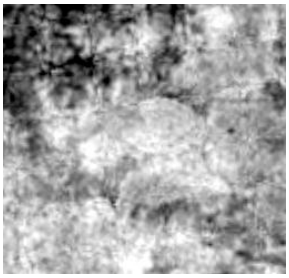

(c) Cobalt Macro-XRF image showing the distribution of cobalt in the focus area.

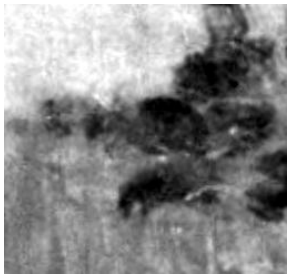

(d) Iron Macro-XRF image showing the distribution of iron in the focus area.

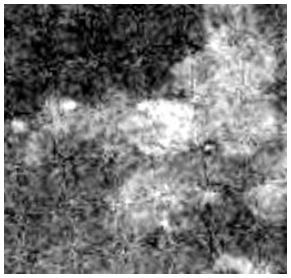

(e) Potassium Macro-XRF image showing the distribution of potassium in the focus area.

Figure 4-47: Close-up of focus area and Macro-XRF images of calcium, cobalt, iron and potassium.
(b) calcium can be related with the pigment of bone black and the high calcium areas are related to the shadows underneath the leaves in the present-day image.
(c) cobalt can be related to smalt and is present in whole of the focus area.
(d)is related to red earth and yellow earth. It shows clearly that there is some concentration in the plant itself, but there is very little present in the leaves themselves.
(e) potassium is related to the pigment of yellow lake. The highest concentration of potassium is in the leaves.

Figure 4-47 shows the Macro-XRF stretched images of the plant. The discussion of these Macro-XRF images is based on the knowledge gathered in section A.
The calcium Macro-XRF stretched image can be related with the pigment of bone black. The white areas in the Macro-XRF image are the shadows underneath the leaves in the original image. In the rest of the area of interest there is also some bone black present, but not in the same quantities.
The cobalt Macro-XRF image is related with the smalt concentration. In this map, the strokes of the brush in the middle of the leaves are visible. Cobalt seems present in relatively high concentrations in the whole area of interest, except where there is a high concentration of calcium, and in the left corner.
The iron map is related to red earth and yellow earth. It shows clearly that there is some concentration in the plant itself, but there is very little present in the leaves themselves.
The potassium map is related to the pigment of yellow lake. The highest concentration of potassium is in the leaves. Here in the Macro-XRF image it is even possible to see the brush strokes made by Rembrandt.

4-5-1-1 Prediction of how the focus area could have appeared

For this prediction, the paint-outs of section C are used. The focus area can be split into two areas, that of the leaves and that of the area surrounding the leaves. In the leaves there is a higher amount of potassium and cobalt, which indicates that yellow lake and smalt were present in high quantities. As both these colours have degraded, this could mean that there was a colour difference between the present day painting and when Rembrandt painted it. Looking at the smalt and yellow lake mixtures as seen in Figure 4-37, the mixture of 25% yellow lake and 75% smalt is very dark and greenish. This might be how the leaves looked like.
The area surrounding the leaves there is cobalt visible in the Macro-XRF image and therefore smalt is present there. Looking at the paint-outs of Figure 4-33 with smalt and comparing it to the paint-outs of Figure 4-34 without smalt, the paint-outs with smalt are darker and cooler in tone than the paint-outs without smalt. The areas surrounding the leaves will presumably look darker and cooler when their colour is digitally reconstructed.

4-5-1-2 Conclusion

To conclude, in the focus area Rembrandt made an ingenious mixture of different pigments. The area can be sub-divided into two main areas; that of the leaves, which might have appeared darker and more greenish, and that of the area surrounding it, which could have appeared darker and cooler.

4-5-2 Section E.1

The focus of this section can be split into two. The goal of the first part is to see the difference between the colour of a sample location in the painting and the paint-out of that sample. The

goal of the second part is to see two digital mixed colours using smalt, yellow lake, and bone black based on the pigment calculations made in section A, and compare the colour with the sample location and the paint-out.
In this section, the sample location of sample 40_7, paint-out of sample 40_7 and two digital reconstructions based on sample 40_7 will be compared using RGB values. All the RGB values are calculated through hyperspectral data. By using hyperspectral data and a standard route to RGB, the effects of different lighting circumstances are eliminated and it is possible to compare them.
Figure 4-48 shows the four colours, all based on sample 40_7.
The first RGB value is taken from the sample 40_7 sample location; seen Figure 4-9.
The second RGB value is based on the paint-out made in section C; see Figure 4-33. One pixel of the paint-out on the black surface, which was not as effected by the specular reflection was used.
The third digital colour mixture is based on the concentration calculations of section A, Table 4-4 sample 40_7, but only the pigments of bone black, smalt, and yellow lake are taken into account.
The fourth digital colour mixture is also based on Table 4-4 sample 40_7, but only half of the concentration of smalt is taken into account.

4-5-2-1 Comparison of the four different colours

The comparison of Figure 4-48 will be split into two parts. The first will focus on the difference between the first two colours, while the second will focus on the digital mixed colours.
Between the sample location in the painting and the paint-out colours there is a slight difference. The colour from the painting is a bit more brownish compared to the paint-out. This was already suggested in section C, that the degraded smalt made the mixture more brownish and non-degraded smalt made the mixture darker and cooler. This difference is also seen in the hyperspectral data of the first colour and the second colour. In the lower wavelengths (400 nm – 500 nm), the second colour has a higher reflection compared to the first colour. While the first colour has a higher reflection from 500 nm – 750 nm, which makes the colour lighter and more brownish
The third colour is digitally mixed. The mixture is solely based on the calculated and normalised pigment concentration of sample 40_7. The colour is very blueish compared to the first two colours. This is due to the fact that the concentration measured is for transparent smalt, while when digital mixing smalt is seen as opaque. If the transparency of smalt had been taken into account it would have less of an effect on the colour and therefore appear less blueish. This would mean that for the digital colour reconstruction the transparency of smalt is not taken into account and the concentration calculated in the samples is therefore too high. The blueish colour is also seen in the hyperspectral data, there is a relative high reflection between the wavelengths 400 nm -500 nm, which creates the blue colour.
The fourth colour is based on the calculated pigment concentration of sample 40_7, but only half the amount of smalt is used. It appears less blue and more in line with the first two colours. If red earth and yellow earth were taken into account, it would most likely result in even less of the blueish tones, since they counter the colour blue. Comparing the hyperspectral data of the third and fourth colour, it shows that the reflection between 400 nm – 5000 nm is less in the fourth colour, which leads to a less blueish appearance.

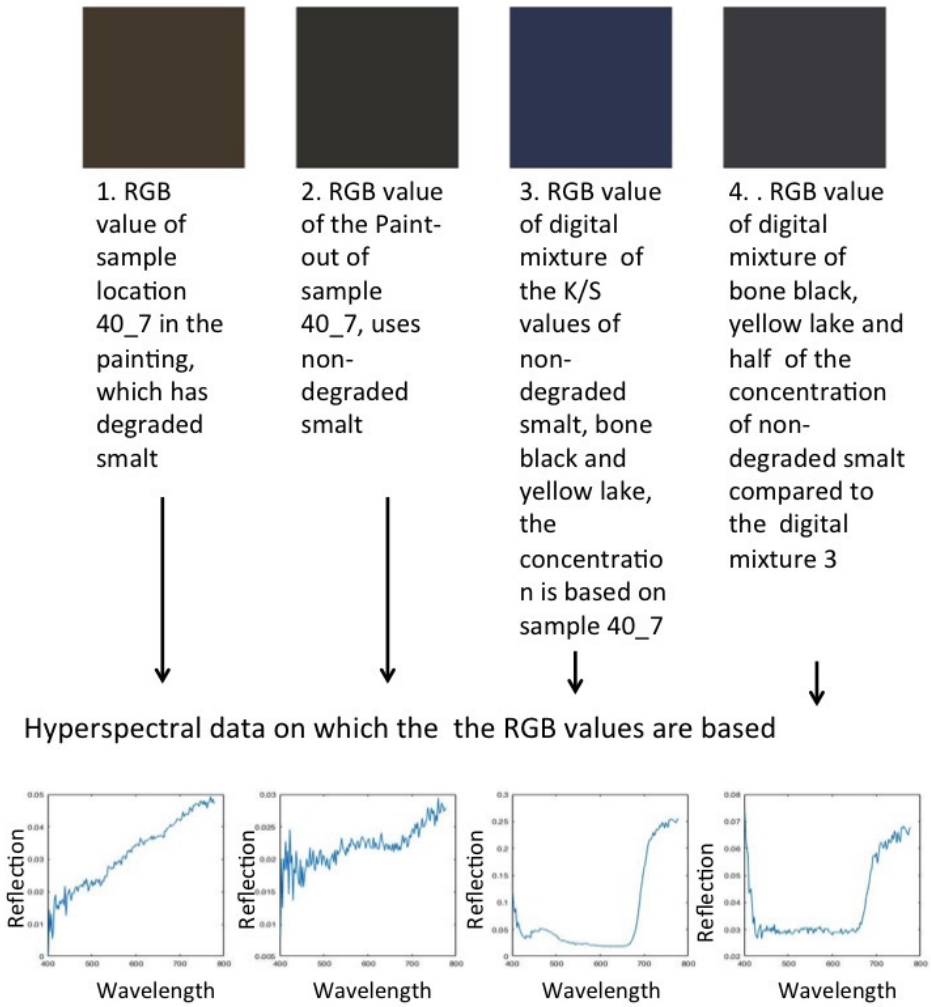

Figure 4-48: Four colours, all based on sample 40_7. The colour from the painting (1) is a bit more brownish compared to the paint-out 2). Using non-degraded smalt makes the colour darker and cooler of tone. 3,the colour is very blueish compared to the first two colours. This is due to the fact that the concentration measured is for transparent smalt, while when digital mixing smalt is seen as opaque. 4, only half the amount of smalt is used. It appears less blue and more in line with the first two colours.
The calculated concentration of smalt should be decreased to make sure that the blue colour is not too dominant. In the next sections the concentration of smalt and yellow lake will vary in different concentration, since the exact concentration is unknown. *Note that the figure brightness is adjusted for printing*

4-5-2-2 Conclusion and discussion

To conclude, there is a small colour difference between the colour of sample location of 40_7 and the paint-out. The colour of non-degraded smalt makes the colour darker and cooler of tone.
Also when digital mixing sample 40_7 transparency is of smalt is not taken into account. Therefore the calculated concentration of smalt should be decreased to make sure that the blue colour is not too dominant. In the next sections the concentration of smalt and yellow lake will vary, since the exact concentration is unknown.

In the future research it could be interesting to investigate the influence of transparency of smalt on the colour of the mixture.
It is also very difficult to see if the amount of yellow lake is correct. This is due to the fact that the mixture of this paragraph is very dark, and yellow lake does not have a high colouring strength.
For this paragraph, only sample 40_7 could be used. This is, because the hyperspectral images of the sample locations of 215/3 and 40_15 are heavily influenced by the specular reflection. Therefore, they could not be used for this comparison. Unfortunately, there was no hyperspectral image made of red earth and yellow earth. This of course is very limiting for accuracy of the outcome. If those were present and more sample points could be used the outcome would be more reliable.

Despite the limitations, Figure 4-48 does show that the calculated and normalised concentrations of smalt have a strong effect on the colour and turn it blueish. This insight will be used in section E.2 and section E.3.

4-5-3 Section E.2

The focus of this section is to see how the parameters will influence the digital colour reconstructions. There are three parameters, which will be individually discussed in a paragraph. The first parameter is the effect of different concentrations of smalt, yellow lake, or a mixture of the two. As seen in the previous section E.1, using the actual concentration of smalt will turn the colour blueish, also from that section it was impossible to determine if the actual concentration of yellow lake created the right colour. Therefore we will vary the concentration of smalt and yellow lake in this section. These will be shown in different concentration steps. The second parameter is that by adding colour back, the original paint mixture will become less in concentration. The third parameter is the effect the degraded smalt has on the matrix and top layer. As stated previously, due to the degradation process of smalt, the oil matrix and top paint layer turn monochrome brown. This brown colour might need to be subtracted from the mixture.

To show the distribution and concentration per pixel, the Macro-XRF intensities (0–1) are multiplied with the top concentration of the pigment (which is varied between 0-1). For instance, if the top concentration of smalt is set at 0.6, (60%), and the pixel in the original Macro-XRF has an intensity of 0.8, it means the concentration of that pixel is 0.48 (48%). This method is used for Macro-XRF images of cobalt and potassium, which indicate the smalt and yellow lake distribution in the painting.
For all these digital colour reconstructions the K/S values are used from the hyperspectral image of the focus area(section B) and the hyperspectral image of the paint-outs of yellow lake, smalt and a mixture of the two (section C, Figure 4-37.
Only a few digital colour reconstructions are discussed, which show the main trend; a wider range of digital colour reconstructions can be seen in appendix E.

4-5-3-1 Concentrations of Smalt and Yellow lake

The focus of this paragraph is on the effect the concentration of smalt and yellow lake has on the colour of the digital colour reconstruction. These colours are placed on a white background and are not digital 'mixed' back in the focus area.
As stated before, the transparency of smalt and yellow lake is not taken into account. If the transparency is taken into account it influences the concentration needed to achieve the same colour effect, as can be seen in section E.1.
This means that the calculated concentrations in section A are different from the concentrations needed to achieve the right colour effect. Here a trend will be shown by changing the concentrations. For the distribution of smalt in the focus area, the Macro-XRF image of cobalt is used, and for the distribution of yellow lake, the Macro-XRF image of potassium.
Figure 4-49 shows the distribution of the different colours in different concentrations.

On the left side of Figure 4-49, the present-day colour of the painting is visible as John Delaney[17] scanned it. The distribution of a particular pigment is based on the Macro-XRF image of the focus area. The concentration of pigment is varied from 20% to 100% in steps of 20%. These concentrations are multiplied with the distribution of Macro-XRF intensities (0–1). This gives an overview of how the colours behaved in the different concentrations.
The first array of Figure 4-49 shows increasing concentrations of smalt. The distribution is

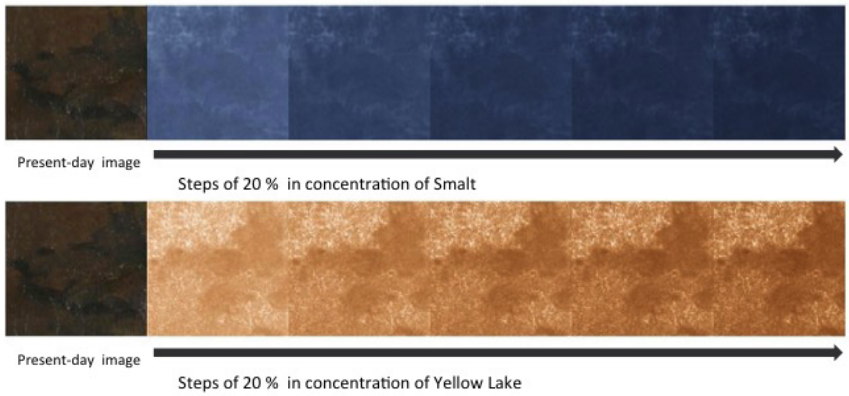

Figure 4-49: Steps in the concentration of smalt and yellow lake
The smalt distribution and concentration is based on the cobalt Macro- XRF image of the focus area. What becomes visible is that the images become progressively darker blue, beside a few spots smalt is very homogeneously distributed.
The yellow lake distribution is based on the potassium Macro-XRF image. It shows that between the leaves the concentration is very large, while there is significantly less yellow lake surrounding the leaves. Also, it shows that the colour in the beginning is yellow, but turns into a more brownish/reddish colour when the concentration increases. *Note that the figure brightness is adjusted for printing*

based on the cobalt Macro- XRF image of the focus area. What becomes visible is that the images become progressively darker blue, beside a few spots smalt is very homogeneously distributed.
The second array of Figure 4-49 shows increasing concentrations of yellow lake. The distribution is based on the potassium Macro-XRF image. What is visible is that the amount of yellow lake between the leaves is very large, while there is significantly less yellow lake surrounding the leaves. Also, it shows that the colour in the beginning is yellow, but turns into a more brownish/reddish colour when the concentration increases, which corresponds with the paint-out made; see Figure 4-37.

Figure 4-50 shows the sequence of yellow lake and smalt are digitally mixed together, both pigments concentration are increased by steps of 20%. The concentration distribution is based on the cobalt Macro-XRF image for smalt and on the potassium Macro-XRF image for yellow lake. It shows that the colour of the leaves is influenced the most by the combination. The two Macro-XRF intensities are both very high in that location. The colour becomes very dark brown. Due to the fact that the yellow lake in large concentrations is a brownish yellow, the leaves do not appear as green as one might have expected. In the area surrounding the leaves, it is clear that blue is the dominant colour.

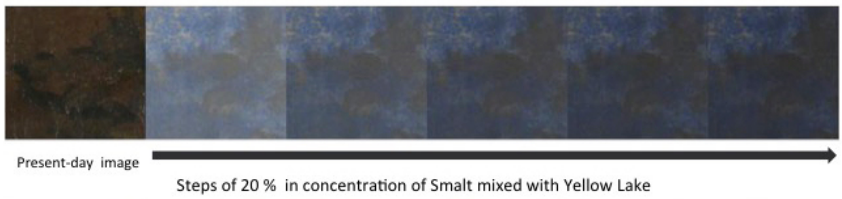

Figure 4-50: Digital mixture of smalt and yellow lake
The concentration distribution is based on the cobalt Macro-XRF image for smalt and on the potassium Macro-XRF image for yellow lake.
The colour of the leaves becomes very dark. Due to the fact that the yellow lake in large concentrations is a brownish yellow. The leaves do not appear as green as one might have expected.*Note that the figure brightness is adjusted for printing*

To conclude, the Macro-XRF image can be used as a guide for the different concentrations of smalt and yellow lake. Smalt has the most effect on the colour of the mixture, while yellow lake has a less pronounced effect. It can also be seen that the mixture of yellow lake and smalt does not turn green, and this is most likely due to the fact that the yellow lake is a brownish yellow colour instead of bright yellow.

4-5-3-2 Concentration for the present-day colour of the background

The focus of this paragraph is on the effect of the concentration of smalt and yellow lake on the present day painting itself. By adding extra colour to the mixture, the concentrations of the other pigments in the paint layer change. The concentration of the K/S value of the painting itself influences the reconstructed image, only it is very difficult to make a good estimation of what the concentration of the present-day K/S value should be, therefore it is also portrayed in steps.

Figure 4-51 shows the original image on the left side and the present-day images chang-

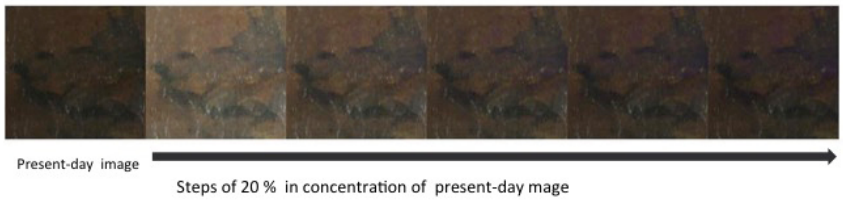

Figure 4-51: Steps in concentration of the present-day image
Between the different concentrations it shows that more specular reflection appears in lower percentages. Also, at the lower concentrations the different colours in the leaves become more visible. *Note that the figure brightness is adjusted for printing*

ing in concentrations. The steps and start at 20% and go to 100% in steps of 20%. Between the different concentrations it shows that more specular reflection appears in lower percentages. Also, at the lower concentrations the different colours in the leaves become more visible.

To conclude, the focus area changes quit a lot, when the concentration changes. Therefore, only a relatively small concentration change should be taken into account, that makes the subtle colour changes visible.

4-5-3-3 Colour of degraded Smalt

As described in Chapter 2, degraded smalt pigment particles turn colourless and grey. The potassium that leaches out binds with the free fatty acids and can migrate towards the outer

surface of the paint layer. This makes the oil matrix and the top layer a monochrome brown. It is clear the current colour of the painting itself is influenced by the colour of degraded smalt and therefore appears brownish.
There is no hyperspectral data of colour of degraded smalt oil matrix or top layer. Therefore, a location was chosen using the Macro-XRF image, where there was a low amount of calcium, iron, and potassium in combination with a very high amount of cobalt. The location is seen in Figure 4-52. Figure 4-53 shows the colour of the degraded smalt in steps of 20%. This is



Figure 4-52: Yellow circle indicates the pixel, which represents the colour of degraded smalt The location was chosen using the Macro-XRF image, where there was a low amount of calcium, iron, and potassium in combination with a very high amount of cobalt.

based on the cobalt Macro-XRF images, since this indicates the smalt distribution. Figure

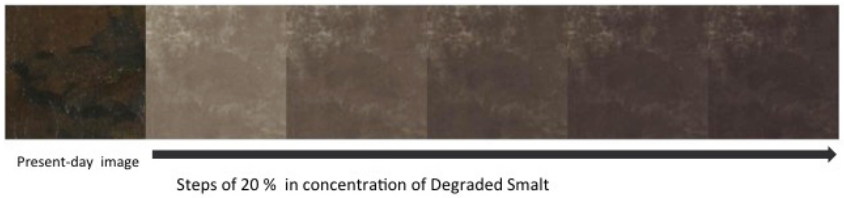

Figure 4-53: Steps in the concentration of the colour degraded smalt. The distribution is based on the cobalt Macro-XRF images, since this indicates the smalt distribution. *Note that the figure brightness is adjusted for printing*

4-54 shows how the present day painting changes if degraded smalt is subtracted from it. What is interesting is that different highlights become better visible. The yellow highlight in the top right corner, for example, is better visible. Most likely the brown colour of the matrix suppressed the vibrant yellow colour. A downside is that the specular reflection becomes more apparent.

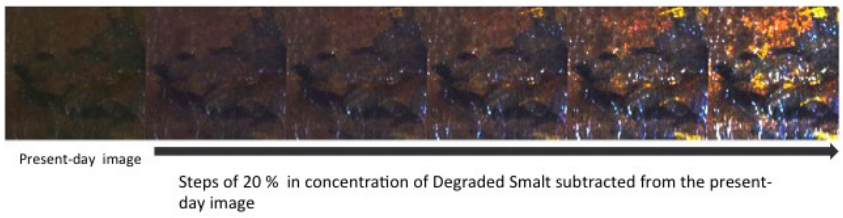

Figure 4-54: Steps in the concentration of degraded Smalt subtracted from the present day colour of the painting. What is interesting is that different highlights become better visible. The yellow highlight in the top right corner, for example, is better visible. *Note that the figure brightness is adjusted for printing*

To conclude, to achieve a just digital colour reconstruction, the brown colour due to potassium leaching in the oil matrix. The brown colour should be subtracted from the present-day image. Since there is no hyperspectral data of degraded smalt matrix, choosing a pixel based on the Macro-XRF images gave the most accurate colour of the degraded smalt matrix.
This paragraph does give an indication of how, besides losing the blue colour, the degradation of smalt affects the colour and how drastic that might be.

4-5-3-4 Conclusion of section E.2 and discussion

In section E.2, the effect of three different parameters were showed and explained.
First, the colour mixtures of smalt and yellow lake and the green colour mixture were investigated. This showed how the Macro-XRF map could be used as a guide for the pigment concentration, also it showed that the colour of the yellow lake was a reddish yellow and therefore the mixture of blue and yellow did not turn green as was previously expected.
Second, by changing the concentration of the original image, there is a noticeable colour change, which should be taken into consideration.
Third is the colour change of the oil matrix and top paint layer by the degradation process of smalt was showed. The browning of the oil matrix and the top paint layer greatly affects the overall colour of the present day painting and must be taken into consideration for the final digital colour reconstruction of the focus area.
Unfortunately, by not taking the transparency of the pigments into account, the previously calculated values from section A cannot be used. Therefore, the figures show different steps in concentration. This of course will considerably affect the accuracy of the outcome, therefore the different digital colour reconstructions can only show a trend that is present, but cannot indicate the most likely outcome.

4-5-4 Section E.3

The focus of this section is to digitally mixing back smalt and yellow lake in the focus area.

As can be seen throughout this chapter, at every step there are many uncertainties. Therefore, it is impossible to pinpoint an exact digital colour reconstruction. The goal of this section is to make a trend visible.
Digital colour reconstructions sequencing will be shown, to indicate the trend, and the rest of the digital colour reconstructions will be shown in appendix E. The two trends here are selected as it was found in section C that smalt concentration has the most noticeable effect on colour compared to yellow lake. Figures 4-55, 4-56 and 4-57 show different digital colour

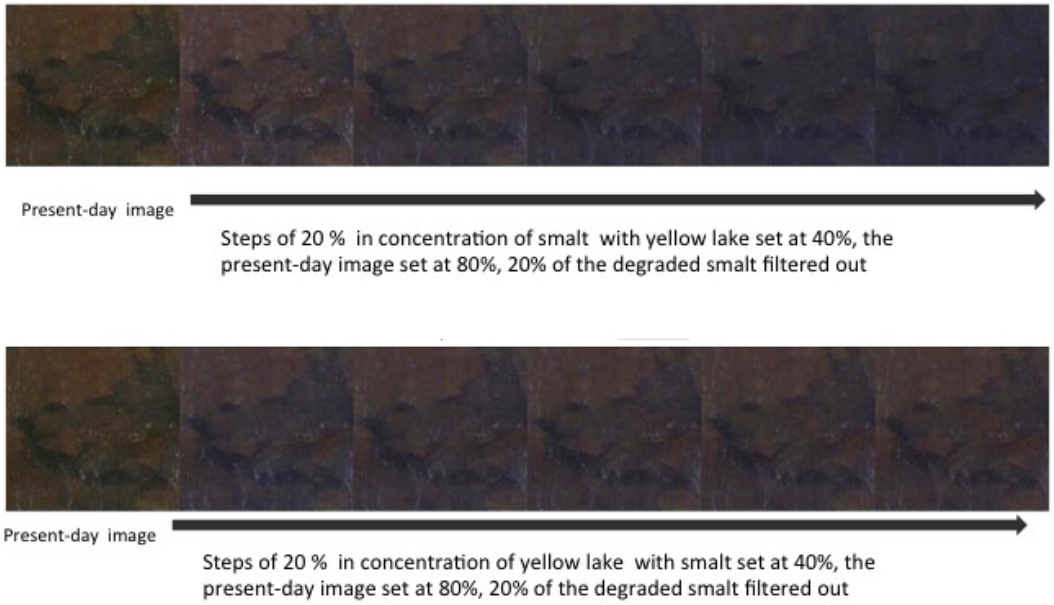

Figure 4-55: Two sequences focusing on the effect of smalt and yellow lake on the focus area. The first array shows that different concentrations of smalt make the background very dark and cool of colour.
The second array shows that different colour concentrations of yellow lake, have less an effect on the focus area. It makes the image a dark and brownish of colour. *Note that the figure brightness is adjusted for printing*

reconstructions. In all the figures, it starts with the present-day image based on the scan of John Delaney[17].
In the first figure, Figure4-55, the focus what the effect is of smalt and yellow lake in different concentrations on the focus area. The first array, it shows an increase of smalt in steps of 20%, while the amount of yellow lake is set at 40%, the concentration of the present-day image is 80% and 20% of degraded smalt is filtered out. It shows that different concentrations of smalt make the background very dark and cool of colour. The second array, it shows an increase of yellow lake in steps of 20%, while the amount of smalt is set at 40%, the concentration of the

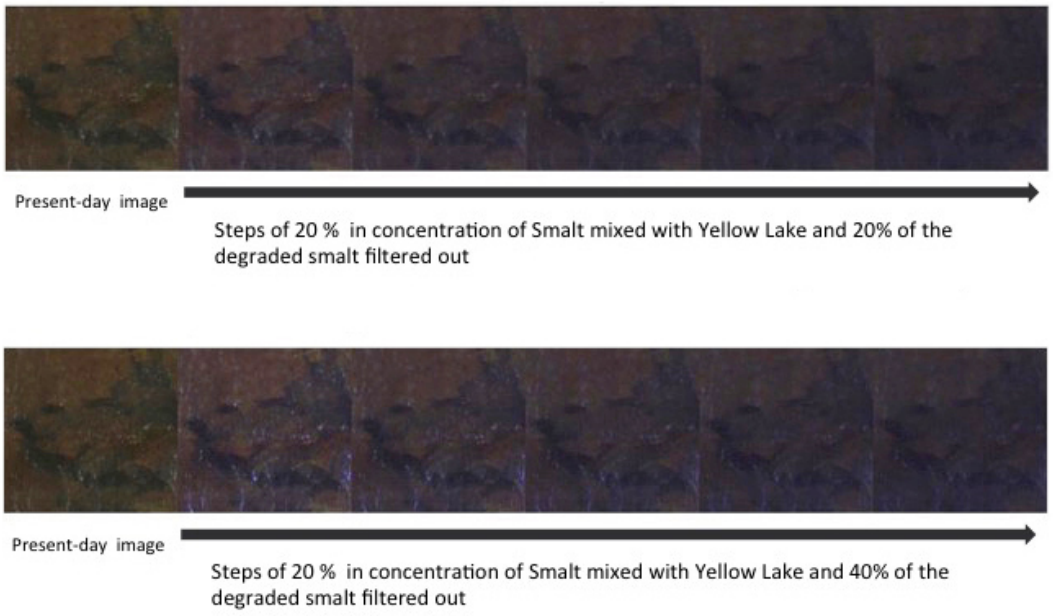

Figure 4-56: Two sequences focussing on the effect of filtering out degraded smalt
In the top array 20% is filtered out and the bottom array 40% is filtered out, while in both the concentration of smalt and yellow increase in steps of 20%. There is little difference between the two arrays, only that in the bottom array, the specular reflection is larger. Both arrays show that the focus area becomes darker and cooler of tone. *Note that the figure brightness is adjusted for printing*

present-day image is 80% and 20% of degraded smalt is filtered out. It shows that different colour concentrations of yellow lake, have less an effect on the focus area. It makes the image a dark brownish of colour.

The second Figure 4-56 shows the effect of different concentration of filtered out degraded smalt. In the top array 20% is filtered out and the bottom array 40% is filtered out, while in both the concentration of smalt and yellow increase in steps of 20%. There is little difference between the two arrays, only that in the bottom array, the specular reflection is larger.

Figure 4-57 shows in the top array an increase of concentration of smalt and yellow lake in steps of 20%, the rest of the sequence the original image is set at 80%. The second array is the same as the previous sequence, but also 20% of the degraded smalt is subtracted from the image.
The concentrations of smalt have a strong influence on the images. It appears that yellow lake does not have the same influence, other than making the leaves even darker as was also seen in Figure 4-55. Also, it shows that subtracting the brown colour of degraded smalt does influence the image. It appears to be even cooler in tone and more blueish dark. Both of the sequences show that when the concentration of smalt and yellow lake increases the colour

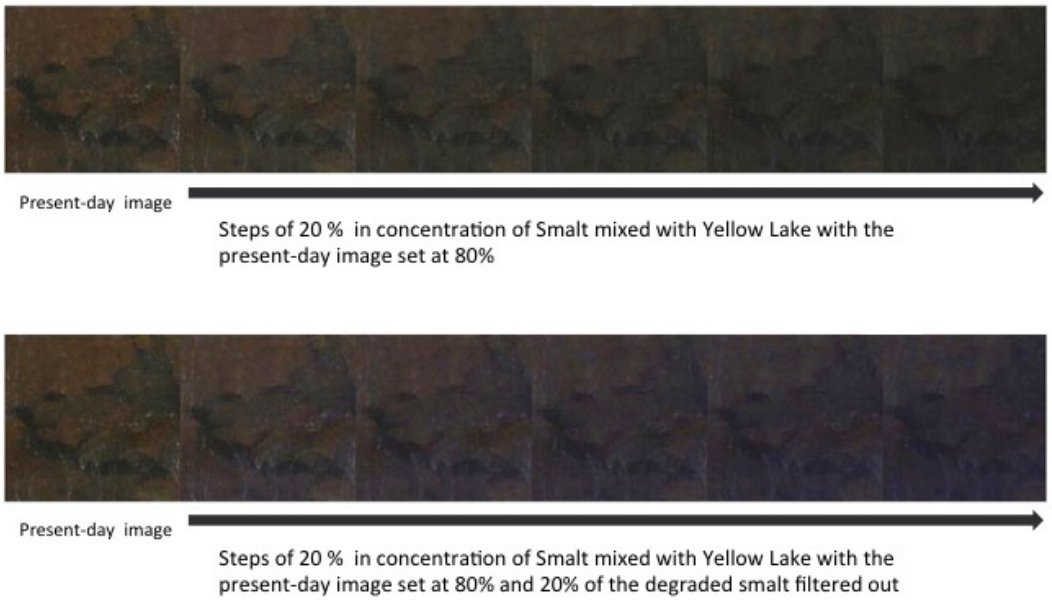

Figure 4-57: Two sequences focussing on the effect of the concentration of the present-day image and a combination of all The first array shows that by increasing the concentration the colour of the focus area becomes darker and cooler of tone. The second array shows that subtracting the brown colour of degraded smalt does influence the image. It appears to be even cooler in tone and more blueish dark compared to the first array. *Note that the figure brightness is adjusted for printing*

becomes darker. Between the two sequences, it is visible that the top is a bit warmer of colour and the bottom cooler. This is due to the fact the brown colour of the degraded smalt is filtered out in the bottom array.

4-5-4-1 Conclusion and discussion

To conclude, in all the sequences it is shown that by adding smalt and yellow lake back into the focus area, the area of interest becomes darker and cooler, which was predicted previously based on the paint-outs. The leaves themselves did not turn green as was expected.

Next we will compare the effect of the two different sections of the focus area: the leaves and the area surrounding them.
In applying the trends to the leave area, we can conclude that the pigment concentration found in leaves themselves did not turn greenish as predicted. This was already seen in section E.2, see Figure 4-50. As stated earlier, this is most likely due to the fact that the yellow lake has a reddish tone in it. Besides that aspect, focusing solely on the colour of the leaves, they appear to be very dark. Therefore, even if the shade of yellow lake was more yellow,

it would probably not have an enormous effect on the colour, as can be seen in the dark paint-outs of tiles in Figure 4-33. The Macro-XRF image of potassium on the other hand shows clearly that Rembrandt deliberately painted large amounts of yellow lake in that area. It would be very unlikely that he did so without there being any effect on the actual painting. It might be that Rembrandt used yellow lake only on the top layer as a highlight and maybe only mixing it in the top layer instead of mixing it throughout the paint mixture. This would probably have a more profound effect on the colour of the leaves.
In applying the trend on the areas surrounding the leaves. It can be concluded that they will become darker and cooler of tone. This would probably mean that if the method is extrapolated over the whole background, it would become darker and cooler of tone.

Although it is impossible to give an exact result of what the focus area could have looked like, this section does show a trend, which is probably the same for the rest of the painting.

4-5-5 Section E.4

The focus of this section is to see how much the focus area is different when placed back inside *The Jewish Bride*.



Steps of 20 % in concentration of smalt mixed with yellow lake with the present-day image set at 80%



Steps of 20 % in concentration of smalt mixed with yellow lake with the present-day image set at 80% and 20% of the degraded smalt filterd out

Figure 4-58: Possible digital colour reconstructions (the dark square in the plant) are placed back in the present-day painting. For this the digital colour reconstruction of Figure 4-57 is used. It shows that the colour change due to smalt and yellow lake degradation is drastic. The digital colour reconstruction is darker and cooler of tone compared to the present-day colour of *The Jewish Bride Note that the figure brightness is adjusted for printing*

Figure 4-58 to show the possible digital colour reconstruction back in the present-day image. The digital colour reconstructions that are placed back can be seen in Figure 4-57. Before discussing the figure, it is important to state two things.
First, the digital colour reconstruction is placed in an image made by the Rijksmuseum. Thus, the lighting will be different between the digital colour reconstruction and the image of the Rijksmuseum. Lighting can influence the colour of an object. This greatly affects the accuracy of the comparison.
Second, as is stated in the Chapter 2, the eye cannot see colour without being influenced by the colour surrounding it, as seen in Figure 2-11. This is the case here also, and therefore certain colours might appear brighter than they did before.

The top array of Figure 4-58 appear more somewhat more greenish than Figure 4-57. This is due to the colour surrounding it, because when looking at the actual RGB values it does not show any large green values.

The second array of Figure 4-58 appears more blueish than that of Figure 4-57. This is due to several reasons. The colour surrounding it makes it appear bluer than it actually is, just as in the previous image. Subtracting the colour of the matrix of degraded smalt in certain parts the craquelé of the area becomes whiter. When adding smalt back those white area turns blueish. These two reasons give an overall blue appearance. Looking at Figure 4-58 all the digital colour reconstructions appear to be darker and have a cooler colour. They are less brown than the rest of the background.
These two sequences are used, since they both portray the trend, that is the focus areas becomes darker and cooler of tone as was suggested from section C and E.1.

If this trend were to be extrapolated over the whole background of *The Jewish Bride*, the brown background especially will be influenced by it. Those smalt areas would become darker and cooler. The black shadow areas will be less affected by the digital colour reconstruction, but will also become slightly darker and cooler. Together, this will mean that the transition from the shadow areas to the rest of the background will look more uniform and have less harsh transitions between shadow and not shadow areas, as right now is seen around the beam above Rebecca.

This will mean a difference for the pictorial image as well. Isaac and Rebecca are all painted in very warm colours, the red dress of Rebecca and the gold outfit of Isaac. By placing them on a darker and cooler background, Rebecca and Isaac's colours will appear even warmer and more attention will be drawn to the couple standing in front of a dark and cool backdrop. Also by this difference between background and foreground, more depth will be created between the couple and the rest of the painting.

4-5-5-1 Conclusion of section E.4

To conclude, comparing the original painting to the digital colour reconstruction, there is a difference, which can be seen in Figure 4-58. It is easy to see that there is a colour difference. The digital colour reconstruction of the focus area appears darker and cooler

in tone. When this trend is extrapolated for the rest of the background, the pictorial image of *The Jewish Bride* will change, since the foreground, Rebecca and Isaac, will appear even warmer of colour and the background very dark and cool.

.

4-5-6 Conclusion of section E and discussion

To conclude, section E shows steps leading to and the actual digital colour reconstruction of the focus area, which gives an indication of what this may have looked like, when Rembrandt painted it.
The trend that appears in the final paragraphs of this section is that the painting becomes a cooler and darker shade. When this trend is extrapolated for the whole painting it influences the pictorial image. Isaac and Rebecca will draw even more attention and their colour scheme will appear warmer, while the background will appear to be further away and even darker.

In section E.1 it becomes clear that although the concentrations of smalt and yellow lake are measured in section A, they cannot provide an accurate image due to the fact that transparency of the two pigments is not taken into account.
In section E.2, when mixing the smalt and the yellow lake, it shows that the colour of the mixture was not green. This has most likely to do with the yellow colour of the yellow lake. The colour might appear yellow, while it actually has a more reddish colour. In the era of Rembrandt there were many different types of yellow lake. Therefore, the type used in this thesis might not have the correct shade.
In section E.3 the trend was made visible in the area surrounding the leaves. The leaves themselves did not change as expected and yellow lake seemed to have little influence on the colour. This could be because instead of mixing the yellow lake completely through the mixture as is done in the digital colour reconstruction, it is actually present in the top surface, where it can affect the colour of the leaves. More research of the focus is needed to see what the layering of the focus area is.
Section E.4 shows the difference in the background and the digital colour reconstruction of the focus area. As already stated, the perception of colour is influenced by the surrounding colours and the lighting also influences the colour. Nonetheless, it shows that the pictorial image might have looked very different. Although it is impossible to an give exact solution, the trend shows that the background of *The Jewish Bride* was darker and cooler of tone.
In section E, all the previous sections are used to digitally colour reconstruct the focus area. The trend that is made visible gives an insight into what *The Jewish Bride* might have looked like when Rembrandt painted it.

Chapter 5

Conclusion

The method suggested in this thesis made it possible to digitally reconstruct the colours of the degraded smalt and yellow lake back into *The Jewish Bride*. Figure 5-1 shows different digital colour reconstructions placed back in the present-day image of *The Jewish Bride*.
Although it is not an exact reconstruction, it does provide an insight of what the painting might have looked like when Rembrandt painted it. It shows a trend that when mixing back smalt and yellow lake, the background would be of darker and cooler colour. There were different steps taken to come to this reconstruction.
First a link was made between pigment concentrations of smalt and yellow lake and their corresponding macro-XRF images of *The Jewish Bride*. It showed that there was a relationship that low amount of cobalt in the Macro-XRF means low amount of smalt and vice versa. The same goes for yellow lake and the potassium Macro-XRF. The macro-XRF images were later used as a guide for the concentration and distribution in the focus area.
Secondly, hyperspectral images made from 400 nm – 1000 nm were made from *The Jewish Bride* as well as all the paint-out tiles. These were transferred in K/S values using the Kubelka-Munk Theory. This allows to digitally mix or remix smalt and yellow lake back into the present-day image.
Thirdly, the Macro-XRF images were used as a guide for the pigment concentration per pixel for the focus area. Also, three different parameters were tested to see their effect on the digital reconstruction. These parameters were the concentration of smalt and yellow lake, the concentration of the present-day image and the concentration of the colour of the degraded smalt matrix.
Finally, these different steps lead to three different sets of digital colour reconstructions, all of which portray the same trend. The trend that became visible is that when the smalt is digitally colour reconstructed, it makes a mixture darker and cooler of tone. This is in line with the conclusions seen from the paint-out in section C and the previous research done by Diana de Man[11].

If this trend were extrapolated for the whole painting itself, this would mean that the shadow areas would appear to be the same, but the transition between the light and shadow areas is less apparent and the whole background will become cooler and darker. This affects the





Figure 5-1: Possible digital colour reconstructions (the dark square in the plant) are placed back in the present-day painting. For this the digital colour reconstruction sof Figure 4-57 is used. It shows that the colour change due to smalt and yellow lake degradation is drastic. The digital colour reconstructions are darker and cooler of tone compared to the present-day colour of *The Jewish Bride Note that the figure brightness is adjusted for printing*

pictorial image, whereby the warm colours of Isaac and Rebecca would become even warmer, while the background would become even cooler and less pronounced.
It is less visible, what the effect is of digitally colour reconstructing yellow lake on the focus

area; this is because the mixture itself is very dark and yellow lake has less of an effect on dark mixtures. This will be discussed in more detail in the next paragraph.
All in all, this method can digitally colour reconstruct faded pigments in a paint mixture as well as take the individual pigment's heterogeneous distribution into account.

5-1 Discussion

The focus of this paragraph is to highlight the main limitations of the method that influence the accuracy of the digital colour reconstruction the most. The method will be set against the requirements stated in the introduction.

5-1-1 Smalt and yellow lake

Smalt and yellow lake are at the basis of this digital colour reconstruction, and therefore will be discussed; first the colour of smalt and yellow lake, after that the K/S value of smalt and yellow lake.

5-1-1-1 The colour of smalt and yellow lake

The colour of smalt is influenced by the cobalt percentages and the particle size. It might be also dependent on the impurities in the glass matrix.
The colour of yellow lake is influenced by the nature of the plant from which it is extracted. The shade of yellow can vary. For this thesis, the smalt and yellow lake colour are set by the previous work done by Diana de Man[11]. This is one of the major parameters for the digital colour reconstruction.
The particle size of the smalt could be better matched. The size of smalt made by Diana de Man[11] varied in size, which influenced the colour. Also, the smalt tile on which the hyperspectral imaging was done is not evenly distributed, and the white tile shines through in many places. Thereby, at the moment of measurement the oil matrix had turned brown, due to lack of exposure to light.
For yellow lake, only one shade of yellow colour was used, while there were a range of yellow colours. As suspected in the beginning, part of the leaves might be green. The yellow lake used is a bit reddish, therefore the outcome of the mixture of smalt and yellow lake is not green. By using a more 'yellow' yellow lake the mix with smalt could turn out green.

In further applications of this method, the particle sizes of smalt and the type of yellow lake could be better matched, so colours are more accurate.

5-1-2 *K/S* values of smalt en yellow lake

Only one of the reflectance spectra pixel of the paint-out of smalt and yellow lake was used to calculate the K/S value of the pigments. This was due to the fact that the paint-outs were not evenly spread out. Also, only the combined value was calculated instead of the K and

S values separately. This influences both the accuracy of the measurement and thereby the outcome.

The assumption of not taking the transparency into account also influences the outcome, as is seen in section E.1. As a result, the calculated pigment concentration of section A could not be verified/used. Therefore, steps of concentrations were used for smalt and yellow lake, instead of one set concentration.

In further application of this method, one must ensure that both the K and S values are measured and to take the transparency into account, new paint-outs should be made through a set method described in literature.

5-1-3 Hyperspectral data

A better hyperspectral image would improve the quality of the the reconstruction.
Section B shows the hyperspectral image of *The Jewish Bride*; it appears that there are areas of specular reflection visible. This highly influenced not only the accuracy of the data set, but also affected the comparison made in section E.1, where only one sample could be compared due to it.
In sections E.3 and E.4, it also shows up in the digital reconstruction, where the craquelé is visible.

5-1-4 Mixing colour with Kubelka-Munk theory

Overall, the digital mixing of colours using the Kubelka-Munk theory gives acceptable results. Only when paint layers are mixed with Kubleka-Munk theory, it does not take layering of the painting into account. Maybe that is why the yellow lake mixed in the plants does not affect the colour as much as expected. If it were a highlight on top of the paint layer in the background, it might be better visible. More research is needed to see if that is the case.

5-1-5 Requirements for the method

When testing the method against the requirements set in the introduction, those are:
It must have a scientific basis.
The method must be easy to use.
The method must be applicable to paint mixtures.
It should have the possibility of being extrapolated to the whole painting.
The method should also be applicable for other paintings.

5-1-5-1 Scientific Approach

The basis of this method is scientific, although due to the various uncertainties the outcome ad to be based on a few assumptions, reducing the accuracy. Through more research, the method might be applied with fewer assumptions, leading to a better outcome.

5-1-5-2 Easy to use

The basis of the method is straightforward, but the steps are time consuming. Different analytical tests must be done, which fall outside the ordinary scope of tests. Also, efforts should be made to see if the outcomes of the digital colour reconstruction match paint-outs of the reconstructed area. In future, a framework may be created to digitally reconstruct degraded pigments, making the whole process easier.

5-1-5-3 Be used in paint mixtures

Using the Kubelka-Munk theory, paints can be mixed digitally into mixtures.
The difficulty of this theory is applying the correct technique for measuring the K/S values, especially for the transparent pigments. This requires different paint-outs and various hyperspectral analysis images. On the upside, it is possible to make a database of all the K/S values of different pigments, which makes this step easier.

5-1-5-4 Extrapolated to the whole painting

Digital colour reconstruction of the entire surface of *The Jewish Bride* is possible, although the current dataset should be updated for this. A part of the images is not scanned with the Macro-XRF scanner and a new hyperspectral scan should be made, since there is a lot of specular reflection in the current scan. By combining the two scans, the specular reflection could be filtered out.

5-1-5-5 Could be used for other paintings

The method used in this thesis can be used on different paintings.
The main limitation is that different data would be required. The micro analytical techniques of cross-section paint analysis are quite standard, while Macro-XRF and hyperspectral scans are less common.

5-1-6 Conclusion

The different aspects in the discussion and those discussed in Chapter 4 make it impossible to make an accurate prediction. Nevertheless, the final digital colour reconstructions of the focus area were in line with predictions made based on the paint-outs and the previous research. More research is needed, though, to improve the accuracy of the method and to make it easier and quicker.

5-2 Further research

The accuracy of the method can be improved in different areas. To achieve that more research is needed. The areas which have the most influence on this will be discussed here. These are smalt and yellow lake, colour of degraded smalt, pigment concentration and Macro-XRF images, and hyperspectral imaging.

5-2-1 Smalt and yellow lake

The colour of smalt and yellow lake itself could be further researched. For smalt, it is interesting to see how much the pigment particle size influences the colour, and if the impurities do influence the colour. For yellow lake, the different colours could be researched and digitally colour reconstructed back into *The Jewish Bride*, to see what effect it has on the painting. Also, it would be interesting to see in what layer the yellow lake is present in the leaves area, since it might be present in the top layer where it will affect the colour more than when it is mixed in.

5-2-2 The Kubelka-Munk theory and transparency pigments

The accuracy can be improved by using K and S values of the pigments, and by taking transparency into account. To achieve this, paint-outs should be made. The method is described in detail in the literature. Not only smalt and yellow lake should be looked at, but an index of the values of a whole range of pigments could be made. If there is an index of pigments with their K/S values, it would be possible to use the Kubelka-Munk theory and calculate their percentage throughout the painting based on the hyperspectral data.

Both of these points will not only influence the accuracy and speed of future digital colour reconstructions, but they will also create a new, tested method for pigment identification.

5-2-3 Accurate colour of degraded smalt

Although degraded smalt particles themselves become colourless, the oil combined with potassium turns brown, as does the top layer of paint. To filter out the right colour of degraded smalt, new paint-outs should be made and aged. Ageing of smalt has already been done in previous research. Instead of looking at the mechanism of smalt degradation, a hyperspectral scan can collect the colour data of the monochrome brown oil matrix and top layer of paint. Through this, a more exact colour of degraded smalt can be filtered out, as can be seen in section E.2; this greatly affects the painting. This can again then be used for future digital colour reconstructions of smalt.

5-2-4 Extrapolating the method to the whole painting

The method is only applied on a small part of the painting, but it could be used on the full-scale image.
Now the effect can only be speculated upon. Most likely it will make the transitions from the shadow area to a lighter area less pronounced and the brownish background will become darker and have a cooler tone.

All in all, this might lead to a new pictorial image of *The Jewish Bride* and create a new insight into the mind of Rembrandt.

Appendix A

XRF

A-1 Workings of the Macro-XRF

The XRF instrument sends outs X-rays. These X-ray can eject an electrons of an atom. The electrons of the outer shells organize themselves to fill the empty space in the K-shell, see figure A-1. By doing this, the electron from an outer shells which has a higher energy level, falls down to the void of a lower energy state. The excess energy is send out as X-rays, which is discreet and element depended. This is measured and it can be linked back to an element.

In a heavier atoms, there are different paths to organize the shell of an atoms after an electron is ejected. There is a preferred order, which are indicated with the letter α and the second with β etc. The jump if electron between shells is indicated with letters. If an electron goes from a L shell to K shell is indicated with the letter K and electron move from the M shell to the L shell,it is indicated with L etc.

From every scanned spot a spectrum is created, which shows the different elements present. To make a visual image, the spot spectrum from an detected element is transferred into a gray scale image. The whiter the pixel is the more a certain element is in that area and vice versa.

There are a few limitations of the XRF. Since it is depended on the weight of the element not all elements are visible. The lightest element that can be detected in the macro-XRF images of *The Jewish Bride*is potassium.

As stated in chapter 2, Rembrandt painted in different layers. With XRF it is impossible to tell from which layer the element comes from. A rough indication is given by the letter of the shell K, L, etc. X-rays from the L-shell are most likely from atoms in the top layer, while X-rays form the K-shell can travel through more layers.

A-2 Distributions of elements in *The Jewish Bride*

The elements that are detected in the Jewish Bride are: arsenic, barium, bismuth, calcium, cobalt, chromium, copper, iron, mercury, potassium, manganese, nickel, lead, tin ,strontium,

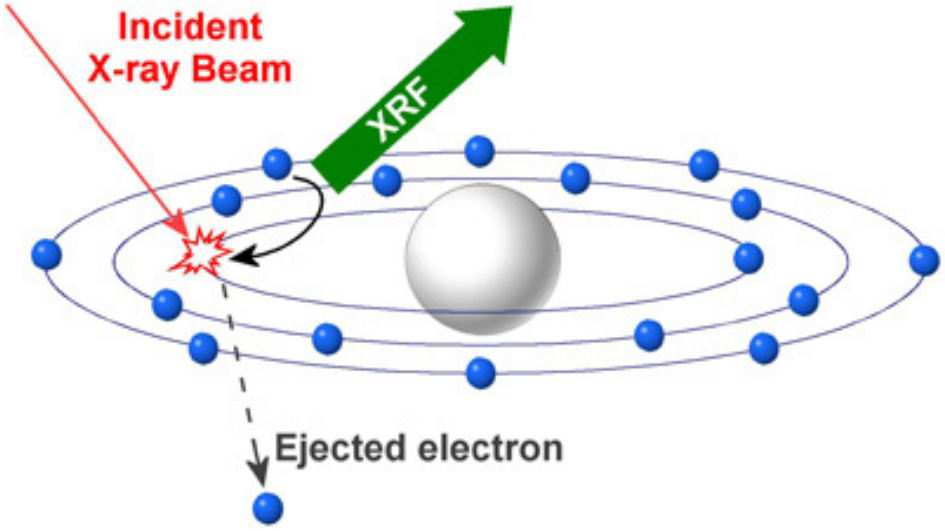

Figure A-1: Working principle of XRF [8]

titanium and zinc. Figure A-2a gives an indication of the scanned area with the yellow border



(a) Yellow marks the scanned area

(b) Shows the X-ray transmission image

Figure A-2: Area scanned and X-ray transmission image

as can be seen an area on the left is not scanned. Figure A-2b is seen the continuum image, which is a normal X-ray image.

A-2-1 Complete overview of the Macro-XRF Maps

This section shows all the macro-XRF images



Arsenic - band K



Barium - band L



Bismuth- band L



Calcium - band K



Cobalt- band K



Chromium - band K



Copper- band K



Iron - band K



Mercury - band L



Potassium - band K



Manganese - band K



Nickel - band K



Lead- band L



Lead - band M



Tin - band K



Tin - band L



Strontium - band K



Titanium - band K



Zinc - band K

Appendix B

Cross-section Samples

The different samples were looked at with the microscope. For the microscope three different lighting settings were used, Bright field, Dark field and ultraviolet with a wavelenght of 365nm. When the samples are looked at with dark field, Shellsol T was used to saturate the samples. Samples 215/1, 215/2 and 215/3 are taken by prof.dr. Arie Wallert[14] and 40_7, 40_12 and 40_15 are taken by dr. Karin Groen[13].

B-1 Sample 215/2

Sampling done by	prof.dr. Arie Wallert
Sample number	215/2
Date	21 December 2011
Spot	73.6 cm from the left, 7.9 cm from the top (measured inside the frame)
Description of spot	Black hat, dark black paint on top orange little head
Purpose	Mixture of black composition of paint layers and same composition 251/1 different samples of the Jewish Bride

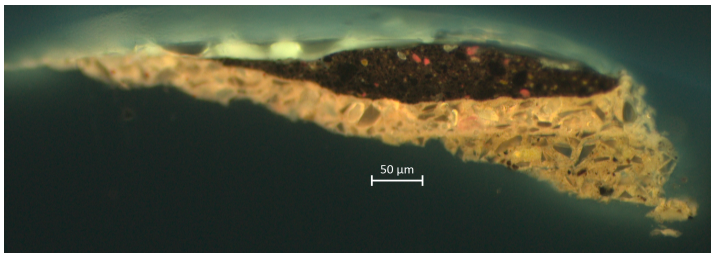

(a) Sample 215/2 UV 365nm

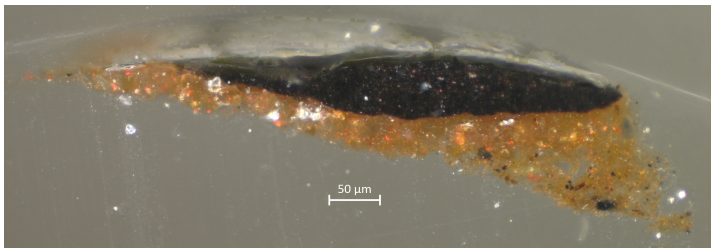

(b) Sample 215/2 Dark Field

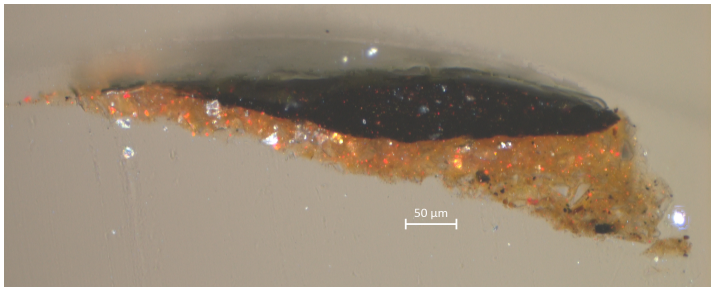

(c) Sample 215/2 Bright Field

Figure B-1: Sample 215/2

B-2 Sample 215/3

Sampling done by	prof.dr. Arie Wallert
Sample number	215/3
Date	21 December 2011
Spot	69.1 cm from the right, 12 cm from the top (measured inside the frame)
Description of spot	Above the head of the Jewish Bride, light black brush stroke in the background
Purpose	Original black colour, as referance for sample 215/1 & sample 215/2

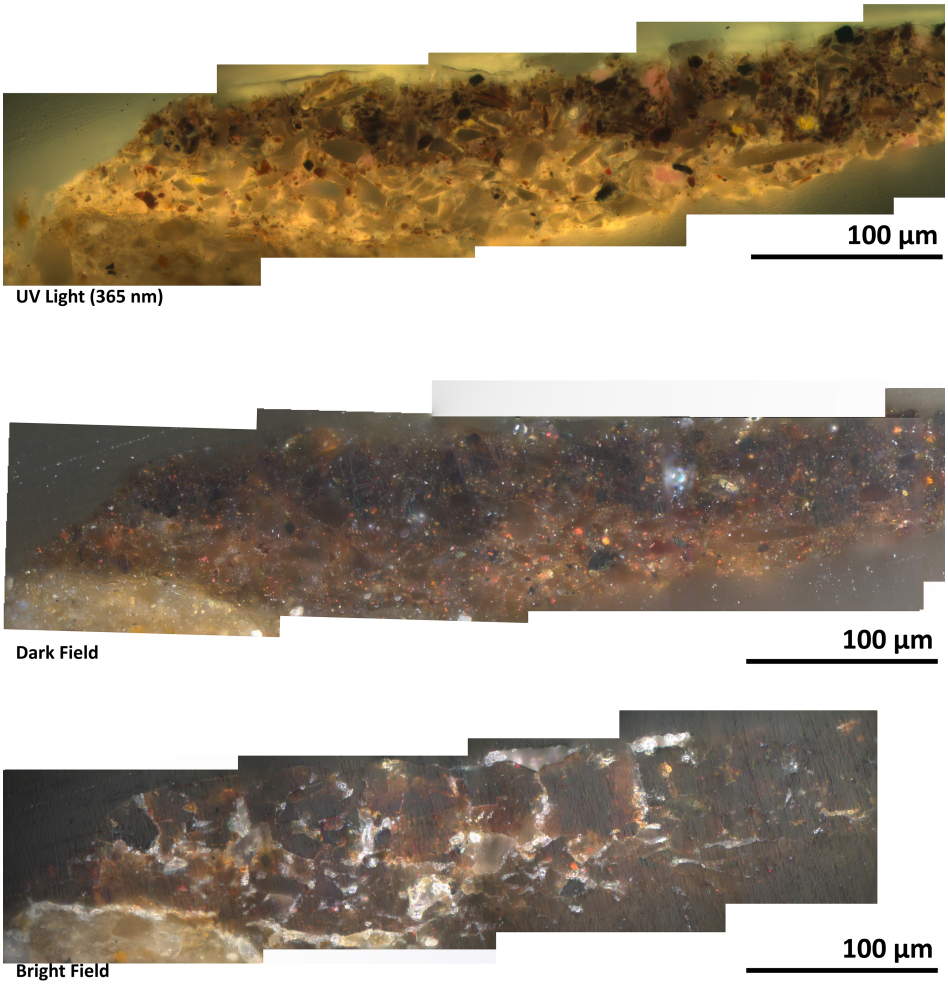

Figure B-2: Sample 215/3

B-3 Sample 40_7

Sampling done by	dr. Karin Groen
Sample number	40_7
Date	15 April 1992
Spot	30 cm from the right, 56 cm from the bottom
Description of spot	Smalt region in the leaves of the flower pot
Purpose	To see the effect the smalt and broken up binding material, as seen in 'The Syndics' of Rembrandt in the Rijksmuseum

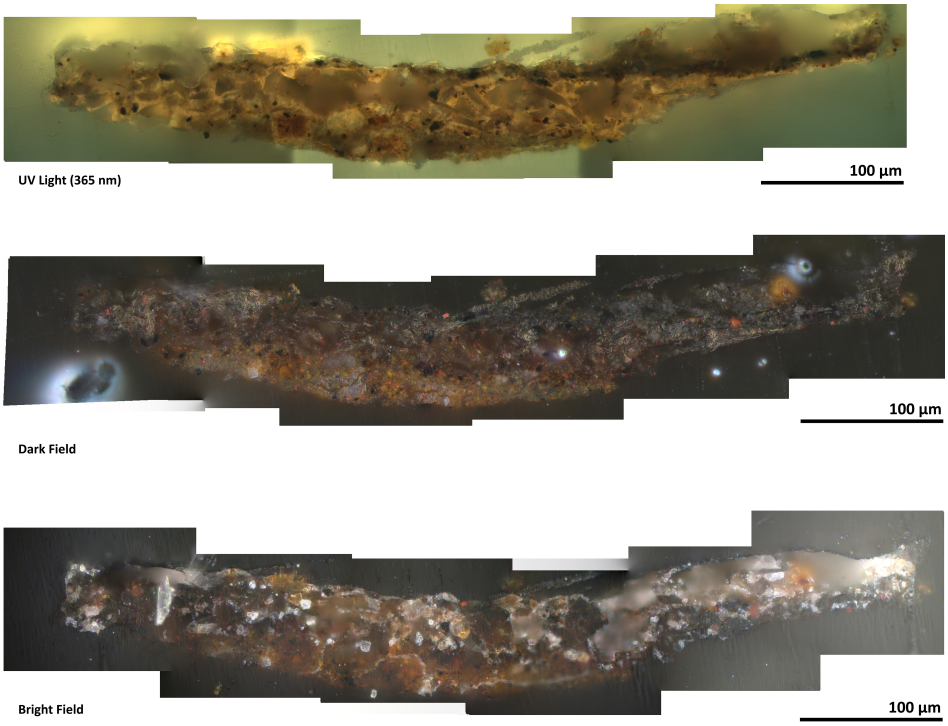

Figure B-3: Sample 40_7

B-4 Sample 40_12

Sampling done by	dr. Karin Groen
Sample number	40_12
Date	2 November 1992
Spot	51.5 cm from the left, 12.5 from the top
Description of spot	Brown background, left of the hat
Purpose	Smooth brown paint on top of cracks, later added Mixture of the brown and black

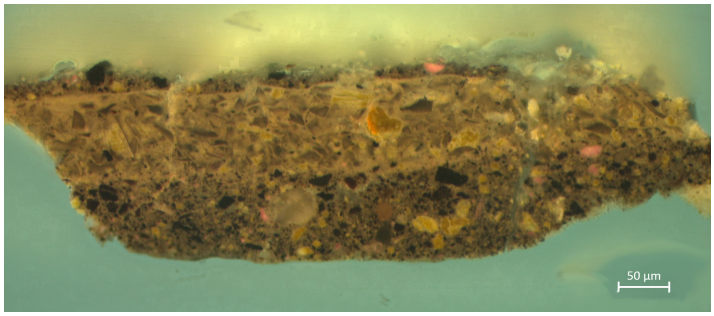

(a) Sample 40_12 UV 365nm

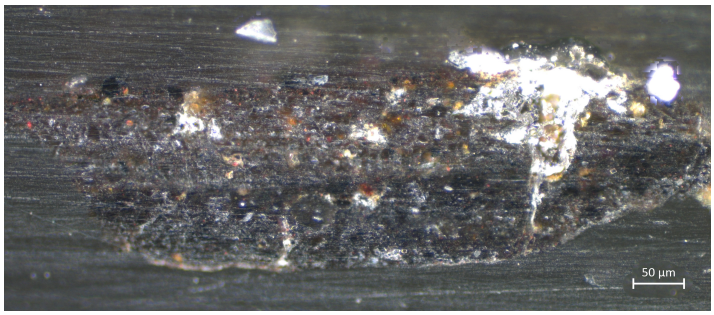

(b) Sample 40_12 Dark Field

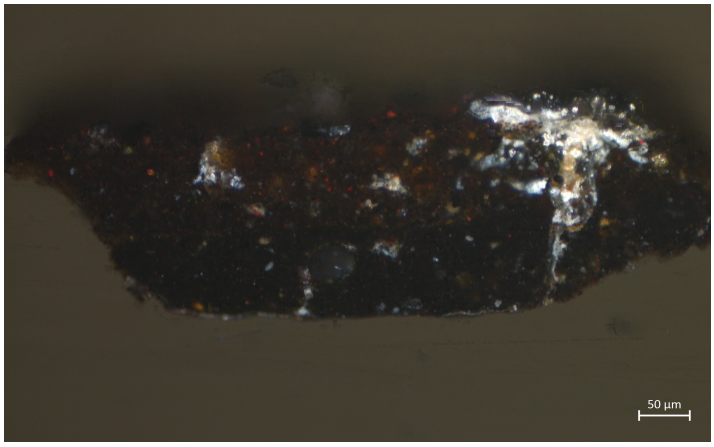

(c) Sample 40_12 Bright Field

Figure B-4: Sample 40_12

B-5 Sample 40_15

Sampling done by	dr. Karin Groen
Sample number	40_15
Date	22 November 1992
Spot	49 cm from the right, 30 cm from the top
Description of spot	Greenish paint right of the dark beam
Purpose	Paint on top of craquelÃľ . Pigment analysis and structure

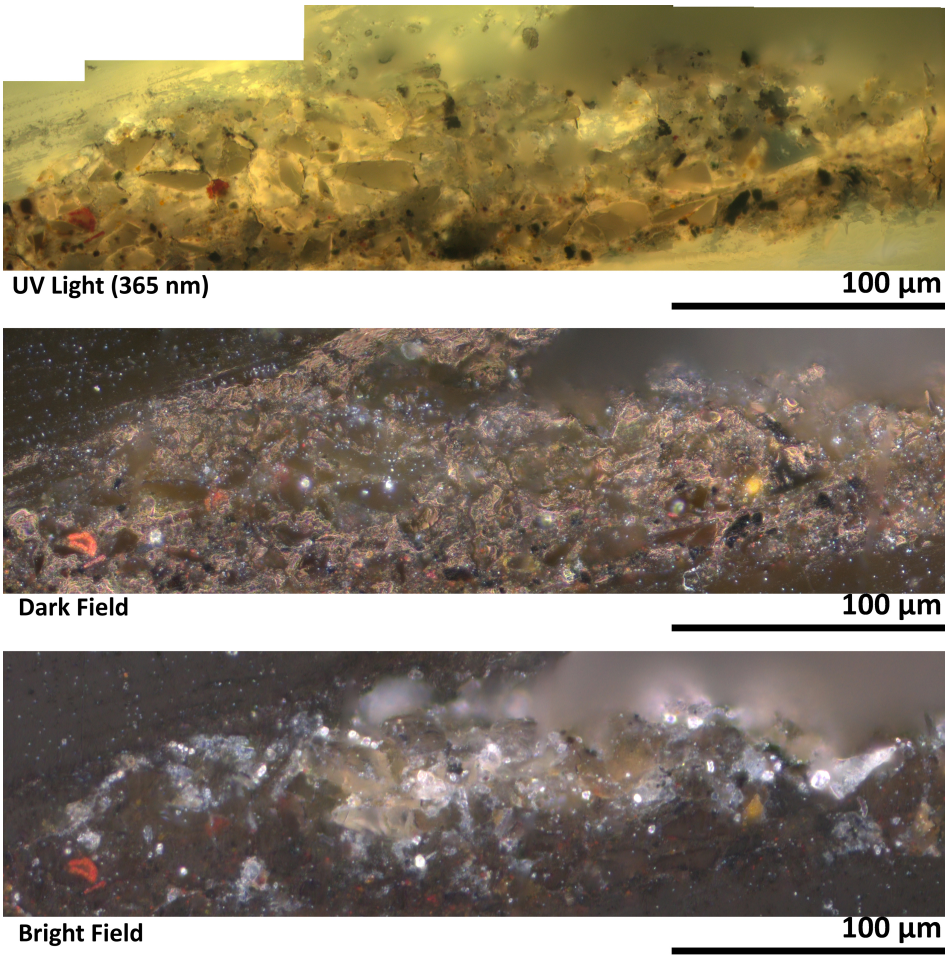

Figure B-5: Sample 40_15

Appendix C

SEM-EDX

Samples 215/2, 215/3, 40_7 , 40_12 and 40_15 and were studied under the SEM-EDX. Sample 215/1 was not scanned, since the sample is parts. The appendix is divided in five sections, each per sample. Each section is sub-divided into the EDX spot and element maps of the sample. In the EDX spot, the location would be indicated. Some of the spectrum quantified data is generated. From that an average and standard deviation is calculated, if they are smalt particles. Other samples only a spectrum image is created, those will be shown at the end of that section.

C-1 SEM-EDX experimental details

The embedded cross-sections were analysed using the SEM-EDX at the FOM Institute AMOLF in Amsterdam. SEM-EDX is a FEI Verios 460 high-pressure electron microscope with an Oxford EDX system. The EDX spot analysis was performed with a 20kV acceleration voltage and a 0.20 nA beam current. To improve the conductivity of the samples they were coated with gold (3 nm). This is done by SC7640 sputter coater (Quorum Technologies, Newhaven, East Sussex, UK). The experiments were performed by Annelies van Loon[15].

C-2 Sample 215/2

C-2-1 EDX spot analysis

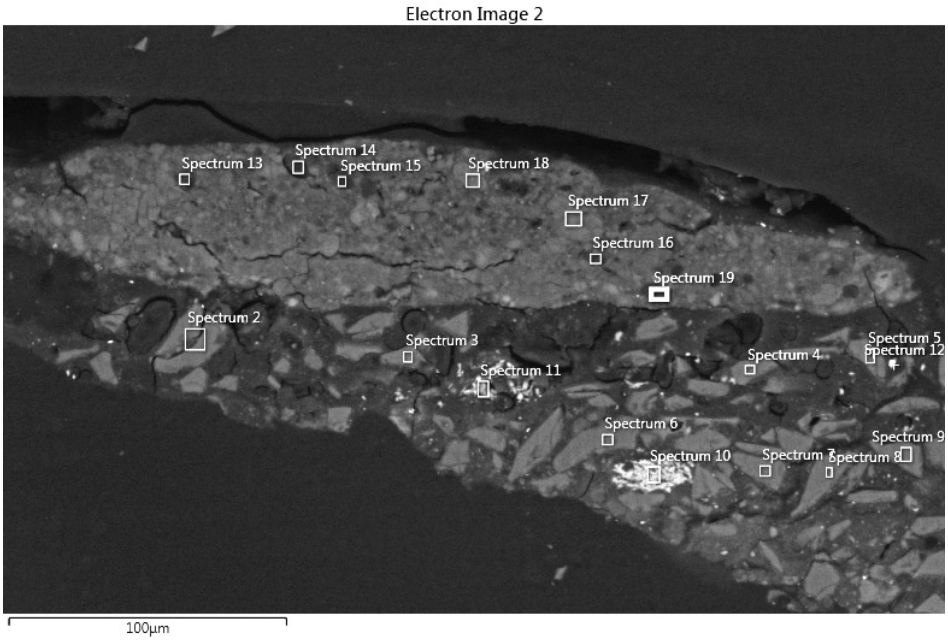

Figure C-1: Sample 215/2 with indicated EDX spots

Table C-1: Quantitative spectrum data of sample 215/2

Wt%	Al_2O_3	SiO_2	K_2O	CaO	FeO	CoO	NiO	As_2O_3	MgO
Spectrum 2	0.92	86.21	0.79	0.71	3.07	4.18	0.83	3.29	0
Spectrum 3	1.62	84.91	0.90	0.93	3.49	3.33	0.89	3.93	0
Spectrum 4	0.82	86.46	0.64	0.43	3.10	4.01	0.59	3.70	0
Spectrum 5	1.02	86.67	0.79	0.51	2.71	3.65	0.83	3.82	0
Spectrum 6	1.31	87.65	0.52	1.92	2.38	2.17	0.76	2.71	0.32
Spectrum 7	0.69	86.45	0.60	0.34	3.13	4.36	0.90	3.54	0
Spectrum 8	0.60	86.86	0.74	0.28	2.89	4.05	1.09	3.51	0

Table C-2: Average wt% and standard deviation of sample 215/2 spectrum spots

	Average	Standard Deviation
Al_2O_3	1.00	0.36
SiO_2	86.46	0.83
K_2O	0.71	0.13
CaO	0.73	0.57
FeO	2.97	0.35
CoO	3.68	0.75
NiO	0.84	0.15
As_2O_3	3.50	0.41
MgO	0.05	0.12

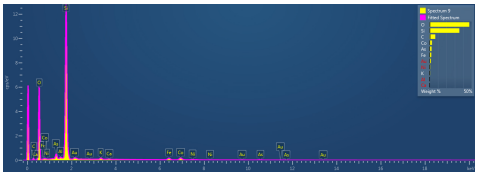

(a) Spectrum 9

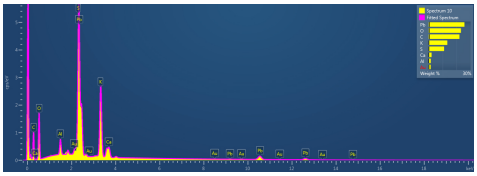

(b) Spectrum 10

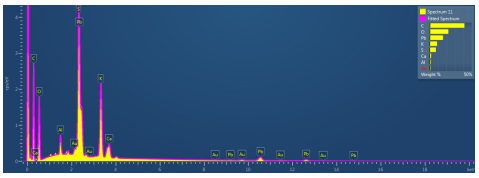

(c) Spectrum 11

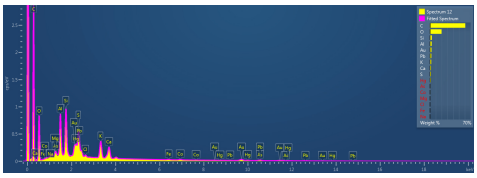

(d) Spectrum 12



(e) Spectrum 13

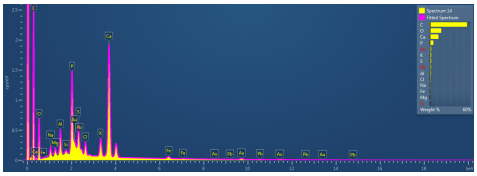

(f) Spectrum 14

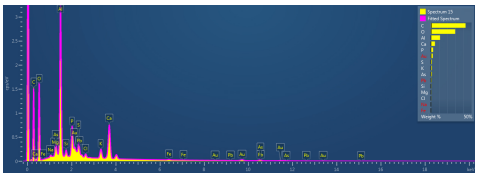

(g) Spectrum 15

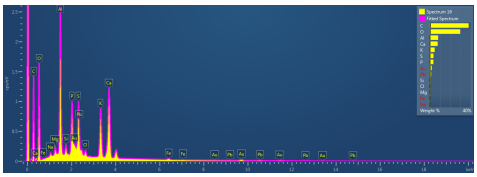

(h) Spectrum 16

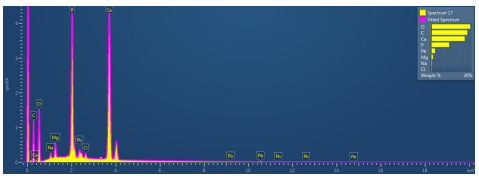

(i) Spectrum 17



(j) Spectrum 18

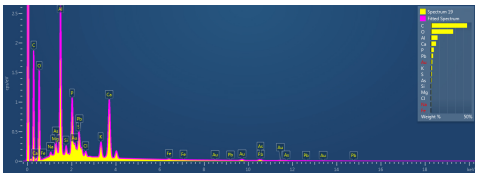

(k) Spectrum 19

Figure C-2: Spectra 9 - 19

C-2-2 Element Map of Sample

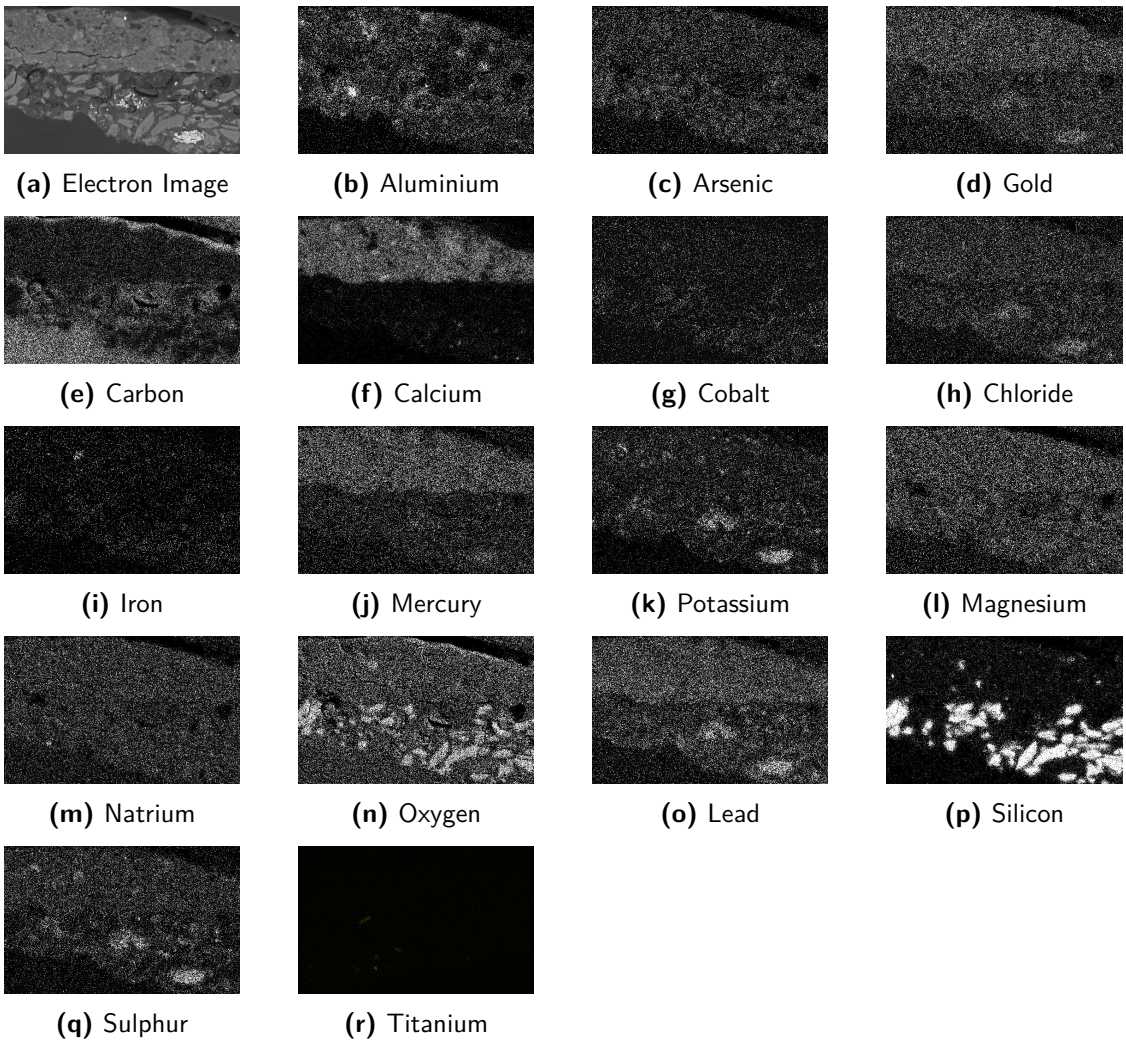

(a) Electron Image **(b)** Aluminium **(c)** Arsenic **(d)** Gold

(e) Carbon **(f)** Calcium **(g)** Cobalt **(h)** Chloride

(i) Iron **(j)** Mercury **(k)** Potassium **(l)** Magnesium

(m) Natrium **(n)** Oxygen **(o)** Lead **(p)** Silicon

(q) Sulphur **(r)** Titanium

Figure C-3: Elemental maps of Sample 215/2

C-3 Sample 215/3

C-3-1 EDX spots

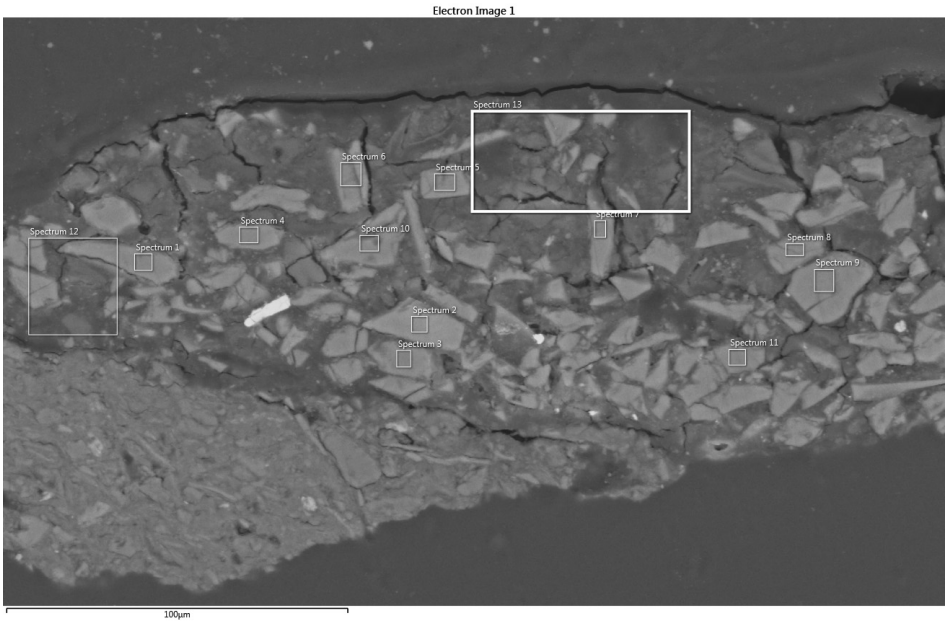

Figure C-4: Sample 215/3 with indicated EDX spots

Table C-3: Quantitative spectra data of sample 215/3

Wt%	Al_2O_3	SiO_2	K_2O	CaO	FeO	CoO	NiO	As_2O_3	PbO
Spectrum 1	0.64	87.62	0.53	0.35	2.88	3.60 0.77	3.61	0	
Spectrum 2	0.88	72.85	12.27	0	2.94	4.98 1.02	5.06	0	
Spectrum 3	0.66	86.98	0.57	0.26	2.99	4.01 0.71	3.81	0	
Spectrum 4	1.40	85.86	0.84	0.01	3.2	2.95 0.90	3.85	0	
Spectrum 5	1.54	84.81	0.6	1.23	3.35	3.45 1.01	4.01	0	
Spectrum 6	0.85	85.5	0.66	0.51	3.00	4.20 0.92	4.36	0	
Spectrum 7	0.78	86.49	0.46	0.51	3.01	3.90 0.88	3.96	0	
Spectrum 8	1.47	84.41	0.68	0.99	3.46	3.11 0.89	3.31	1.67	
Spectrum 9	2.86	83.13	1.27	0.17	2.95	3.60 0.12	5.90	0	
Spectrum 10	1.06	87.09	0.47	0.39	2.76	3.81 0.72	3.69	0	
Spectrum 11	0.60	87.07	0.53	0.30	2.86	3.90 0.88	3.85	0	
Spectrum 12	4.81	70.01	1.71	4.82	4.61	2.93 0.76	3.14	7.21	
Spectrum 13	9.60	56.45	3.28	9.21	3.63	2.18 0.47	2.39	12.78	

Table C-4: Average wt% and standard deviation of sample 215/3 sample spots

	Average	Standard Deviation
Al_2O_3	2.09	2.54
SiO_2	81.41	9.34
K_2O	1.84	3.23
CaO	1.44	2.65
FeO	3.20	0.49
CoO	3.59	0.70
NiO	0.77	0.24
As_2O_3	3.92	0.86
PbO	1.67	3.89

C-3-2 Element map of sample

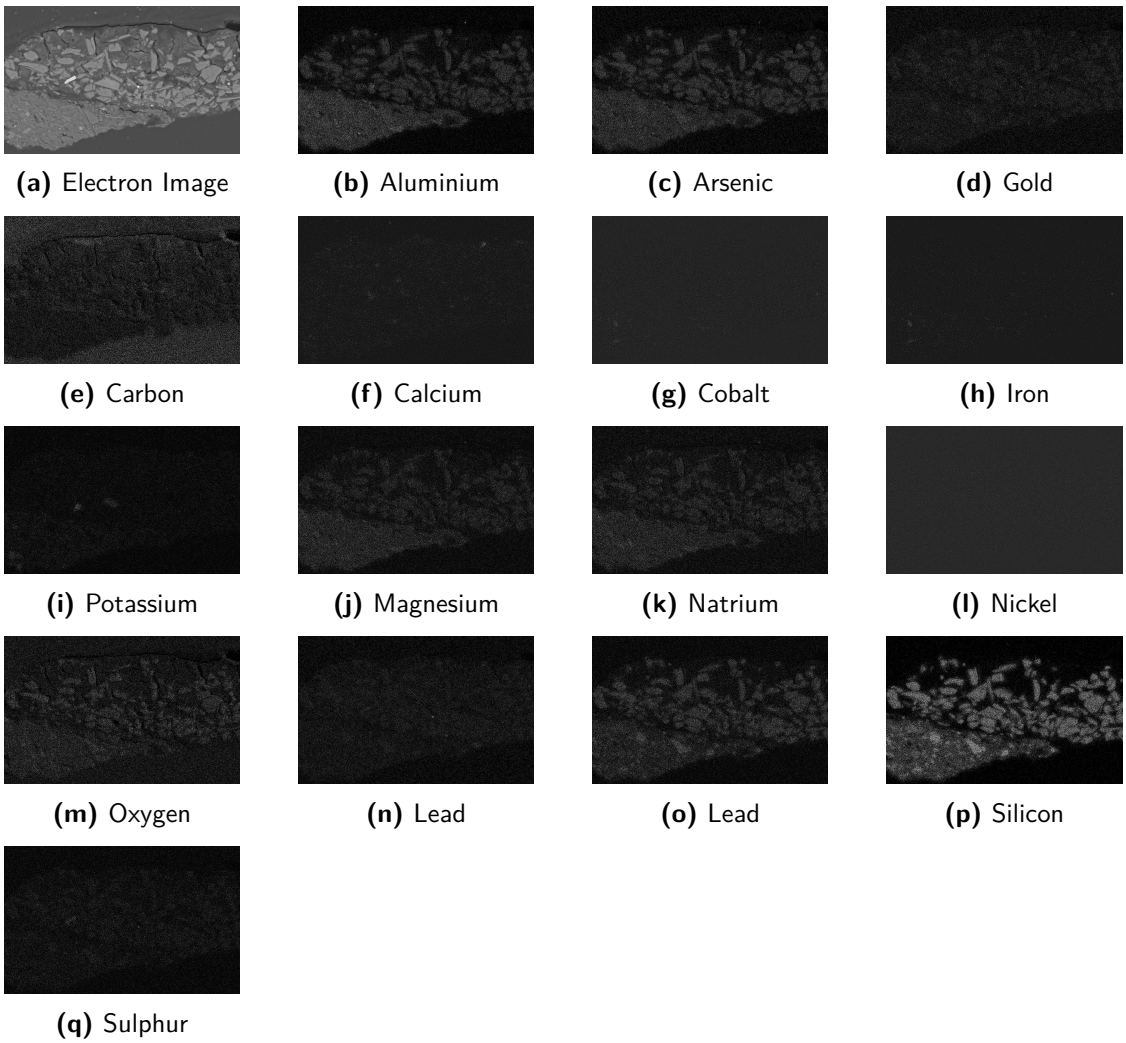

(a) Electron Image **(b)** Aluminium **(c)** Arsenic **(d)** Gold

(e) Carbon **(f)** Calcium **(g)** Cobalt **(h)** Iron

(i) Potassium **(j)** Magnesium **(k)** Natrium **(l)** Nickel

(m) Oxygen **(n)** Lead **(o)** Lead **(p)** Silicon

(q) Sulphur

Figure C-5: Elemental maps of Sample 215/3

C-4 Sample 40_7

C-4-1 EDX spot analysis

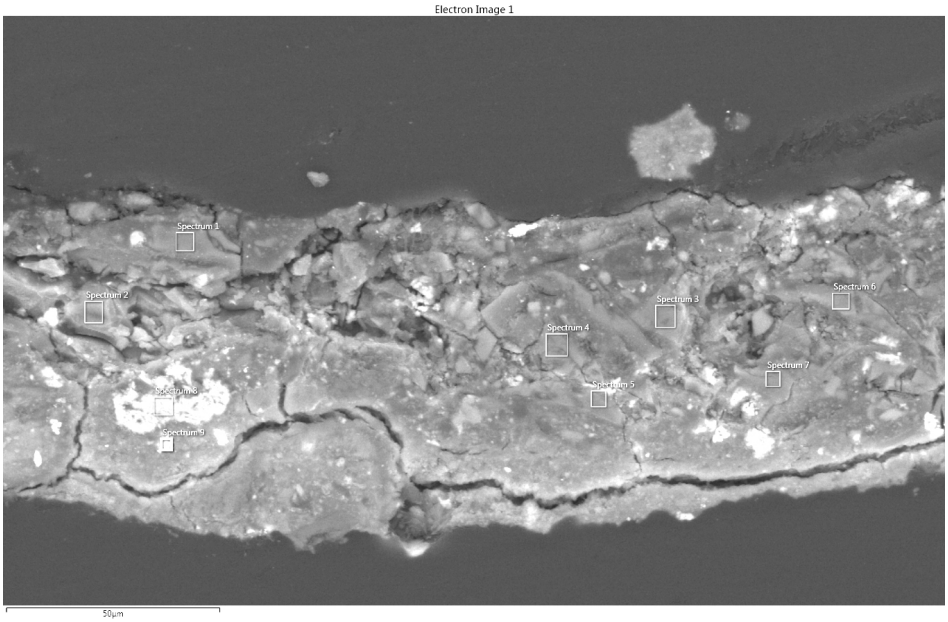

Figure C-6: Sample 40_7 with indicated EDX spots

Table C-5: Quantitative spectra data of sample 40_7

Wt%	$Al_2O_3\%$	$SiO_2\%$	$K_2O\%$	$CaO\%$	$FeO\%$	$CoO\%$	$NiO\%$	$As_2O_3\%$
Spectrum 1	0.91	86.69	0.71	0.75	2.64	3.45	0.75	4.11
Spectrum 2	0.82	87.25	0.76	0.23	2.66	3.53	0.73	4.02
Spectrum 3	0.73	86.85	0.63	0.39	2.58	3.44	0.82	4.56
Spectrum 4	1.05	86.57	0.88	1.75	2.27	2.86	0.37	4.24
Spectrum 5	2.07	82.58	2.34	2.26	3.58	2.62	0.60	3.94
Spectrum 6	0.99	88.19	0.59	0.55	2.32	2.96	0.36	4.04
Spectrum 7	3.32	80.39	2.39	2.06	4.14	2.82	0.40	4.49

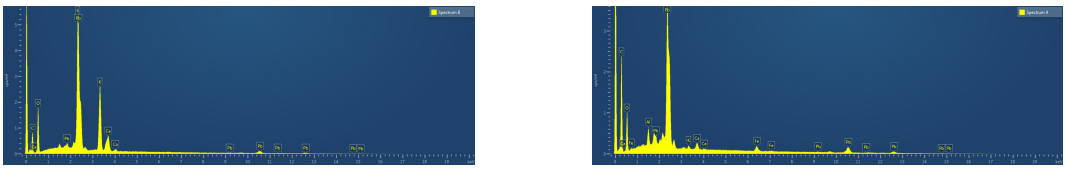

(a) Spectrum 8 **(b)** Spectrum 9

Figure C-7: Spectra 8 & 9

Table C-6: Average wt% and standard Deviation of sample 40_7 sample spots

	Average	Standard Deviation
Al_20_3	1.41	0.95
SiO_2	85.50	2.87
K_2O	1.19	0.811
CaO	1.14	0.85
FeO	2.88	0.70
CoO	3.09	0.37
NiO	0.58	0.20
As_2O_3	4.20	0.24

C-4-2 Element Map of Sample

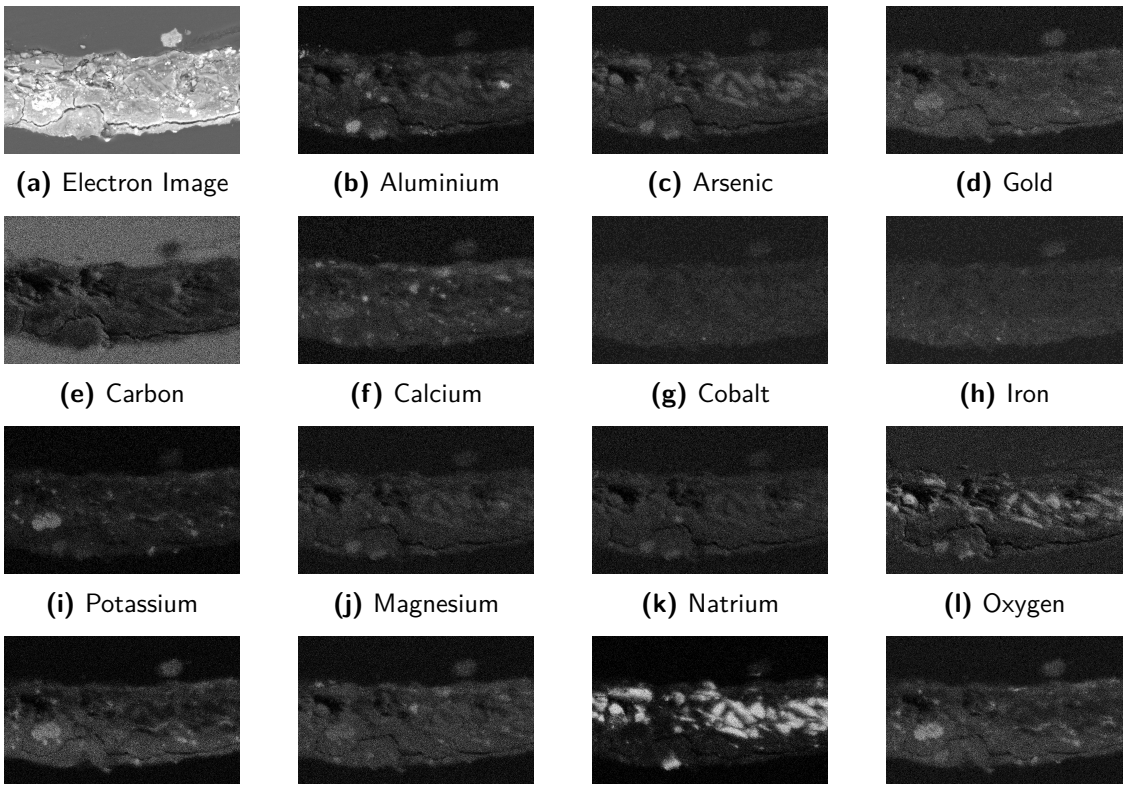

(a) Electron Image **(b)** Aluminium **(c)** Arsenic **(d)** Gold

(e) Carbon **(f)** Calcium **(g)** Cobalt **(h)** Iron

(i) Potassium **(j)** Magnesium **(k)** Natrium **(l)** Oxygen

(m) Lead **(n)** Phosphorus **(o)** Silicon **(p)** Sulpher

Figure C-8: Elemental maps of Sample 40_7

C-5 Sample 40_12

C-5-1 EDX spots

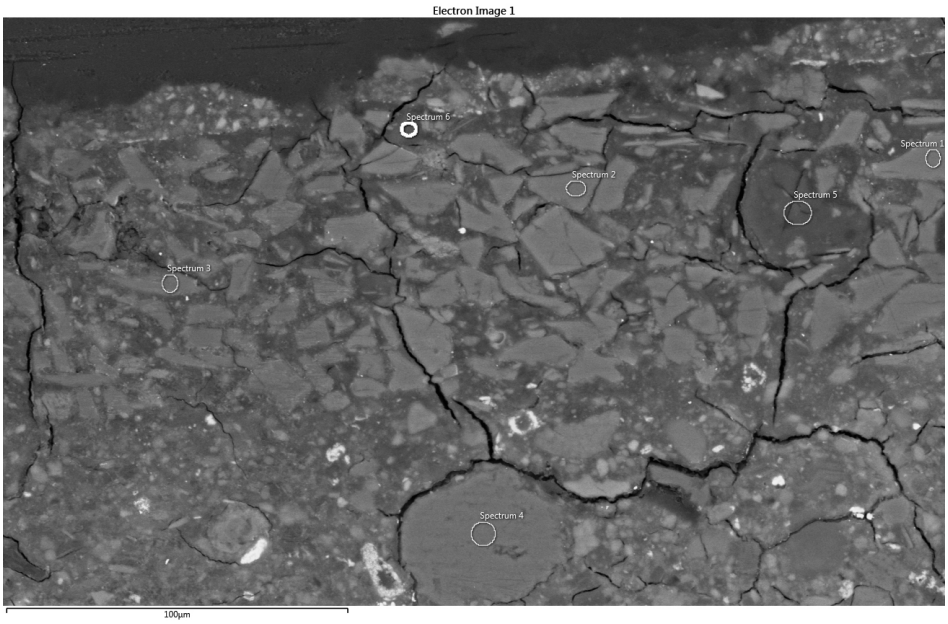

Figure C-9: Sample 40_12 with indicated EDX spots

Table C-7: Quantitative spectrum data of sample 40_12

Wt%	Al_2O_3	SiO_2	K_2O	CaO	FeO	CoO	NiO	As_2O_3	Au_2O_3	Bi_2O_3	SO_3
Spectrum 1	0.96	75.52	1.03	0.61	3.07	4.48	0.71	4.87	6.8	1.33	0.31
Spectrum 2	0.80	80.64	0.72	0.33	3.31	3.81	0.37	3.48	6.35	0	0
Spectrum 3	0.90	81.56	0.88	0.49	2.74	3.78	0.73	3.52	5.17	0	0

Table C-8: Average wt% and standard Deviation of sample 40_12 sample spots

	Average	Standard Deviation
Al_2O_3	0.89	0.08
SiO_2	79.24	3.25
K_2O	0.88	0.16
CaO	0.48	0.14
FeO	3.04	0.29
CoO	4.02	0.40
NiO	0.60	0.20
As_2O_3	3.96	0.79
Au_2O_3	6.11	0.84
Bi_2O_3	0.44	0.77
SO_3	0.10	0.18

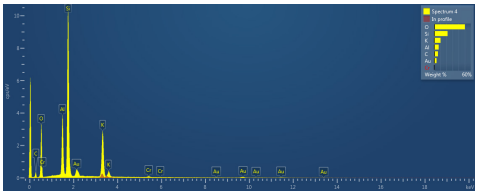

(a) Spectrum 4

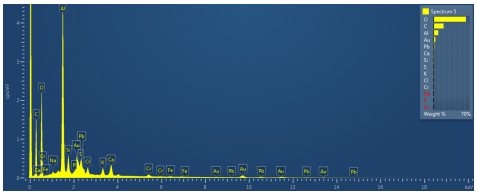

(b) Spectrum 5

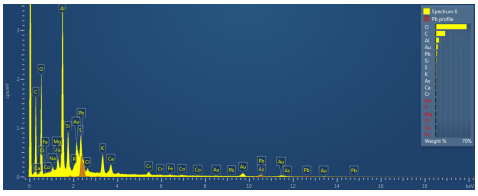

(c) Spectrum 6

Figure C-10: Spectra 4-6

C-5-2 Element Map of Sample

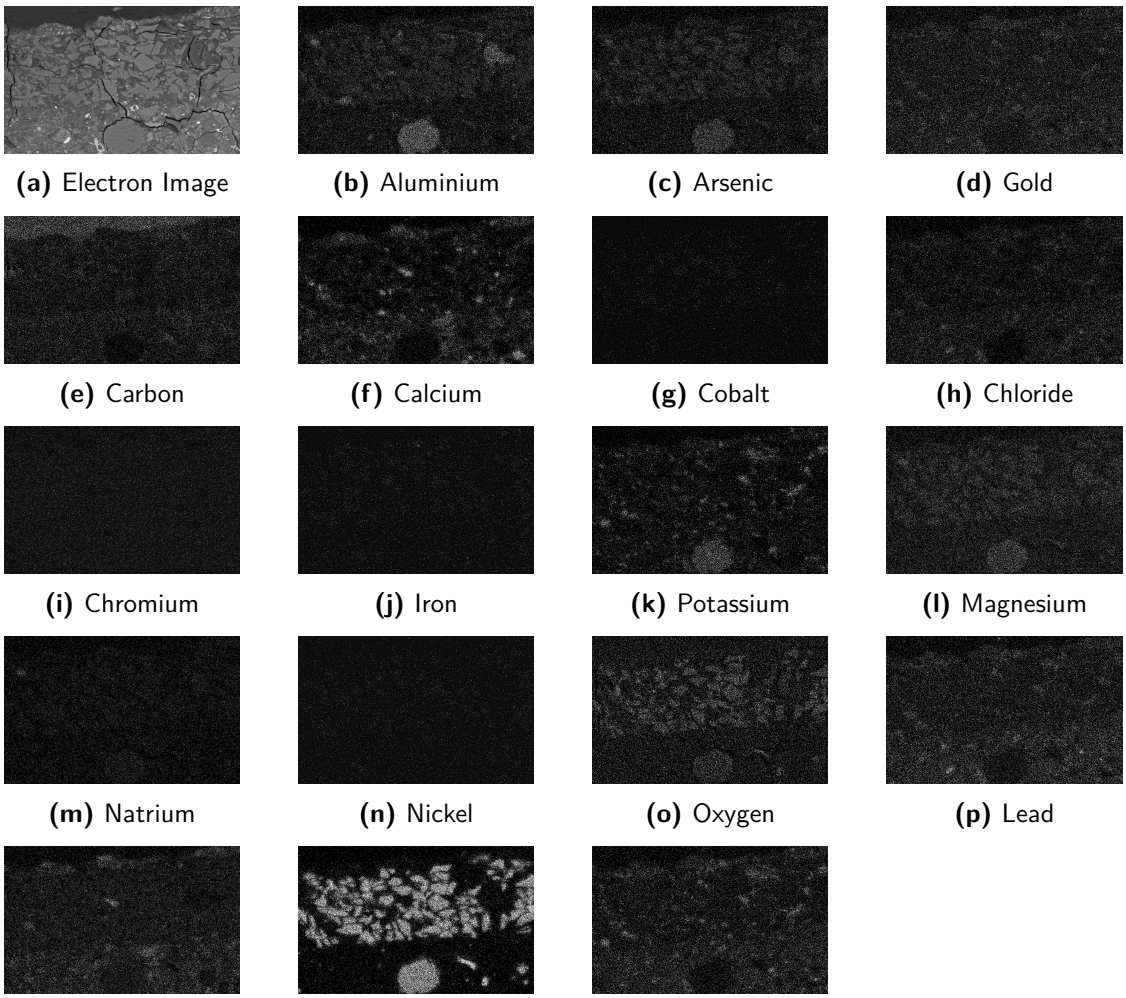

(a) Electron Image **(b)** Aluminium **(c)** Arsenic **(d)** Gold

(e) Carbon **(f)** Calcium **(g)** Cobalt **(h)** Chloride

(i) Chromium **(j)** Iron **(k)** Potassium **(l)** Magnesium

(m) Natrium **(n)** Nickel **(o)** Oxygen **(p)** Lead

(q) Phosphorus **(r)** Silicon **(s)** Sulphur

Figure C-11: Elemental maps of Sample 40_12

C-6 Sample 40_15

C-6-1 EDX Spots

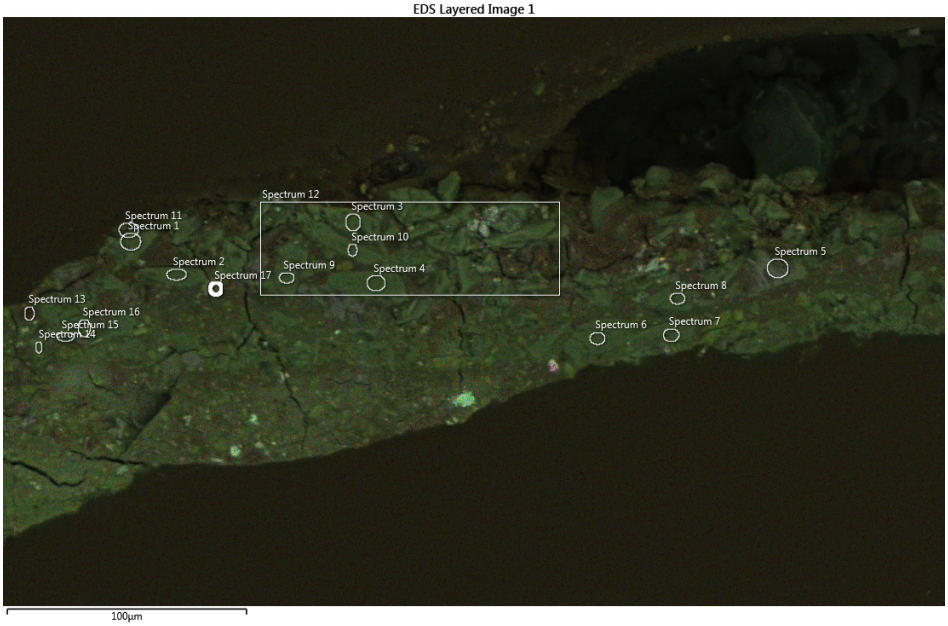

Figure C-12: Sample 40_15 with indicated EDX spots

Table C-9: Quantitative spectra data of sample 40_15

Wt%	$Al_2O_3\%$	$SiO_2\%$	$K_2O\%$	$CaO\%$	$FeO\%$	$CoO\%$	$NiO\%$	$As_2O_3\%$	$PbO\%$
Spectrum 1	0.78	85.59	0.87	0.89	2.85	4.14	0.85	4.04	-
Spectrum 2	0.90	87.14	0.44	0.57	2.64	3.74	0.74	3.83	-
Spectrum 3	1.36	86.03	0.58	0.68	3.41	3.24	0.78	3.93	-
Spectrum 4	0.74	87.28	0.49	0.31	2.93	3.94	0.73	3.59	-
Spectrum 5	1.29	71.87	14.21	-	2.70	3.83	0.74	5.36	-
Spectrum 6	0.95	87.11	0.47	0.34	3.50	3.78	-	3.86	-
Spectrum 7	2.05	82.93	1.33	2.25	3.35	3.80	0.76	3.54	-
Spectrum 8	0.74	87.28	0.49	0.31	2.93	3.94	0.73	3.59	-
Spectrum 9	1.26	85.96	0.69	0.51	2.80	3.75	0.91	4.12	-
Spectrum 10	1.51	85.74	0.59	0.66	3.34	3.42	0.77	3.97	-
Spectrum 11	2.90	77.43	1.65	3.40	3.03	3.12	0.76	3.35	4.37
Spectrum 12	4.97	68.73	3.62	4.14	3.16	2.66	0.72	3.13	8.87
Spectrum 14	1.62	82.42	0.66	1.33	3.34	4.04	0.95	5.63	-
Spectrum 15	1.75	83.06	0.88	2.42	3.91	3.66	0.94	3.30	-

Table C-10: Elements of smalt particles in sample 40_15

Smalt particles 40_15	Average	Standard Deviation
Al_2O_3	1.38	0.65
SiO_2	84.99	2.92
K_2O	0.79	0.38
CaO	1.13	1.05
FeO	3.16	0.37
CoO	3.67	0.30
NiO	1.09	0.92
As_2O_3	3.40	1.16
PbO	0.40	1.32

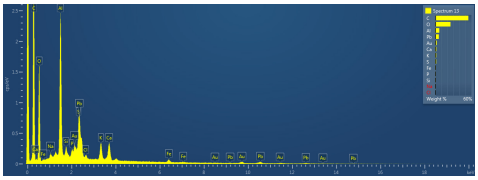

(a) Spectrum 13

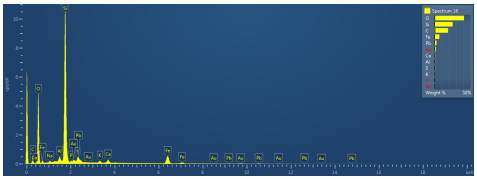

(b) Spectrum 16

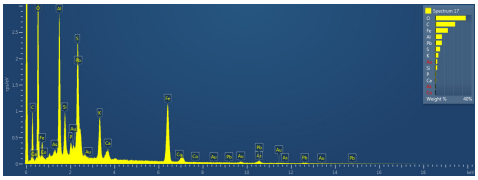

(c) Spectrum 17

Figure C-13: Spectra 13, 16 and 17

C-6-2 Element Map of Sample

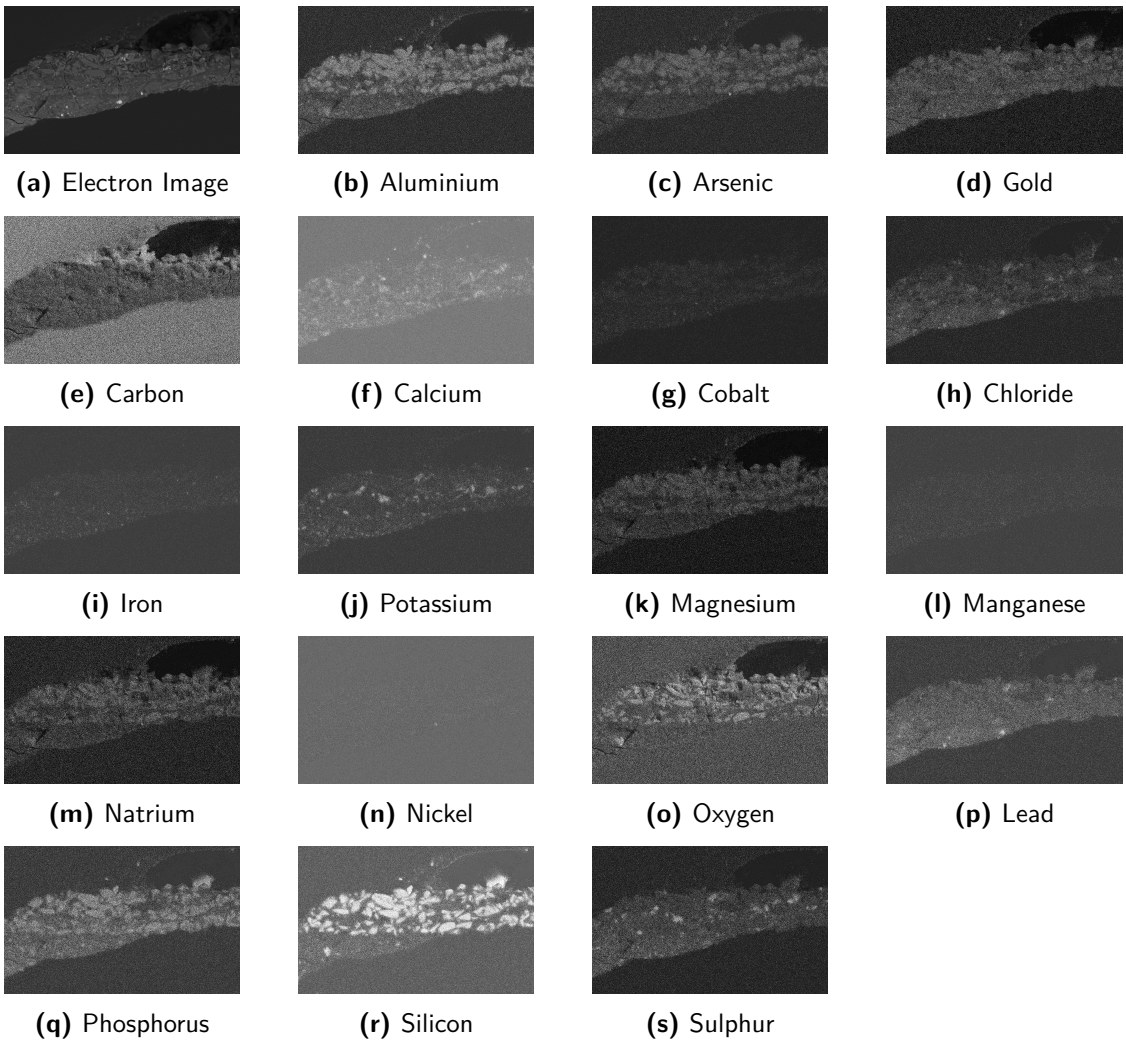

(a) Electron Image **(b)** Aluminium **(c)** Arsenic **(d)** Gold

(e) Carbon **(f)** Calcium **(g)** Cobalt **(h)** Chloride

(i) Iron **(j)** Potassium **(k)** Magnesium **(l)** Manganese

(m) Natrium **(n)** Nickel **(o)** Oxygen **(p)** Lead

(q) Phosphorus **(r)** Silicon **(s)** Sulphur

Figure C-14: Elemental maps of Sample 40_15

C-7 Reconstruction of Sample 40_15

C-7-1 Element maps of sample

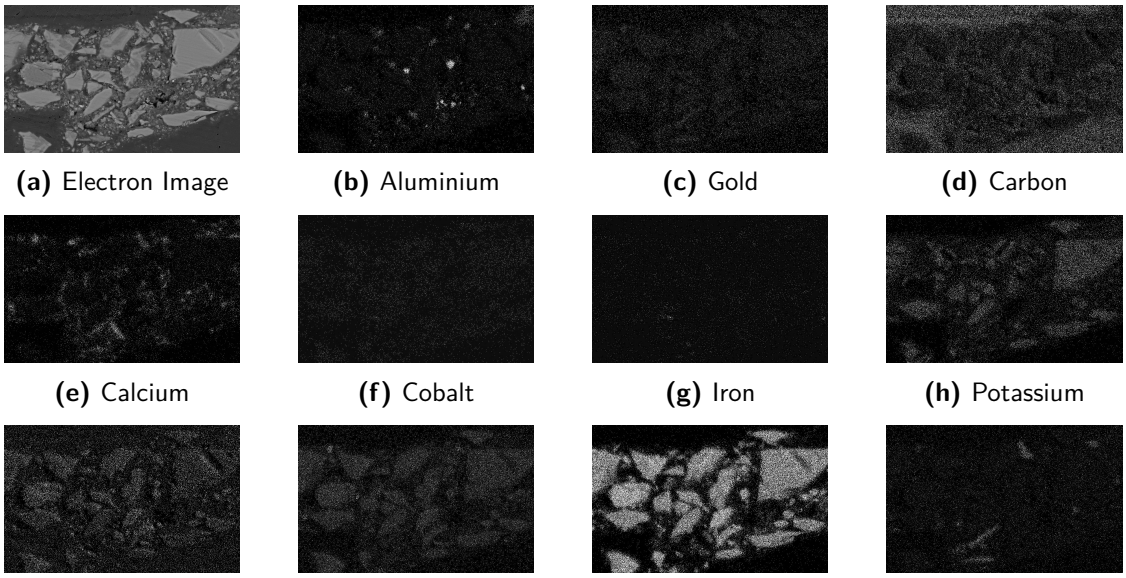

(a) Electron Image **(b)** Aluminium **(c)** Gold **(d)** Carbon

(e) Calcium **(f)** Cobalt **(g)** Iron **(h)** Potassium

(i) Oxygen **(j)** Phosphorus **(k)** Silicon **(l)** Sulphur

Figure C-15: Elemental maps of reconstruction of sample 40_15

Appendix D

Paintouts

D-1 Paint-outs

The paint-outs were based on the work done by Diana de Man (MA Conservation and Restoration of Paintings, University of Amsterdam)[11]. Together the two sets of paint-outs could complement each other. Diana de Man [11] made paint-outs for her thesis, based on the painting of *Homereus* by Rembrandt. For her Master project, she also made smalt, red lake, and yellow lake based on old recipes. [10]

D-1-1 Material used and method

D-1-1-1 Material

The pigments used were the same as for Diana de Man's[11] paint-outs; see Table D-1[11]. The paint-outs were painted on black and white tiles. This is because the tiles do not react with the paint.

Table D-1: Pigments used for Paint outs

Pigment	Abbreviations	Name
Bone Black	BB	Kremer Beinschwarz 47100
Red Earth	RE	Kremer venetian red 40510
Smalt		4% Cobalt made by Diana de Man (UvA C& R 2015)[10]
Yellow Earth	YE	Kremer French Yellow Ochre 40030
Yellow Lake	YL	Made by Diana de Man (UvA C& R 2015) using unripe buckthorn berries [10]

The paint-outs painted on black and white tiles. This as the tiles do not react with the paint.

D-1-1-2 Method

Diana de Man[11] used a drawback bar to determine the thickness of the paint layer. A drawback bar is a slider were the height can vary so the paint is spread evenly. With a drawback bar paint is spread over a relatively large surface area. The amount of smalt was limited,therefore a different method was used where less paint is needed.
Cover slips (No. 1) which are small glass squares 0.13-16 mm in height were used. These slips were placed on top of tiles to create small slits and were held in place with tape. The paint mixtures were spread with a pallet knife between the slits. This leads to small paint-outs with the same thickness.

D-1-2 Translation from volume to weight

The cross-section pigment concentrations were measured in volume percentages. Due to the fact that the amount of smalt was limited, volume was changed into weight. When measuring weight instead of volume, smaller amounts can be used.
The measured volume and weight per dry pigment and oil is seen in table D-2.

Table D-2: Volume and weight per dry pigment and oil

Pigment	Volume(ml)	gram
Bone Black	1.000	0.579
Red Earth	1.000	0.670
Smalt	1.000	0.993
Yellow Earth	1.000	0.596
Yellow Lake	1.000	0.598
Oil	1.000	0.914

To ensure that the percentage of pigment suspended in the oil is known, the volume fraction of pigment plus oil and pigment was calculated. This can be seen in table D-3.

Table D-3: Amount of oil per pigment and fraction

	Weight (gram)	Oil volume used (ml)	Oil weight used (grams)	Weight total (grams)	Total weight/ Pigment weight
Boneblack	2.070	3.0	2.74	4.81	2.33
red earth	2.588	1.5	1.37	3.96	1.53
smalt	3.229	1.75	1.6	4.83	1.50
yellow Earth	2.001	1.5	1.37	3.37	1.69
Yellow Lake	2.841	2.5	2.29	5.12	1.80

While mixing the pigments with oil, Diana de Man[11] confirmed that the viscosity of the paints was the same as when she used them. Since the test was done over a couple of days, in the end a few extra drops of oil were added to ensure that the paint had the same viscosity.

D-1-3 Paint-outs

For the paint-outs, different steps were taken to get from percentage to total weight. This is seen in figure D-1.

As it is easier to start with percentages, this was used. After that a set amount of volume

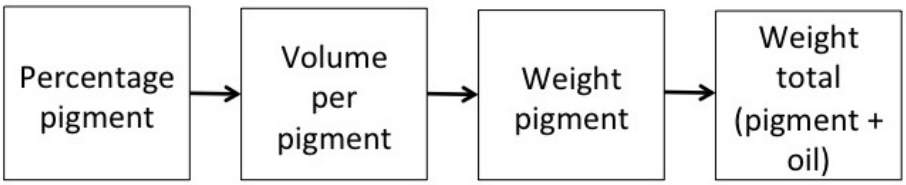

Figure D-1: Steps from pigment prectage to total weight (pigment+oil)

was taken per paint-out, which led to volume per pigment. From the volume per pigment the weight per pigment was calculated. By using the fraction between total weight and pigment weight, the total amount of weight (pigment plus oil) was computed. In total four different paint-out sets were made.

D-1-3-1 First set of paint-outs

The goal for this set was to see how the cross-section samples looked like with non- degraded smalt and yellow lake. The samples 215/3, 40_7 and 40_15 were used and their volume percentages were previously calculated.

D-1-3-2 Second set of paint-outs

The goal of this set was to see what the first set of paint-outs would look like if no smalt were used. By comparing the two, the influence of smalt on colour and texture is seen.

D-1-3-3 Third set of paint-outs

In this set, the goal was to see how the pigments, bone black, red earth and yellow earth, and yellow lake influenced the colour. This was done by setting sample 40_15 as average and changing one of the pigments accordingly, while the rest of the pigment percentages stayed the same. This resulted in 16 different paint-outs, as seen in table D-4

Table D-4: Third set of paint-outs

Test Boneblack	-4.0%	-2.0%	Sample 40_15	+2.0%	+4.0%
Test Red Earth	-5.0%	-2.5%	Sample 40_15	+2.5%	+5.0%
Test Yellow Earth	-5.0%	-2.5%	Sample 40_15	+2.5%	+5.0%
Test Yellow Lake	-5.0%	-2.5%	Sample 40_15	+2.5%	+5.0%

D-1-3-4 Fourth set of paint-outs

The goal in this set was to see how bone black, red earth, yellow earth, and yellow lake react when mixed only with smalt. Three sets of mixtures were made; pigment 25% -75% smalt, pigment 50%-50% smalt, and pigment 75%-25% smalt. This gave a clear insight into how the two pigments behave when mixed with smalt.

D-2 Tile set 1

These are the samples of the paint-outs based on cross-section Samples and paint-outs with different fractions.



(a) Tile 1 samples on white

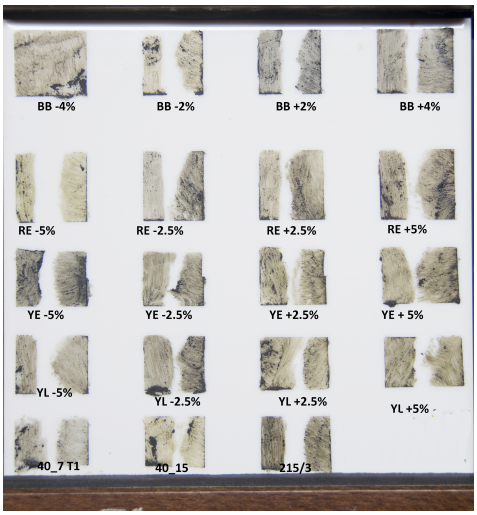

(b) Tile 1 samples on white applied with brush



(c) Tile 1 samples on black tile

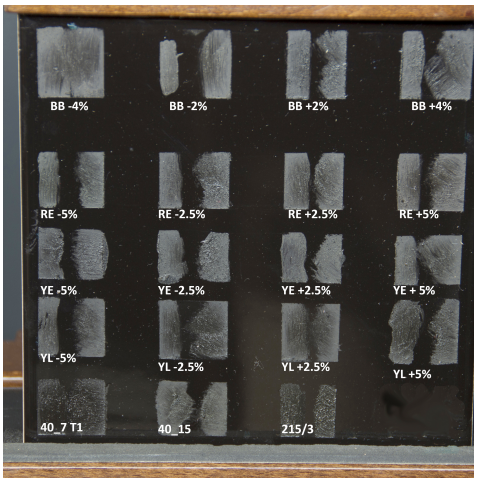

(d) Tile 1 samples on black tile applied with brush

Figure D-2: Tile set 1

D-3 Tile set 2

These are the samples without smalt.

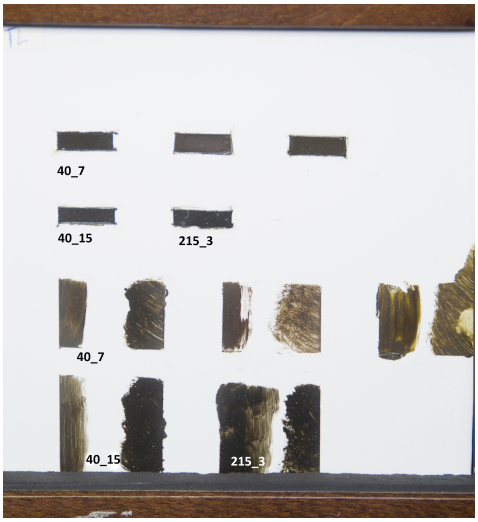

(a) Tile 2 samples on white tile

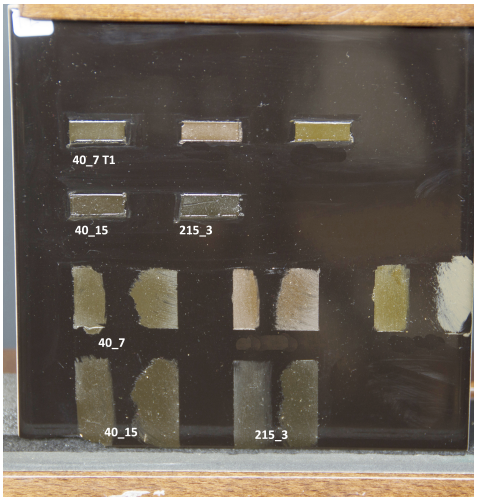

(b) Tile 2 samples on black tile

Figure D-3: Tile set 2

D-4 Tile set 3

These are the samples of the paint-outs with smalt and one other pigment with different and concentration.

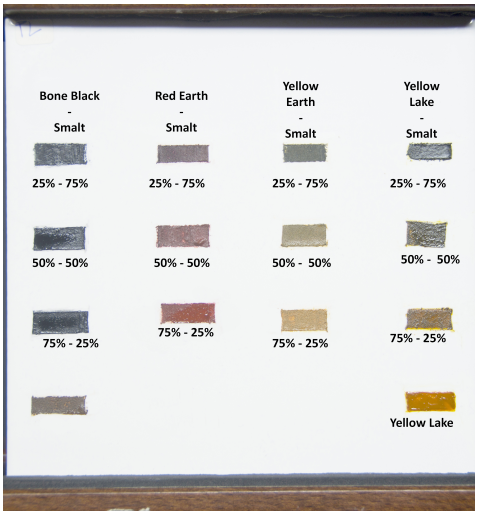

(a) Tile 3 samples on white

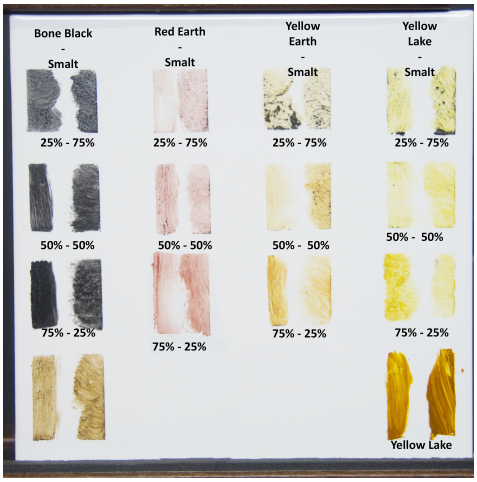

(b) Tile 3 samples on white applied with brush

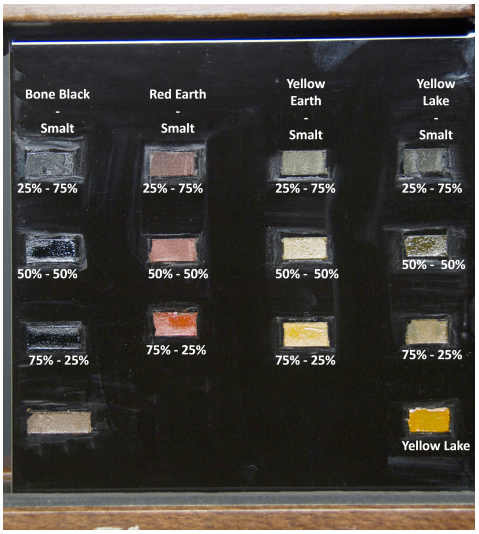

(c) Tile 3 samples on white

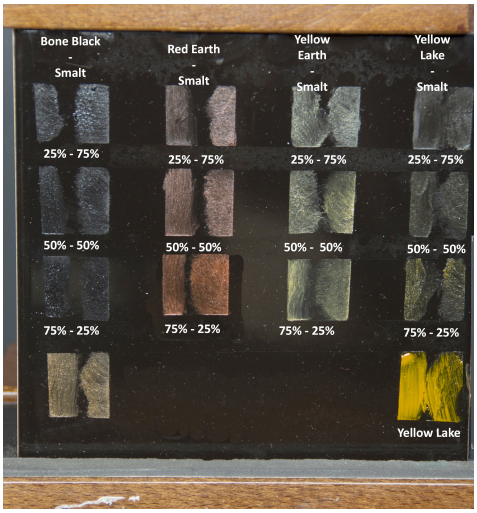

(d) Tile 3 samples on black applied with brush

Figure D-4: Tile set 3

Appendix E

Digital Colour Reconstructions

This appendix will show more digital colour reconstructions. These will give a more of an insight.

E-1 Yellow lake and Smalt

Figure E-1 shows 100 images of the focus area with increasing concentration of smalt and yellow lake. For yellow lake, the macro-XRF image of potassium is used as a guide and for smalt, the macro-XRF image of cobalt is used. The concentration increases in steps of 10%.

E-2 The background without the colour of the degraded matrix and yellow lake

Figure E-2 shows 100 images of the focus area with increasing concentration of yellow lake, while the focus area is decreased with the colour of degraded smalt. For yellow lake, the macro-XRF image of potassium is used as a guide and for degraded smalt colour, the macro-XRF image of cobalt is used. The steps are that of 10%. By subtracting the colour of degraded smalt the colour becomes lighter and more specular reflection appears. Smalt makes the painting progressively darker/bluer.

E-3 The background without the colour of the degraded matrix and yellow lake

Figure E-3 shows 100 images of the focus area with increasing concentration of yellow lake, while the focus area is decreased of the colour of degraded smalt. For smalt, the macro-XRF image of cobalt is used as a guide and for degraded smalt colour, the macro-XRF image of

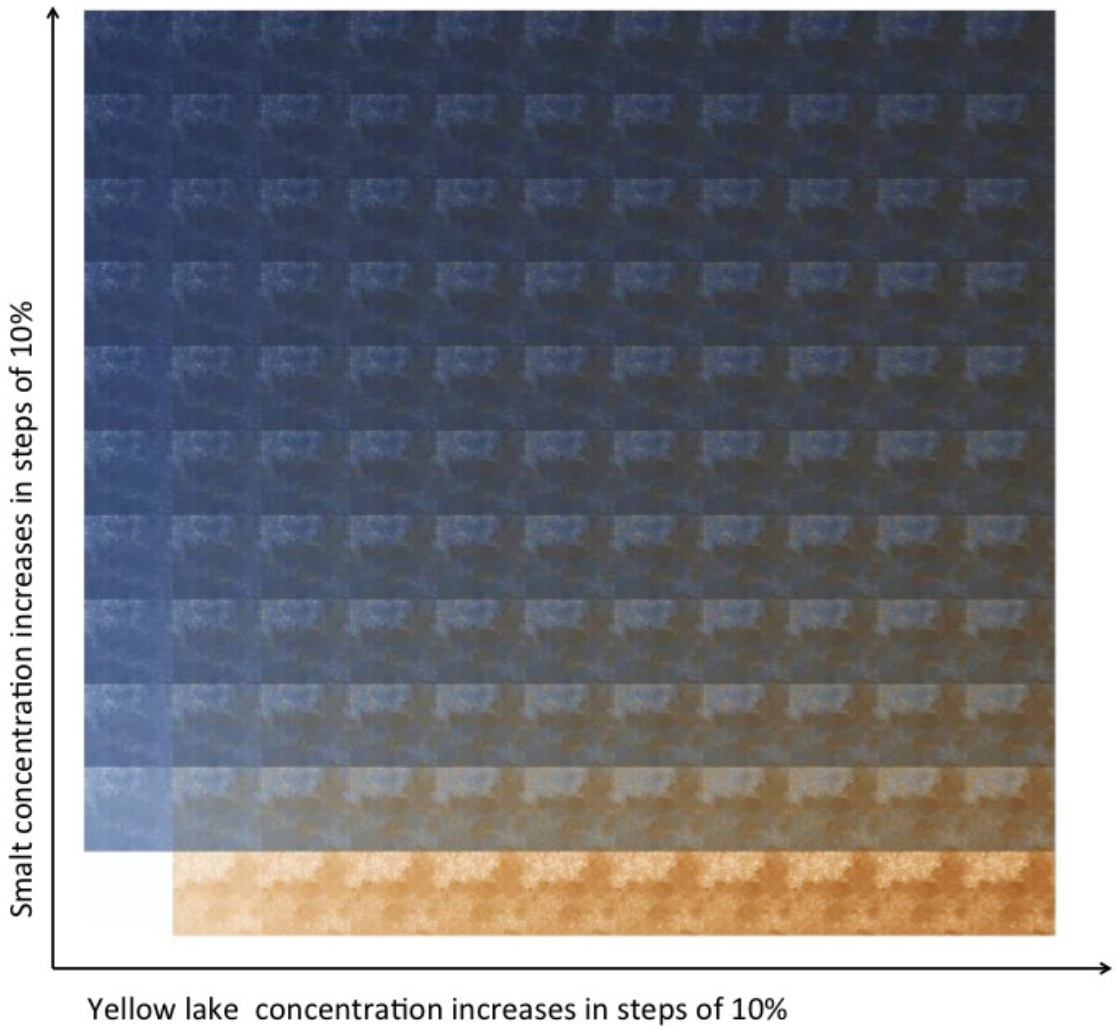

Figure E-1: The focus area with increasing concentration of smalt and yellow lake
It shows that in almost every concentration the area surrounding the leaves appear blue, while the leaves turn brownish due to the fact of the mix of blue and 'reddish' yellow.

cobalt is used. The steps are that of 10%. By subtracting the colour of degraded smalt the colour becomes lighter and more specular reflection appears. Yellow lake makes the painting progressively darker and more brown.

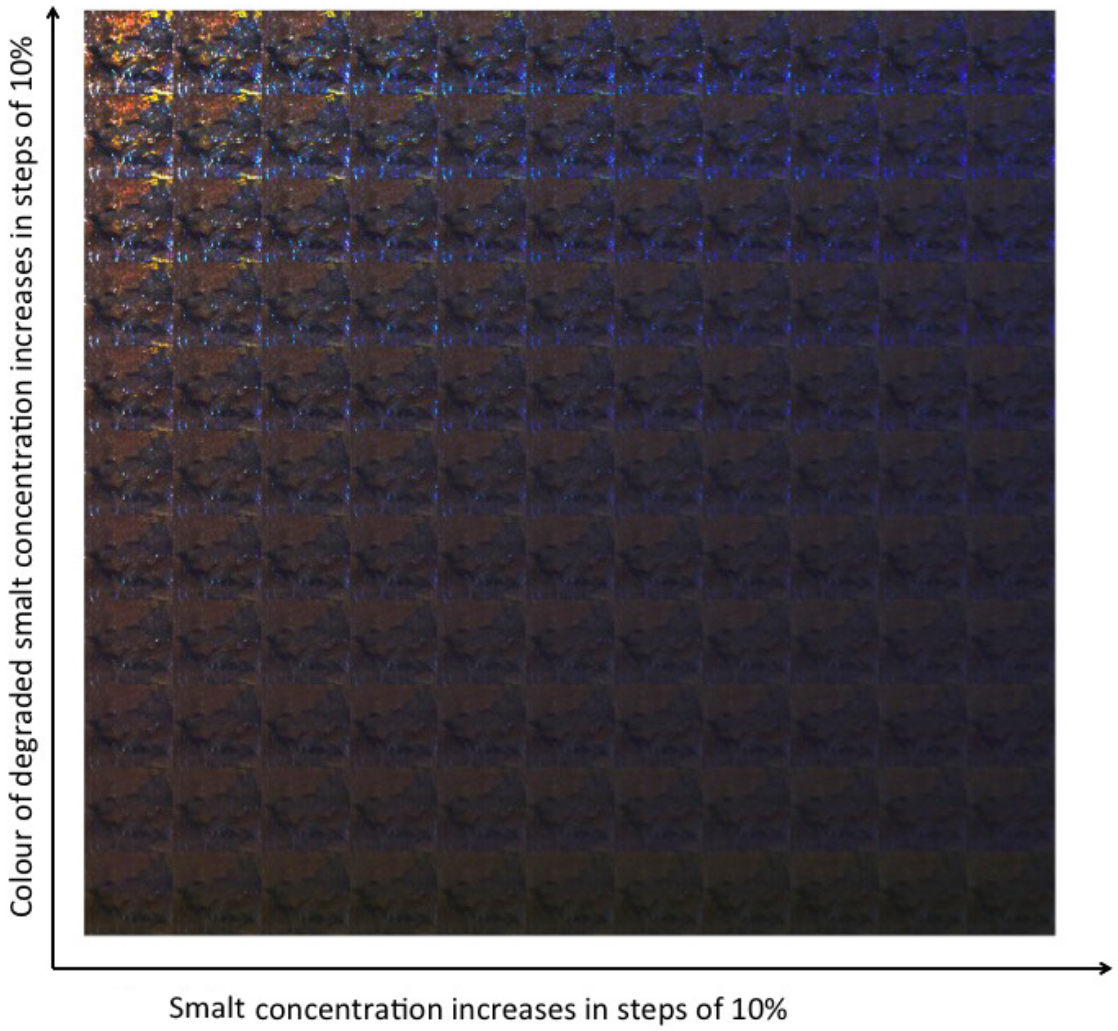

Figure E-2: The focus area with increasing concentration of yellow lake and increasing amount of degraded smalt is filtered out. By subtracting the colour of degraded smalt the colour becomes lighter and more specular reflection appears. Smalt makes the painting progressively darker/bluer.

E-4 Expansion of figure 4-57

Figure E-4 shows 100 images of the focus area with increasing concentration of yellow lake and smalt. The original image is set at 80%. For smalt, the macro-XRF image of cobalt is used as a guide and for yellow lake, the macro-XRF image of potassium is used. The steps are that of 10%. It shows that that the focus area get progressively darker and cooler of tone FigureE-4 shows 100 images of the focus area with increasing concentration of yellow lake and smalt. The original image is set at 80% and 20% of the colour of degraded smalt

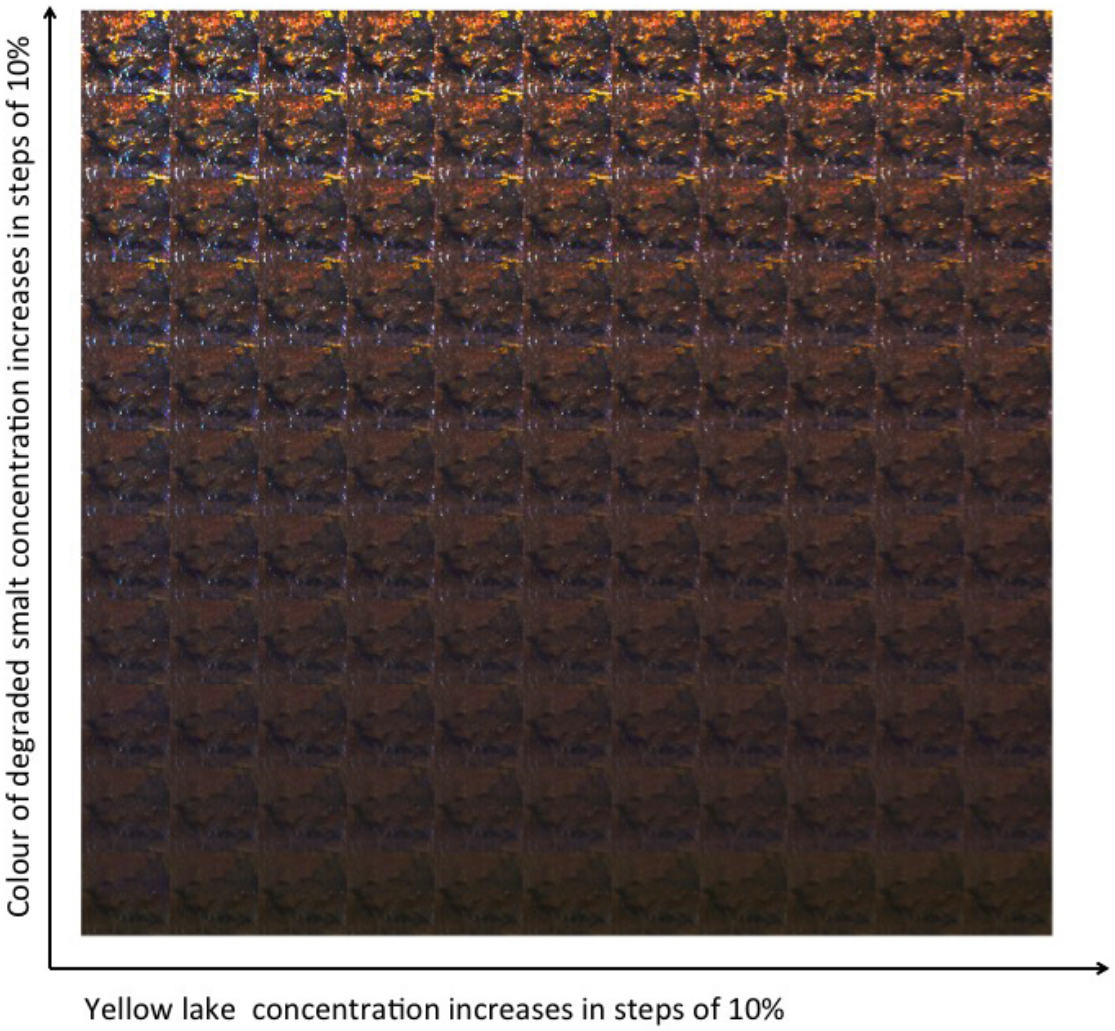

Figure E-3: The focus area with increasing concentration of smalt and increasing amount of degraded smalt is filtered out.
By subtracting the colour of degraded smalt the colour becomes lighter and more specular reflection appears. Yellow lake makes the painting progressively darker and more brown.

is subtracted based on the cobalt distribution. For smalt, the macro-XRF image of cobalt is used as a guide and for yellow lake, the macro-XRF image of potassium is used. The steps are that of 10%. It shows that that the focus area get progressively darker and cooler of tone All in all, it can be stated that by mixing back yellow lake and smalt back, the focus area becomes darker and cooler of tone.

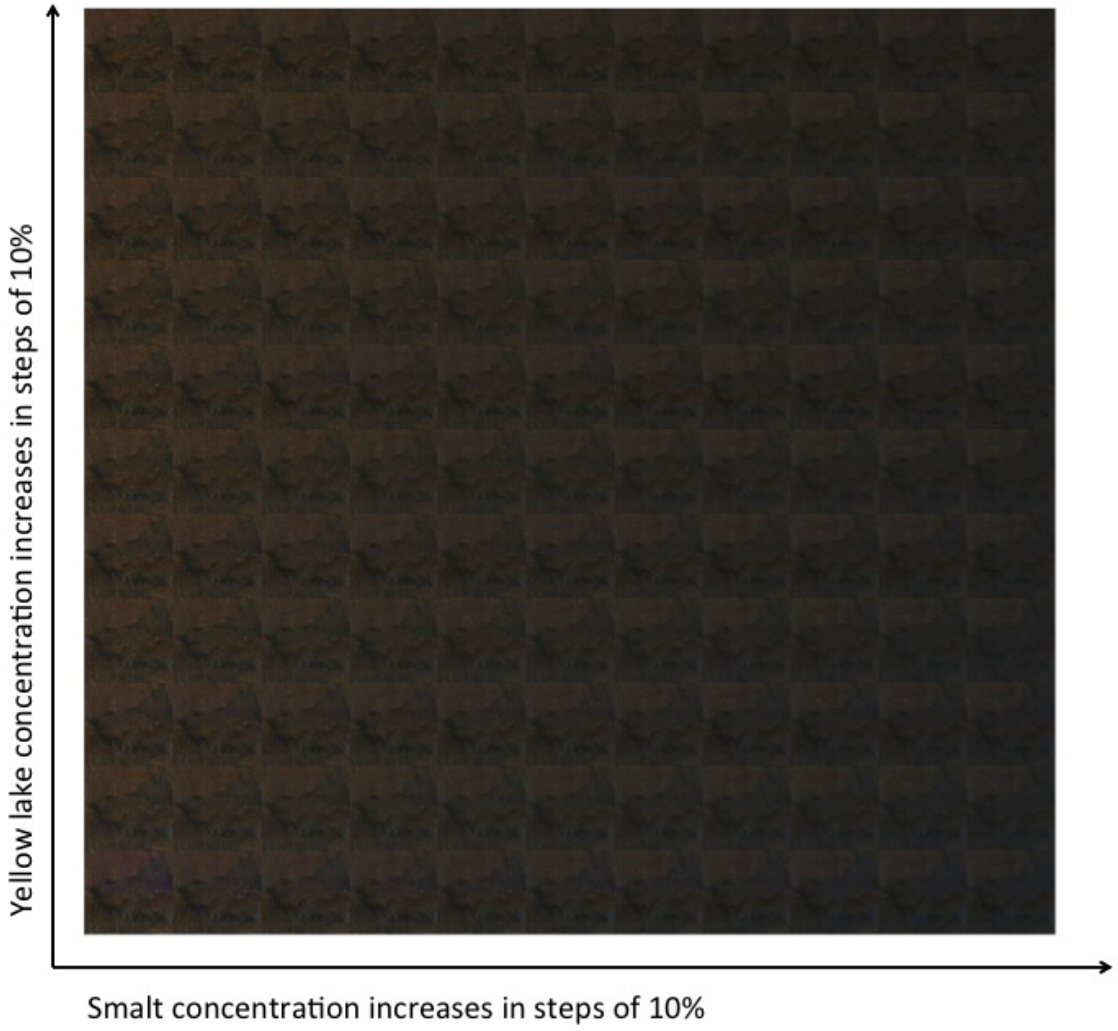

Figure E-4: The original image set at 80% with increasing concentration in steps of 10% of smalt and yellow lake. It shows that that the focus area get progressively darker and cooler of tone.

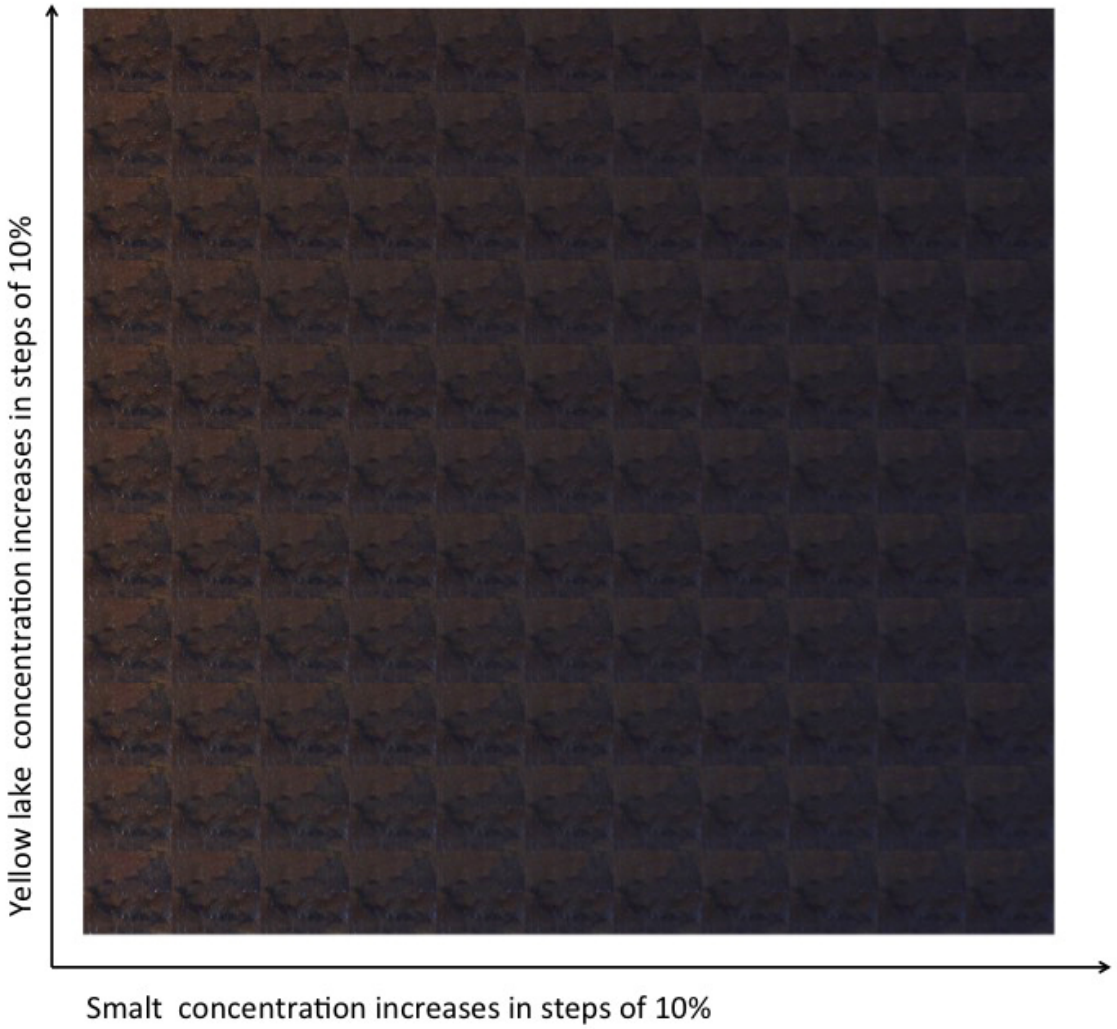

Figure E-5: The original image set at 80% and 20% of the colour of degraded smalt is subtracted, with increasing concentration in steps of 10% of smalt and yellow lake. It shows that that the focus area get progressively darker and cooler of tone.

Appendix F

Matlab

These functions are used in the process of filtering out pigment particles. In Table F-1, only a very short description is given.

Table F-1: Matlab functions

Name	Function	Works on
Contrast stretching	Expands the range of intensities so it uses the full intensity range of an image	Coloured image and grey scale
Sharpening	Intensities changes are highlighted	Coloured image and grey scale
Colour Threshold	Filters out a specific range of colours, used for separating them out of of an image	Coloured image and grey scale
Area open	Removes clusters of pixels that are smaller than a set amount of pixels	Binary image (black and white)
Erosion	Shrinks the white pixel cluster	Binary image (black and white)
Dilation	Increases the white pixel cluster	Binary image (black and white)
Opening	First erosion and after dilation: removes small objects and smooths the contours of the white pixel cluster.	Binary image (black and white)
Closing	First dilation, after erosion: eliminates small holes and smooths the contours of the white pixel cluster.	Binary image (black and white)
Fill holes	Fills holes in a white pixel cluster.	Binary image (black and white)

Bibliography

[1] "Rijksmuseum, portret van een paar als isaak en rebekka, bekend als de joodse bruid." http://hdl.handle.net/10934/RM0001.COLLECT.5223. Accessed: 2017-04-03.

[2] "Rkd, isaak en rebecca bespied door abimelek bij het minnekozen (genesis 26:8), ca.1665." https://rkd.nl/nl/explore/images/257818. Accessed: 2017-05-28.

[3] A. K. R. Choudhury, *Principles of Colour and Appearance Measurement Volume 2: Object appearance, colour perception and instrumental measurement*. Woodhead Publishing, 2014.

[4] J. Dik, *Scientific Analysis of Historical Paint and the Implications for Art History and Art Conservation: The Case Studies of Naples Yellow and Discoloured Smalt*. Universiteit van Amsterdam [Host], 2003.

[5] "prof.dr. joris dik, antoni van leeuwenhoek professor materials technology - materials in art and archaeology at tu delft." https://www.tudelft.nl/staff/j.dik/.

[6] "Chemical and engineering news, van gogh's fading colors inspire scientific inquiry." http://cen.acs.org/articles/94/i5/Van-Goghs-Fading-Colors-Inspire.html. Accessed: 2017-06-17.

[7] "Wikepedia, illuminant d65." https://en.wikipedia.org/wiki/Illuminant_D65. Accessed: 2017-09-28.

[8] N. Eastaugh, V. Walsh, T. Chaplin, and R. Siddall, *Pigment Compendium A Dictionary of Historical Pigments A Dictionary of Historical Pigments*. Elsevier Science, 2004.

[9] "Horiba, x-ray fluorescence - the basic process." http://www.horiba.com/scientific/products/x-ray-fluorescence-analysis/tutorial/x-ray-fluorescence-the-basic-process/. Accessed: 2017-05-28.

[10] D. de Man, "Invloed van smalt in de homerus van rembrandt," Master's thesis, University of Amsterdam, 2015.

[11] "Diana de man, ma conservation and restoration of paintings, universiteit van amsterdam." https://www.linkedin.com/in/diana-de-man-a8a25aa3/?ppe=1.

[12] A. K. R. Choudhury, *Principles of Colour and Appearance Measurement Volume 1: Object appearance, colour perception and instrumental measurement*. Woodhead Publishing, 2014.

[13] "dr. karin groen, chemist and research technician, rembrandt research project."

[14] "prof. dr. arie wallert, chair atelier practice, univeristy of amsterdam / rijksmuseum." https://www.codart.nl/guide/curators/arie-wallert/.

[15] "dr. annelies van loon, paintings research scientist, rijksmuseum / tu delft." https://www.researchgate.net/profile/Annelies_Van_Loon.

[16] "drs. petria noble, head of paintings conservation, rijksmuseum in amsterdam." https://www.codart.nl/guide/curators/petria-noble/.

[17] "dr. john delaney, senior imaging scientist, national gallery of art, washington, dc." https://www.nga.gov/audio-video/video/chemical-imaging.html.

[18] E. van de Wetering and R. van Rijn, *Rembrandt: The Painter at Work*. Amsterdam University Press, 2009.

[19] e. David Bomford, Jo Kirby, *Art in the making Rembrandt*. National Gallery Company Limited, 2006.

[20] R. Harley, *Artists' Pigments C.1600-1835: A Study in English Documentary Sources*. Butterworth Scientific, 1982.

[21] I. Cianchetta, I. Colantoni, F. Talarico, F. d'Acapito, A. Trapananti, C. Maurizio, S. Fantacci, and I. Davoli, "Discoloration of the smalt pigment: experimental studies and ab initio calculations," *J. Anal. At. Spectrom.*, vol. 27, pp. 1941–1948, 2012.

[22] L. Robinet, M. Spring, S. Pagés-Camagna, D. Vantelon, and N. Trcera, "Investigation of the discoloration of smalt pigment in historic paintings by micro-x-ray absorption spectroscopy at the co k-edge," *Analytical Chemistry*, vol. 83, no. 13, pp. 5145–5152, 2011.

[23] J. T. Bruno Mühlethaler, "Smalt," *Studies in Conservation*, vol. 14, no. 2, pp. 47–61, 1969.

[24] L. Robinet, M. Spring, and S. Pages-Camagna, "Vibrational spectroscopy correlated with elemental analysis for the investigation of smalt pigment and its alteration in paintings," *Anal. Methods*, vol. 5, pp. 4628–4638, 2013.

[25] A. van Loon, *Color Changes and Chemical Reactivity in Seventeenth-century Oil Paintings*. 2008.

[26] D. Saunders and J. Kirby, "Light-induced colour changes in red and yellow lake pigments," *National Gallery Technical Bulletin*, vol. 15, 1994.

[27] R. W. Marika Spring, Nicholas Penny and M. Wyld, "Colour change in the conversion of the magdalen attributed to pedro campaña," *National Gallery Technical Bulletin*, vol. 22, 2001.

[28] "The art institute of chicago,4/1/2016 session 1 of 3: Color change in 19th century art." https://www.youtube.com/watch?v=XRa6bGTBuzc. Accessed: 2017-05-28.

[29] W. S. Taft and J. W. Mayer, *The Science of Paintings*. Springer, 2000.

[30] J. Plesters, "A preliminary note on the incidence of discolouration of smalt in oil media," *Studies in Conservation*, vol. 14, no. 2, pp. 62–74, 1969.

[31] R. McDonald, S. of Dyers, and Colourists, *Colour Physics for Industry*. Society of Dyers and Colourists, 1997.

[32] R. Johnston-Feller, *Color Science in the Examination of Museum Objects: nondestructive procedures*. The]. Paul Getty Trust, 2001.

[33] L. Bressel and O. Reich, "Theoretical and experimental study of the diffuse transmission of light through highly concentrated absorbing and scattering materials. part monte carlo simulations," *jqsrt*, vol. 146, pp. 190–198, oct 2014.

[34] M. Senthilkumar, "5 - use of artificial neural networks (anns) in colour measurement," in *Colour Measurement* (M. Gulrajani, ed.), Woodhead Publishing Series in Textiles, pp. 125 – 146, Woodhead Publishing, 2010.

[35] MATLAB, *version 9.0 (R2016a)*. Natick, Massachusetts: The MathWorks Inc., 2016.

[36] K. Janssens, G. V. D. Snickt, M. Alfeld, P. Noble, A. van Loon, J. Delaney, D. Conover, J. Zeibel, and J. Dik, "Rembrandt's *Saul and David* (c. 1652): Use of multiple types of smalt evidenced by means of non-destructive imaging," *Microchemical Journal*, vol. 126, pp. 515 – 523, 2016.

[37] M. Kubik, "5 hyperspectral imaging: A new technique for the non-invasive study of artworks," in *Physical Techniques in the Study of Art, Archaelogy and Cultural Heritage* (D. Creagh and D. Bradley, eds.), pp. 199 – 259, Elsevier, 2007.